

Deep Learning Statistical Arbitrage*

Jorge Guíjarro-Ordóñez[†]

Markus Pelger[‡]

Greg Zanolli[§]

This draft: September 25, 2022

First draft: March 15, 2019

Abstract

Statistical arbitrage exploits temporal price differences between similar assets. We develop a unifying conceptual framework for statistical arbitrage and a novel data driven solution. First, we construct arbitrage portfolios of similar assets as residual portfolios from conditional latent asset pricing factors. Second, we extract their time series signals with a powerful machine-learning time-series solution, a convolutional transformer. Lastly, we use these signals to form an optimal trading policy, that maximizes risk-adjusted returns under constraints. Our comprehensive empirical study on daily US equities shows a high compensation for arbitrageurs to enforce the law of one price. Our arbitrage strategies obtain consistently high out-of-sample mean returns and Sharpe ratios, and substantially outperform all benchmark approaches.

Keywords: statistical arbitrage, pairs trading, machine learning, deep learning, big data, stock returns, convolutional neural network, transformer, attention, factor model, market efficiency, investment.

JEL classification: C14, C38, C55, G12

*We thank Robert Anderson, Jose Blanchet, Marcelo Fernandes, Kay Giesecke, Lisa Goldberg, Amit Goyal (discussant), Bryan Kelly, Robert Korajczyk, Martin Lettau, Sophia Li, Marcelo Medeiros, Scott Murray, George Papanicolaou, Guofu Zhou (discussant) and seminar and conference participants at Stanford, UC Berkeley, Rutgers University, GSU CEAR Finance Conference, NBER-NSF Time-Series Conference, AI and Big Data in Finance Research Seminar, AI in Fintech Forum, World Congress of the Bachelier Finance Society, Society of Financial Econometrics Annual Conference, the Econometric Research in Finance Workshop, the Meeting of the Brazilian Finance Society, World Online Seminars on Machine Learning in Finance, the Machine Learning and Quantitative Finance Workshop at Oxford, Annual Bloomberg-Columbia Machine Learning in Finance Workshop, NVIDIA AI Webinar, Vanguard Academic Seminar, INFORMS and the Western Conference on Mathematical Finance for helpful comments. We thank MSCI for generous research support.

[†]Stanford University, Department of Mathematics, Email: jguiord@stanford.edu.

[‡]Stanford University, Department of Management Science & Engineering, Email: mpelger@stanford.edu.

[§]Stanford University, Department of Management Science & Engineering, Email: gzanolli@stanford.edu.

I. Introduction

Statistical arbitrage is one of the pillars of quantitative trading, and has long been used by hedge funds and investment banks. The term statistical arbitrage encompasses a wide variety of investment strategies, which identify and exploit temporal price differences between similar assets using statistical methods. Conceptually, they are based on relative trades between a stock and a mimicking portfolio. The mimicking portfolio is constructed to be “similar” to the target stock, usually based on historical co-movements in the price time-series or similar firm characteristics. When the spread between the prices of the two comparison assets widens, the arbitrageur sells the winner and buys the loser. If their prices move back together, the arbitrageur will profit. While Wall Street has developed a plethora of proprietary tools for sophisticated arbitrage trading, there is still a lack of understanding of how much arbitrage opportunity is actually left in financial markets. In this paper we answer the two key questions around statistical arbitrage: What are the important elements of a successful arbitrage strategy and how much realistic arbitrage is in financial markets?

Every statistical arbitrage strategy needs to solve the following three fundamental problems: Given a large universe of assets, what are long-short portfolios of similar assets? Given these portfolios, what are time series signals that indicate the presence of temporary price deviations? Last, but not least, given these signals, how should an arbitrageur trade them to optimize a trading objective while taking into account possible constraints and market frictions? Each of these three questions poses substantial challenges, that prior work has only partly addressed. First, it is a hard problem to find long-short portfolios for all stocks as it is a priori unknown what constitutes “similarity”. This problem requires considering all the big data available for a large number of assets and times, including not just conventional return data but also exogenous information like asset characteristics. Second, extracting the right signals requires detecting flexibly all the relevant patterns in the noisy, complex, low-sample-size time series of the portfolio prices. Last but not least, optimal trading rules on a multitude of signals and assets are complicated and depend on the trading objective. All of these challenges fundamentally require flexible estimation tools that can deal with many variables. It is a natural idea to use machine learning techniques like deep neural networks to deal with the high dimensionality and complex functional dependencies of the problem. However, our problem is different from the usual prediction task, where machine learning tools excel. We show how to optimally design a machine learning solution to our problem that leverages the economic structure and objective.

In this paper, we propose a unifying conceptual framework that generalizes common approaches to statistical arbitrage. Statistical arbitrage can be decomposed into three fundamental elements: (1) arbitrage portfolio generation, (2) arbitrage signal extraction and (3) the arbitrage allocation decision given the signal. By decomposing different methods into their arbitrage portfolio, signal and allocation element, we can compare different methods and study which components are the most relevant for successful trading. For each step we develop a novel machine learning implementation, which we compare with conventional methods. As a result, we construct a new deep learning statistical arbitrage approach. Our new approach constructs arbitrage portfolios with a conditional

latent factor model, extracts the signals with the currently most successful machine learning time-series method and maps them into a trading allocation with a flexible neural network. These components are integrated and optimized over a global economic objective, which maximizes the risk-adjusted return under constraints. Empirically, our general model outperforms out-of-sample the leading benchmark approaches and provides a clear insight into the structure of statistical arbitrage.

To construct arbitrage portfolios, we introduce the economically motivated asset pricing perspective to create them as residuals relative to asset pricing models. This perspective allows us to take advantage of the recent developments in asset pricing and to also include a large set of firm characteristics in the construction of the arbitrage portfolios. We use fundamental risk factors and conditional and unconditional statistical factors for our asset pricing models. Similarity between assets is captured by similar exposure to those factors. Hence, arbitrage portfolios are trades relative to mimicking stock portfolios, which are well-diversified portfolios with the same exposure to risk factors. In the case of statistical principal component factors, the mimicking portfolios correspond to assets with the highest correlation with the target stocks. Arbitrage Pricing Theory provides a justification for mean reversion patterns. It implies that, with an appropriate model, the corresponding factor portfolios represent the “fair price” of each of the assets. Therefore, the residual portfolios relative to the asset pricing factors capture the temporary deviations from the fair price of each of the assets and should only temporally deviate from their long-term mean. Importantly, the residuals are tradeable portfolios, which are only weakly cross-sectionally correlated, and close to orthogonal to firm characteristics and systematic factors. These properties allow us to extract a stationary time-series model for the signal.

To detect time series patterns and signals in the residual portfolios, we introduce a filter perspective and estimate them with a flexible data-driven filter based on convolutional networks combined with transformers. In this way, we do not prescribe a potentially misspecified function to extract the time series structure, for example, by estimating the parameters of a given parametric time-series model, or the coefficients of a decomposition into given basis functions, as in conventional methods. Instead, we directly learn in a data-driven way what the optimal pattern extraction function is for our trading objective. The convolutional transformer is the ideal method for this purpose. Convolutional neural networks are the state-of-the-art AI method for pattern recognition, in particular in computer vision. In our case they identify the local patterns in the data and may be thought as a nonlinear and learnable generalization of conventional kernel-based data filters. Transformer networks are the most successful AI model for time series in natural language processing. In our model, they combine the local patterns to global time-series patterns. Their combination results in a data-driven flexible time-series filter that can essentially extract any complex time-series signal, while providing an interpretable model.

To find the optimal trading allocation, we propose neural networks to map the arbitrage signals into a complex trading allocation. This generalizes conventional parametric rules, for example fixed rules based on thresholds, which are only valid under strong model assumptions and a small signal

dimension. Importantly, these components are integrated and optimized over a global economic objective, which maximizes the risk-adjusted return under constraints. This allows our model to learn the optimal signals and allocation for the actual trading objective, which is different from a prediction objective. The trading objective can maximize the Sharpe ratio or expected return subject to a risk penalty, while taking into account constraints important to real investment managers, such as restricting turnover, leverage, or proportion of short trades.

Our comprehensive empirical out-of-sample analysis is based on the daily returns of roughly the 550 largest and most liquid stocks in the U.S. from 1998 to 2016. We estimate the out-of-sample residuals on a rolling window relative to the empirically most important factor models. These are observed fundamental factors, for example the Fama-French 5 factors and price trend factors, locally estimated latent factors based on principal component analysis (PCA) or locally estimated conditional latent factors that include the information in 46 firm-specific characteristics and are based on the Instrumented PCA (IPCA) of Kelly et al. (2019). We extract the trading signal with one of the most successful parametric models, based on the mean-reverting Ornstein-Uhlenbeck process, a frequency decomposition of the time-series with a Fourier transformation and our novel convolutional network with transformer. Finally, we compare the trading allocations based on parametric or nonparametric rules estimated with different risk-adjusted trading objectives.

Our empirical main findings are five-fold. First, our deep learning statistical arbitrage model substantially outperforms all benchmark approaches out-of-sample. In fact, our model can achieve an impressive annual Sharpe ratio larger than four. While respecting short-selling constraints we can obtain annual out-of-sample mean returns of 20%. This performance is four times better than one of the best parametric arbitrage models, and twice as good as an alternative deep learning model without the convolutional transformer filter. These results are particularly impressive as we only trade the largest and most liquid stocks. Hence, our model establishes a new standard for arbitrage trading.

Second, the performance of our deep learning model suggests that there is a substantial amount of short-term arbitrage in financial markets. The profitability of our strategies is orthogonal to market movements and conventional risk factors including momentum and reversal factors and does not constitute a risk-premium. Our strategy performs consistently well over the full time horizon. The model is extremely robust to the choice of tuning parameters, and the period when it is estimated. Importantly, our arbitrage strategy remains profitable in the presence of realistic transaction and holdings costs. Arbitrage signals are persistent over short time horizons. While arbitrageurs correct most mispricing over the horizon of a month, around half of the Sharpe ratio can persist for a holding period of one week. Assessing the amount of arbitrage in financial markets with unconditional pricing errors relative to factor models or with parametric statistical arbitrage models, severely underestimates the amount of statistical arbitrage.

Third, the trading signal extraction is the most challenging and separating element among different arbitrage models. Surprisingly, the choice of asset pricing factors has only a minor effect on the overall performance. Residuals relative to the five Fama-French factors and five locally

estimated principal component factors perform very well with out-of-sample Sharpe ratios above 3.2 for our deep learning model. Five conditional IPCA factors increase the out-of-sample Sharpe ratio to 4.2, which suggests that asset characteristics provide additional useful information. Increasing the number of risk factors beyond five has only a marginal effect. Similarly, the other benchmark models are robust to the choice of factor model as long as it contains sufficiently many factors. The distinguishing element is the time-series model to extract the arbitrage signal. The convolutional transformer doubles the performance relative to an identical deep learning model with a pre-specified frequency filter. Importantly, we highlight that time-series modeling requires a time-series machine learning approach, which takes temporal dependency into account. An off-the-shelf nonparametric machine learning method like conventional neural networks, that estimates an arbitrage allocation directly from residuals, performs substantially worse.

Fourth, successful arbitrage trading is based on local asymmetric trend and reversion patterns. Our convolutional transformer framework provides an interpretable representation of the underlying patterns, based on local basic patterns and global “dependency factors”. The building blocks of arbitrage trading are smooth trend and reversion patterns. The arbitrage trading is short-term and the last 30 trading days seem to capture the relevant information. Interestingly, the direction of policies is asymmetric. The model reacts quickly on downturn movements, but more cautiously on uptrends. More specifically, the “dependency factors” which are the most active in downturn movements focus only on the most recent 10 days, while those for upward movements focus on the first 20 days in a 30-day window.

Fifth, time-series-based trading patterns should be extracted from residuals and not directly from returns. For an appropriate factor model, the residuals are only weakly correlated and close to stationary in both, the time and cross-sectional dimension. Hence, it is meaningful to extract a uniform trading pattern, that is based only on the past time-series information, from the residuals. In contrast stock returns are dominated by a few factors, which severely limits the actual independent time-series information, and are strongly heterogeneous due to their variation in firm characteristics. While the level of stock returns is extremely hard to predict, even with flexible machine learning methods, residuals capture relative movements and remove the level component. These properties make residuals analyzable from a purely time-series based perspective and, unlike the existing literature, they allow us to incorporate alternative data into the portfolio construction process. This also highlights a fundamental difference with most of the existing financial machine learning literature: We do not use characteristics to get features for prediction, but rather to obtain the data orthogonal to these features.

Related Literature

Our paper builds on the classical statistical arbitrage literature, in which the three main problems of portfolio generation, pattern extraction, and allocation decision have traditionally been considered independently. Classical statistical methods of generating arbitrage portfolios have mostly focused on obtaining multiple pairs or small portfolios of assets, using techniques like the

distance method of Gatev et al. (2006), the cointegration approach of Vidyamurthy (2004), or copulas as in Rad et al. (2016). In contrast, more general methods that exploit large panels of stock returns include the use of PCA factor models, as in Avellaneda and Lee (2010) and its extension in Yeo and Papanicolaou (2017), and the maximization of mean-reversion and sparsity statistics as in d’Aspremont (2011). We include the model of Yeo and Papanicolaou (2017) as the parametric benchmark model in our study as it has one of the best empirical performances among the class of parametric models. Our paper contributes to this literature by introducing a general asset pricing perspective to obtain the arbitrage portfolios as residuals. This allows us to take advantage of conditional asset pricing models, that include time-varying firm characteristics in addition to the return time-series, and provides a more disciplined, economically motivated approach. The signal extraction step for these models assumes parametric time series models for the arbitrage portfolios, whereas the allocations are often decided from the estimated parameters by using stochastic control methods or given threshold rules and one-period optimizations. Some representative papers of the first approach include Jurek and Yang (2007), Mudchanatongsuk et al. (2008), Cartea and Jaimungal (2016), Lintilhac and Tourin (2016) and Leung and Li (2015), whereas the second one is illustrated by Elliott et al. (2005) and Yeo and Papanicolaou (2017). Both approaches are special cases of our more general framework. Mulvey et al. (2020) and Kim and Kim (2019) are examples of including machine learning elements within the parametric statistical arbitrage framework, by either solving a stochastic control problem with neural networks or estimating a time-varying threshold rule with reinforcement learning.

Our paper is complementary to the emerging literature that uses machine learning methods for asset pricing. While the asset pricing literature aims to explain the risk premia of assets, our focus is on the residual component which is not explained by the asset pricing models. Chen et al. (2022), Bryzgalova et al. (2019) and Kozak et al. (2020) estimate the stochastic discount factor (SDF), which explains the risk premia of assets, with deep neural networks, decision trees or elastic net regularization. These papers employ advanced statistical methods to solve a conditional method of moment problem in the presence of many variables. The workhorse models in equity asset pricing are based on linear factor models exemplified by Fama and French (1993, 2015). Recently, new methods have been developed to extract statistical asset pricing factors from large panels with various versions of principal component analysis (PCA). The Risk-Premium PCA in Lettau and Pelger (2020a,b) includes a pricing error penalty to detect weak factors that explain the cross-section of returns. The high-frequency PCA in Pelger (2020) uses high-frequency data to estimate local time-varying latent risk factors and the Instrumented PCA (IPCA) of Kelly et al. (2019) estimates conditional latent factors by allowing the loadings to be functions of time-varying asset characteristics. Gu et al. (2021) generalize IPCA to allow the loadings to be nonlinear functions of characteristics. Giglio and Xiu (2021) use PCA factors to account for missing priced factors in risk premia estimation. He et al. (2022) highlight the important insight that the time-series of residuals can be informative for trading. They test asset pricing models by studying the profitability of trading residuals based on high-minus-low sorting strategies of prior residual returns.

Our paper is related to the growing literature on return prediction with machine learning methods, which has shown the benefits of regularized flexible methods. In their pioneering work Gu et al. (2020) conduct a comparison of machine learning methods for predicting the panel of individual U.S. stock returns based on the asset-specific characteristics and economic conditions in the previous period. Freyberger et al. (2020) use different methods for predicting stock returns. In a similar spirit, Bianchi et al. (2019) predict bond returns, Li and Rossi (2020) predict mutual fund returns, and Bali et al. (2022) predict option returns. A related stream extends cross-sectional machine learning prediction to higher moments and residuals, which are used for investment decisions. Li and Tang (2022) use machine learning to predict risk measures and estimate conditional volatilities. Kaniel et al. (2022) and DeMiguel et al. (2022) predict the skill of mutual fund managers based on residuals from benchmark asset pricing factors. The return prediction literature is fundamentally estimating the risk premia of assets, while our focus is on understanding and exploiting the temporal deviations thereof. This different goal is reflected in the different methods that are needed. These return predictions estimate a nonparametric cross-sectional model between current returns and large set of covariates from the last period, but do not estimate a time-series model. In contrast, the important challenge that we solve is to extract a complex time-series pattern.

A related stream of the return prediction literature forecasts returns using past returns, generally followed by some long-short investment policy based on the prediction. For example, Krauss et al. (2017) use various machine learning methods for this type of prediction.¹ However, they use general nonparametric function estimates, which are not specifically designed for time-series data. Lim and Zohren (2020) show that it is important for machine learning solutions to explicitly account for temporal dependence when they are applied to time-series data. Murray et al. (2021) and Jiang et al. (2022) build on this insight and use machine learning to learn price trends for return forecasting. Forecasting returns and building a long-short portfolio based on the prediction is different from statistical arbitrage trading as it combines a risk premium and potential arbitrage component. It is not based on temporary price differences and also in general not orthogonal to common risk factors and market movements. In this paper we highlight the challenge of inferring complex time-series information and argue that using returns directly as an input to a time-series machine learning method, can be suboptimal as returns are dominated by a few factor time-series and are heterogeneous due to cross-sectionally and time-varying characteristics. In contrast, appropriate residuals are close to uncorrelated and locally cross-sectionally stationary. Hence, appropriate residuals allow the extraction of a complex time-series pattern.

Naturally, our work overlaps with the literature on using machine learning tools for investment. The SDF estimated by asset pricing models, like in Chen et al. (2022) and Bryzgalova et al. (2019), directly maps into a conditionally mean-variance efficient portfolio and hence an attractive investment opportunity. However, by construction this investment portfolio is not orthogonal but fully exposed to systematic risk, which is exactly the opposite for an arbitrage portfolio. Prediction approaches also imply investment strategies, typically long-short portfolios based on the predic-

¹Similar studies include Fischer et al. (2019), Chen et al. (2018), Huck (2009), and Dunis et al. (2006).

tion signal. However, estimating a signal with a prediction objective, is not necessarily providing an optimal signal for investment. Bryzgalova et al. (2019) and Chen et al. (2022) illustrate that machine learning models that use a trading objective can result in a substantially more profitable investment than models that estimate a signal with a prediction objective, while using the same information as input and having the same flexibility. This is also confirmed in Cong et al. (2020), who use an investment objective and reinforcement learning to construct machine learning investment portfolios. Our paper contributes to this literature by estimating investment strategies, that are orthogonal to systematic risk and are based on a trading objective with constraints.

Finally, our approach is also informed by the recent deep learning for time series literature. The transformer method was first introduced in the groundbreaking paper by Vaswani et al. (2017). We are the first to bring this idea into the context of statistical arbitrage and adopt it to the economic problem.

II. Model

The fundamental problem of statistical arbitrage consists of three elements: (1) The identification of similar assets to generate arbitrage portfolios, (2) the extraction of time-series signals for the temporary deviations of the similarity between assets and (3) a trading policy in the arbitrage portfolios based on the time-series signals. We discuss each element separately.

A. Arbitrage portfolios

We consider a panel of excess returns $R_{n,t}$, that is the return minus risk free rate of stock $n = 1, \dots, N_t$ at time $t = 1, \dots, T$. The number of available assets at time t can be time-varying. The excess return vector of all assets at time t is denoted as $R_t = \begin{pmatrix} R_{1,t} & \dots & R_{N_t,t} \end{pmatrix}^\top$.

We use a general asset pricing model to identify similar assets. In this context, similarity is defined as the same exposure to systematic risk, which implies that assets with the same risk exposure should have the same fundamental value. We assume that asset returns can be modeled by a conditional factor model:

$$R_{n,t} = \beta_{n,t-1}^\top F_t + \epsilon_{n,t}.$$

The K factors $F \in \mathbb{R}^{T \times K}$ capture the systematic risk, while the risk loadings $\beta_{t-1} \in \mathbb{R}^{N_t \times K}$ can be general functions of the information set at time $t - 1$ and hence can be time-varying. This general formulation includes the empirically most successful factor models. In our empirical analysis we will include observed traded factors, e.g. the Fama-French 5 factor model, latent factors based on the principal components analysis (PCA) of stock returns and conditional latent factors estimated with Instrumented Principal Component Analysis (IPCA).

Without loss of generality, we can treat the factors as excess returns of traded assets. Either the factors are traded, for example a market factor, in which case we include them in the returns

R_t . Otherwise, we can generate factor mimicking portfolios by projecting them on the asset space, as for example with latent factors:

$$F_t = w_{t-1}^F{}^\top R_t.$$

We define *arbitrage portfolios* as residual portfolios $\epsilon_{n,t} = R_{n,t} - \beta_{n,t-1}^\top F_t$. As factors are traded assets, the arbitrage portfolios are themselves traded portfolios. Hence, the vector of residual portfolios equals

$$\epsilon_t = R_t - \beta_{t-1} w_{t-1}^F{}^\top R_t = \underbrace{\left(I_{N_t} - \beta_{t-1} w_{t-1}^F{}^\top \right)}_{\Phi_{t-1}} R_t = \Phi_{t-1} R_t. \quad (1)$$

Arbitrage portfolios are trades relative to mimicking stock portfolios. The factor component in the residuals corresponds to a well-diversified mimicking portfolio, that is is “close” to the specific stock in the relative trade. More specifically, in the case of PCA factors, we construct well-diversified portfolios of stocks that have the highest correlation with each target stock in the relative trades. This is conceptually the same idea as using some form of clustering algorithm to construct a portfolio of highly correlated stocks.² Hence, residuals of PCA factors construct relative trades based on correlations in past return time-series. In the case of IPCA factors, we intuitively construct for each stock a well-diversified mimicking portfolio that is as similar as possible in terms of the underlying firm characteristics. Hence, the mimicking portfolio represents an asset with very similar firm fundamentals. Lastly, for Fama-French factors, we construct mimicking portfolios with the same exposure to those fundamental factors. In all cases, the choice of factor model implies a notation of similarity. By construction the mimicking portfolio and the target stock have identical loadings to the selected factors.

Arbitrage trading relative to mimicking portfolios takes advantage of all assets in the market. In practice and modern statistical arbitrage theory, it has replaced the more restrictive idea of pairs trading, which considers relative trades between only two stocks. On an intuitive level, the mimicking portfolio represents the reference asset in the relative trade. It can be constructed even if there does not exist an individual stock that is highly correlated with a target stock.

Our arbitrage portfolios based on residuals also allow us to benefit from an asset pricing perspective. Arbitrage portfolios are projections on the return space that annihilate systematic asset risk. For an appropriate asset pricing model, the residual portfolios should not earn a risk premium. This is the fundamental assumption behind any arbitrage argument. As deviations from a mean of zero have to be temporary, arbitrage trading bets on the mean revision of the residuals. In particular, for an appropriate factor model the residuals are expected to have the following properties: First, the unconditional mean of the arbitrage portfolios is zero, $\mathbb{E}[\epsilon_{n,t}] = 0$. Second, the arbitrage portfolios are only weakly cross-sectionally dependent. We confirm empirically that once we use sufficiently many statistical or fundamental factors the residuals are indeed close to uncorrelated

²In fact, under appropriate assumptions a clustering problem can be solved by a latent factor estimation.

and have an average mean close to zero. However, while the asset pricing perspective provides a theoretical argument for mean reversion in residuals, our approach is still valid even if we omit some relevant risk factors. The relative trades would then only exploit the temporal time-series deviations from the risk factors captured by the mimicking portfolios.

We denote by \mathcal{F}_{t-1} the filtration generated by the returns R_{t-1} , which include the factors, and the information set that captures the risk exposure β_{t-1} , which is typically based on asset specific characteristics or past returns.

B. Arbitrage signal

The *arbitrage signal* is extracted from the time-series of the arbitrage portfolios. These time-series signals are the input for a trading policy. An example for an arbitrage signal would be a parametric model for mean reversion that is estimated for each arbitrage portfolio. The trading strategy for each arbitrage portfolio would depend on its speed of mean reversion and its deviation from the long run mean. More generally, the arbitrage signal is the estimation of a time-series model, which can be parametric or nonparametric. An important class of models are filtering approaches. Conceptually, time-series models are multivariate functional mappings between sequences, which take into account the temporal order of the elements and potentially complex dependencies between the elements of the input sequence.

We apply the signal extraction to the time-series of the last L lagged residuals, which we denote in vector notation as

$$\epsilon_{n,t-1}^L := \begin{pmatrix} \epsilon_{n,t-L} & \cdots & \epsilon_{n,t-1} \end{pmatrix}.$$

The arbitrage signal function is a mapping $\theta \in \Theta$ from \mathbb{R}^L to \mathbb{R}^p , where Θ defines an appropriate function space:

$$\theta(\cdot) : \epsilon_{n,t-1}^L \rightarrow \theta_{n,t-1}.$$

The signals $\theta_{n,t-1} \in \mathbb{R}^p$ for the arbitrage portfolio n at time t only depend on the time-series of lagged returns $\epsilon_{n,t-1}^L$. Note that the dimensionality of the signal can be the same as for the input sequence. Formally, the function θ is a mapping from the filtration $\mathcal{F}_{n,t-1}^{\epsilon,L}$ generated by $\epsilon_{n,t-1}^L$ into the filtration $\mathcal{F}_{n,t-1}^\theta$ generated by $\theta_{n,t-1}$ and $\mathcal{F}_{n,t-1}^\theta \subseteq \mathcal{F}_{n,t-1}^{\epsilon,L}$. We use the notation of evaluating functions elementwise, that is $\theta(\epsilon_{t-1}^L) = \begin{pmatrix} \theta_{1,t-1} & \cdots & \theta_{N_t,t-1} \end{pmatrix} = \theta_{t-1} \in \mathbb{R}^{N_t}$ with $\epsilon_{t-1}^L = \begin{pmatrix} \epsilon_{1,t-1} & \cdots & \epsilon_{N_t,t-1} \end{pmatrix}$.

The arbitrage signal $\theta_{n,t-1}$ is a sufficient statistic for the trading policy; that is, all relevant information for trading decisions is summarized in it. This also implies that two arbitrage portfolios with the same signal get the same weight in the trading strategy. More formally, this means that the arbitrage signal defines equivalence classes for the arbitrage portfolios. The most relevant signals summarize reversal patterns and their direction with a small number of parameters. A potential

trading policy could be to hold long positions in residuals with a predicted upward movement and go short in residuals that are in a downward cycle.

This problem formulation makes two implicit assumptions. First, the residual time-series follow a stationary distribution conditioned on its lagged returns. This is a very general framework that includes the most important models for financial time-series. Second, the first L lagged returns are a sufficient statistic to obtain the arbitrage signal $\theta_{n,t-1}$. This reflects the motivation that arbitrage is a temporary deviation of the fair price. The lookback window can be chosen to be arbitrarily large, but in practice it is limited by the availability of lagged returns.

C. Arbitrage trading

The trading policy assigns an investment weight to each arbitrage portfolio based on its signal. The allocation weight is the solution to an optimization problem, which models a general risk-return tradeoff and can also include trading frictions and constraints. An important case are mean-variance efficient portfolios with transaction costs and short sale constraints.

An arbitrage allocation is a mapping from \mathbb{R}^p to \mathbb{R} in a function class \mathbf{W} , that assigns a weight $w_{n,t-1}^\epsilon$ for the arbitrage portfolio $\epsilon_{n,t-1}$ in the investment strategy using only the arbitrage signal $\theta_{n,t}$:

$$\mathbf{w}^\epsilon : \theta_{n,t-1} \rightarrow w_{n,t-1}^\epsilon.$$

Given a concave utility function $U(\cdot)$, the allocation function is the solution to

$$\max_{\mathbf{w}^\epsilon \in \mathbf{W}, \theta \in \Theta} \mathbb{E}_{t-1} [U(w_{t-1}^R R_t)] \quad (2)$$

$$\text{s.t.} \quad w_{t-1}^R = \frac{w_{t-1}^\epsilon{}^\top \Phi_{t-1}}{\|w_{t-1}^\epsilon{}^\top \Phi_{t-1}\|_1} \quad \text{and} \quad w_{t-1}^\epsilon = \mathbf{w}^\epsilon(\theta(\epsilon_{t-1}^L)). \quad (3)$$

In the presence of trading costs, we calculate the expected utility of the portfolio net return by subtracting from the portfolio return $w_{t-1}^R R_t$ the trading costs that are associated with the stock allocation w_{t-1}^R . The trading costs can capture the transaction costs from frequent rebalancing and the higher costs of short selling compared to long positions. The stock weights w_{t-1}^R are normalized to add up to one in absolute value, which implicitly imposes a leverage constraint. The conditional expectation uses the general filtration \mathcal{F}_{t-1} .

This is a combined optimization problem, which simultaneously solves for the optimal allocation function and arbitrage signal function. As the weight is a composition of the two functions, i.e. $w_{t-1}^\epsilon = \mathbf{w}^\epsilon(\theta(\epsilon_{t-1}^L))$, the decomposition into a signal and allocation function is in general not uniquely identified. This means there can be multiple representations of θ and \mathbf{w}^ϵ , that will result in the same trading policy. We use a decomposition that allows us to compare the problem to classical arbitrage approaches, for which this separation is uniquely identified. The key feature of the signal function θ is that it models a time-series, that means it is a mapping that explicitly models

the temporal order and the dependency between the elements of ϵ_{t-1}^L . The allocation function \mathbf{w}^ϵ can be a complex nonlinear function, but does not explicitly model time-series behavior. This means that \mathbf{w}^ϵ is implicitly limited in the dependency patterns of its input elements that it can capture.

We will consider arbitrage trading that maximizes the Sharpe ratio or achieves the highest average return for a given level of variance risk. More specifically we will solve for

$$\max_{\mathbf{w}^\epsilon \in \mathbf{W}, \theta \in \Theta} \frac{\mathbb{E}[w_{t-1}^R{}^\top R_t]}{\sqrt{\text{Var}(w_{t-1}^R{}^\top R_t)}} \quad \text{or} \quad \max_{\mathbf{w}^\epsilon \in \mathbf{W}, \theta \in \Theta} \mathbb{E}[w_{t-1}^R{}^\top R_t] - \gamma \text{Var}(w_{t-1}^R{}^\top R_t) \quad (4)$$

$$\text{s.t.} \quad w_{t-1}^R = \frac{w_{t-1}^\epsilon{}^\top \Phi_{t-1}}{\|w_{t-1}^\epsilon{}^\top \Phi_{t-1}\|_1} \quad \text{and} \quad w_{t-1}^\epsilon = \mathbf{w}^\epsilon(\theta(\epsilon_{t-1}^L)). \quad (5)$$

for some risk aversion parameter γ . We will consider this formulation with and without trading costs.³

Many relevant models estimate the signal and allocation function separately. The arbitrage signals can be estimated as the parameters of a parametric time-series model, the serial moments for a given stationary distribution or a time-series filter. In these cases, the signal estimation solves a separate optimization problem as part of the estimation. Given the signals, the allocation function is the solution of

$$\max_{\mathbf{w}^\epsilon \in \mathbf{W}} \mathbb{E}_{t-1}[U(w_{t-1}^R R_t)] \quad \text{s.t.} \quad w_{t-1}^R = \frac{w^\epsilon(\theta_{t-1})^\top \Phi_{t-1}}{\|w^\epsilon(\theta_{t-1})^\top \Phi_{t-1}\|_1}. \quad (6)$$

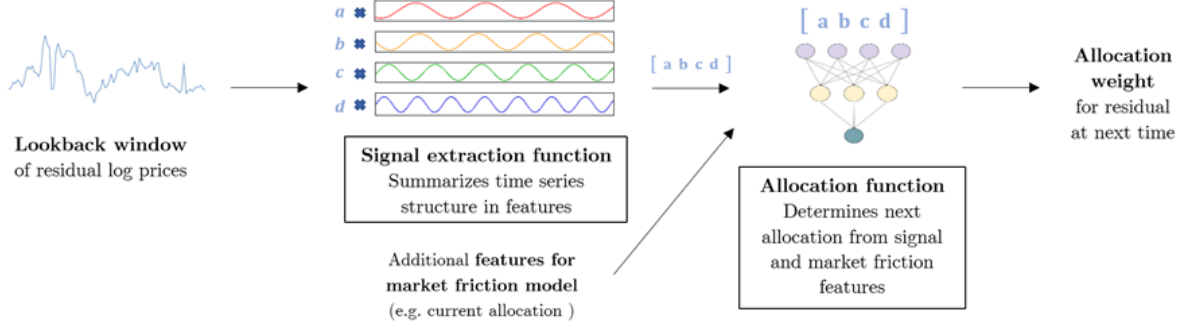
We provide an extensive study of the importance of the different elements in statistical arbitrage trading. We find that the most important driver for profitable portfolios is the arbitrage signal function; that is, a good model to extract time-series behavior and to time the predictable mean reversion patterns is essential. The arbitrage portfolios of asset pricing models that are sufficiently rich result in roughly the same performance. Once an informative signal is extracted, parametric and nonparametric allocation functions can take advantage of it. We find that the key element is to consider a sufficiently general class of functions Θ for the arbitrage signal and to estimate the signal that is the most relevant for trading. In other words, the largest gains in statistical arbitrage come from flexible time-series signals θ and a joint optimization problem.

D. Models for Arbitrage Signal and Allocation Functions

In this section we introduce different functional models for the signal and allocation functions. They range from the most restrictive assumptions for simple parametric models to the most flexible model, which is our sophisticated deep neural network architecture. The general problem is the estimation of a signal and allocation function given the residual time-series. Here, we take the

³While the conventional mean-variance optimization applies a penalty to the variance, we found that it is numerically beneficial to use the standard deviation instead. Both formulations describe the same fundamental trade-off.

Figure 1: Conceptual Arbitrage Model



This figure illustrates the conceptual structure of our statistical arbitrage framework. The model takes as input the last L cumulative returns of a residual portfolio on a lookback window at a given time and outputs the predicted optimal allocation weight for that residual for the next time. The model is composed of a signal extraction function and an allocation function.

residual returns as given, i.e. we have selected an asset pricing model. In order to illustrate the key elements of the allocation functions, we consider trading the residuals directly. Projecting the residuals back into the original return space is identical for the different methods and discussed in the empirical part. The conceptual steps are illustrated in Figure 1.

The input to the signal extraction functions are the last L cumulative residuals. We simplify the notation by dropping the time index $t - 1$ and the asset index n and define the generic input vector

$$x := \mathbf{Int}(\epsilon_{n,t-1}^L) = \left(\epsilon_{n,t-L} \quad \sum_{l=1}^2 \epsilon_{n,t-L-1+l} \quad \cdots \quad \sum_{l=1}^L \epsilon_{n,t-L-1+l} \right).$$

Here the operation $\mathbf{Int}(\cdot)$ simply integrates a discrete time-series. We can view the cumulative residuals as the residual “price” process. We discuss three different classes of models for the signal function θ that vary in the degree of flexibility of the type of patterns that they can capture. Similarly, we consider different classes of models for the allocation function w^ϵ .

D.1. Parametric Models

Our first benchmark method is a parametric model and corresponds to classical mean-reversion trading. In this framework, the cumulative residuals x are assumed to be the discrete realizations of continuous time model:

$$x = \begin{pmatrix} X_1 & \cdots & X_L \end{pmatrix}.$$

Following the influential papers by Avellaneda and Lee (2010) and Yeo and Papanicolaou (2017) we model X_t as an Ornstein-Uhlenbeck (OU) process

$$dX_t = \kappa(\mu - X_t)dt + \sigma dB_t$$

for a Brownian motion B_t . These are the standard models for mean-reversion trading and Avellaneda and Lee (2010) among others have shown their good empirical performance.

The parameters of this model are estimated from the moments of the discretized time-series, as described in detail along with the other implementation details in Appendix B.B. The parameters for each residual process, the last cumulative sum and a goodness of fit measure form the signals for the Ornstein-Uhlenbeck model:

$$\theta^{\text{OU}} = \begin{pmatrix} \hat{\kappa} & \hat{\mu} & \hat{\sigma} & X_L & R^2 \end{pmatrix}.$$

Following Yeo and Papanicolaou (2017) we also include the goodness of fit parameter R^2 as part of the signal. R^2 has the conventional definition of the ratio of squared values explained by the model normalized by total squared values. If the R^2 value is too low, the predictions of the model seem to be unreliable, which can be taken into account in a trading policy. Hence, for each cumulative residual vector $\epsilon_{n,t-1}^L$ we obtain the signal

$$\theta_{n,t-1}^{\text{OU}} = \begin{pmatrix} \hat{\kappa}_{n,t-1} & \hat{\mu}_{n,t-1} & \hat{\sigma}_{n,t-1} & \sum_{l=1}^L \epsilon_{n,t-1+l} & R_{n,t-1}^2 \end{pmatrix}.$$

Avellaneda and Lee (2010) and Yeo and Papanicolaou (2017) advocate a classical mean-reversion thresholding rule, which implies the following allocation function⁴:

$$\mathbf{w}^{\epsilon|\text{OU}}(\theta^{\text{OU}}) = \begin{cases} -1 & \text{if } \frac{X_L - \mu}{\sigma/\sqrt{2\kappa}} > c_{\text{thresh}} \text{ and } R^2 > c_{\text{crit}} \\ 1 & \text{if } \frac{X_L - \mu}{\sigma/\sqrt{2\kappa}} < -c_{\text{thresh}} \text{ and } R^2 > c_{\text{crit}} \\ 0 & \text{otherwise} \end{cases}$$

The threshold parameters c_{thresh} and c_{crit} are tuning parameters. The strategy suggests to buy or sell residuals based on the ratio $\frac{X_L - \mu}{\sigma/\sqrt{2\kappa}}$. If this ratio exceeds a threshold, it is likely that the process reverts back to its long term mean, which starts the trading. If the R^2 value is too low, the predictions of the model seem to be unreliable, which stops the trading. This will be our parametric benchmark model. It has a parametric model for both the signal and allocation function.

Figure A.2 in the Appendix illustrates this model with an empirical example. In this figure we show the allocation weights and signals of the Ornstein-Uhlenbeck with threshold model as well as the more flexible models that we are going to discuss next. The models are estimated on the empirical data, and the residual is a representative empirical example. In more detail, we consider the residuals from five IPCA factors and estimate the benchmark models as explained in the empirical Section III.N. The left subplots display the cumulative residual process along with the out-of-sample allocation weights w_i^ϵ that each model assigns to this specific residual. The evaluation of this illustrative example is a simplification of the general model that we use in our empirical main analysis. In this example, we consider trading only this specific residual and hence normalize the

⁴The allocation function is derived by maximizing an expected trading profit. This deviates slightly from our objective of either maximizing the Sharpe ratio or the expected return subject to a variance penalty. As this is the most common arbitrage trading rule, we include it as a natural benchmark.

weights to $\{-1, 0, 1\}$. In our empirical analysis we trade all residuals and map them back into the original stock returns. The middle column shows the time-series of estimated out-of-sample signals for each model, by applying the θ_l arbitrage signal function to the previous $L = 30$ cumulative returns of the residual. The right column displays the out-of-sample cumulative returns of trading this particular residual based on the corresponding allocation weights.

The last row in Figure A.2 shows the results for the OU+Threshold model. The cumulative return of trading this residual is negative, suggesting that the parametric model fails. The residual time-series with the corresponding allocation weights in subplot (g) explain why. The trading allocation does not assign a positive weight during the uptrend and wrongly assigns a constant negative weight, when the residual price process follows a mean-reversion pattern with positive and negative returns. A parametric model can break down if it is misspecified. This is not only the case for trend patterns, but also if there are multiple mean reversion patterns of different frequencies. Subplot (h) shows the signal.⁵ We see that changes in the allocation function are related to sharp changes in at least one of the signals, but overall, the signal does not seem to represent the complex price patterns of the residual.

A natural generalization is to allow for a more flexible allocation function given the same time-series signals. We will consider for all our models also a general feedforward neural network (FFN) to map the signal into an allocation weight. FFNs are nonparametric estimators that can capture very general functional relationships.⁶ Hence, we also consider the additional model that restricts the signal function, but allows for a flexible allocation function:

$$w^{\epsilon|\text{OU-FFN}}(\theta^{\text{OU}}) = g^{\text{FFN}}(\theta^{\text{OU}}).$$

We will show empirically that the gains of a flexible allocation function are minor relative to the very simple parametric model.

D.2. Pre-Specified Filters

As a generalization of the restrictive parametric model of the last subsection, we consider more general time-series models. Many relevant time-series models can be formulated as filtering problems. Filters are transformations of time-series that provide an alternative representation of the original time-series which emphasizes certain dynamic patterns.

A time-invariant linear filter can be formulated as

$$\theta_l = \sum_{j=1}^L W_j^{\text{filter}} x_j,$$

⁵For better readability we have scaled the parameters of the OU process by a factor of five, but this still represents the same model as the scaling cancels out in the allocation function. As a minor modification, we use the ratio $\sigma/\sqrt{2\kappa}$ as a signal instead of two individual parameters, as the conventional regression estimator of the OU process directly provides the ratio, but requires additional moments for the individual parameters. However, this results in an equivalent presentation of the model as only the ratio enters the allocation function.

⁶Appendix B.A provides the details for estimating a FFN as a functional mapping $g^{\text{FFN}} : \mathbb{R}^p \rightarrow \mathbb{R}$.

which is a linear mapping from \mathbb{R}^L into \mathbb{R}^L with the matrix $W^{\text{filter}} \in \mathbb{R}^{L \times L}$. The estimation of causal ARMA processes is an example for such filters. A spectral decomposition based on a frequency filter is the most relevant filter for our problem of finding mean reversion patterns.

A Fast Fourier Transform (FFT) provides a frequency decomposition of the original time-series and separates the movements into mean reverting processes of different frequencies. FFT applies the filter $W_j^{\text{FFT}} = e^{\frac{2\pi i}{L}j}$ in the complex plane, but for real-valued time-series it is equivalent to fitting the following model:

$$x_l = a_0 + \sum_{j=1}^{L/2-1} \left(a_j \cdot \cos\left(\frac{2\pi j}{L}l\right) + b_j \cdot \sin\left(\frac{2\pi j}{L}l\right) \right) + a_{L/2} \cos(\pi l).$$

The FFT representation is given by coefficients of the trigonometric representation

$$\theta^{\text{FFT}} = \begin{pmatrix} a_0 & \cdots & a_{L/2} & b_1 & \cdots & b_{L/2-1} \end{pmatrix} \in \mathbb{R}^L.$$

The coefficients a_l and b_l can be interpreted as “loadings” or exposure to long or short-term reversal patterns. Note that the FFT is an invertible transformation. Hence, it simply represents the original time-series in a different form without losing any information. It is based on the insight that not the magnitude of the original data but the relative relationship in a time-series matters.

We use a flexible feedforward neural network for the allocation function

$$\mathbf{w}^{\epsilon|\text{FFT}}(\theta^{\text{FFT}}) = \mathbf{g}^{\text{FFN}}(\theta^{\text{FFT}}).$$

The usual intuition behind filtering is to use the frequency representation to cut off frequencies that have low coefficients and therefore remove noise in the representation. The FFN is essentially implementing this filtering step of removing less important frequencies.

We illustrate the model within our running example in Figure A.2. The middle row shows the results for the FFT+FFN model. The cumulative residual in subplot (d) seems to be a combination of low and high-frequency movements with an initial trend component. The signal in subplot (e) suggests that the FFT filter seems to capture the low frequency reversal pattern. However, it misses the high-frequency components as indicated by the simplistic allocation function. The trading strategy takes a long position for the first half and a short position for the second part. While this simple allocation results in a positive cumulative return, in this example it neglects the more complex local reversal patterns.

While the FFT framework is an improvement over the simple OU model as it can deal with multiple combined mean-reversion patterns of different frequencies, it fails if the data follows a pattern that cannot be well approximated by a small number of the pre-specified basis functions.

For completeness, our empirical analysis will also report the case of a trivial filter, which simply

takes the residuals as signals, and combines them with a general allocation function:

$$\begin{aligned}\theta^{\text{ident}}(x) &= x = \theta^{\text{ident}} \\ \mathbf{w}^{\epsilon|\text{FFN}}(\theta^{\text{ident}}) &= \mathbf{g}^{\text{FFN}}(x).\end{aligned}$$

This is a good example to emphasize the importance of a time-series model. While FFNs are flexible in learning low dimensional functional relationships, they are limited in learning a complex dependency model. For example, the FFN architecture we consider is not sufficiently flexible to learn the FFT transformation and hence has a worse performance on the original time-series compared to frequency-transformed time-series. While Xiaohong Chen and White (1999) have shown that FFNs are “universal approximators” of low-dimensional functional relationships, they also show that FFN can suffer from a curse of dimensionality when capturing complex dependencies between the input. Although the time domain and frequency domain representations of the input are equivalent under the Fourier transform, clearly the time-series model implied by the frequency domain representation allows for a more effective learning of an arbitrage policy. However, the choice of the pre-specified filter limits the time-series patterns that can be exploited. The solution is our data driven filter presented in the next section.

D.3. Convolutional Neural Network with Transformer

Our benchmark machine learning model is a Convolutional Neural Network (CNN) combined with a Transformer. It uses the most advanced state-of-the art machine learning tools tailored to our problem. Convolutional networks are in fact the most successful networks for computer vision, i.e. for pattern detection. Transformers have rapidly become the model of choice for sequence modeling such as Natural Language Processing (NLP) problems, replacing older recurrent neural network models such as the Long Short-Term Memory (LSTM) network.

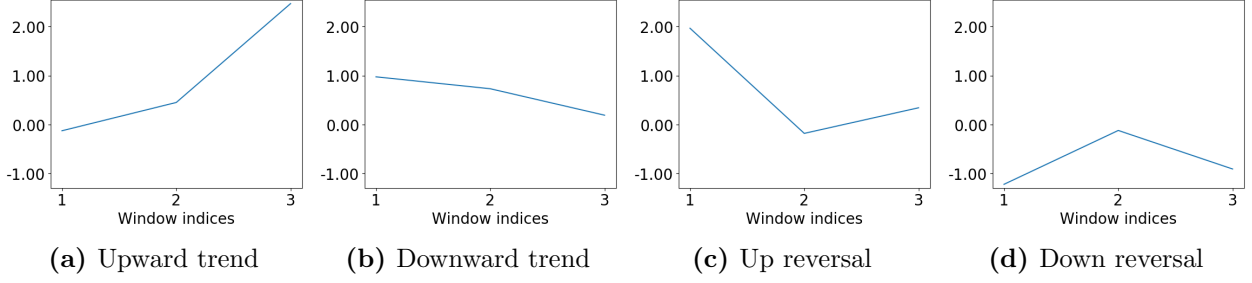
The CNN and transformer framework has two key elements: (1) Local filters and (2) the temporal combination of these local filters. The CNN can be interpreted as a set of data driven flexible local filters. A transformer can be viewed as a data driven flexible time-series model to capture complex dependencies between local patterns. We use the CNN+Transformer to generate the time-series signal. The allocation function is then modeled as a flexible data driven allocation with an FFN.

The CNN estimates D local filters of size D_{size} :

$$y_l^{(0)} = \sum_{m=1}^{D_{\text{size}}} W_m^{(0)} x_{l-m+1}$$

for a matrix $W^{(0)} \in \mathbb{R}^{D_{\text{size}} \times D}$. The local filters are a mapping from $x \in \mathbb{R}^L$ to $y^{(0)} \in \mathbb{R}^{L \times D}$ given by the convolution $y^{(0)} = W^{(0)} * x$. Figure 2 shows examples of these local filters for $D_{\text{size}} = 3$. The values of $y^{(0)}$ can be interpreted as the “loadings” or exposure to local basis patterns. For

Figure 2: Examples of Local Filters



These figures show the most important local filters estimated for the benchmark model in our empirical analysis. These are projections of our higher dimensional nonlinear filter from a 2-layer CNN into two-dimensional linear filters.

example, if x represents a global upward trend, its filtered representation should have mainly large values for the local upward trend filter.

The convolutional mapping can be repeated in multiple layers to obtain a multi-layer CNN. First, the output of the first layer of the CNN is transformed nonlinearly by applying the $\text{ReLU}(\cdot)$ function:

$$x_{l,d}^{(1)} = \text{ReLU} \left(y_{l,d}^{(0)} \right) := \max(y_{l,d}^{(0)}, 0).$$

The second layer is given by a higher dimensional filtering projection:

$$y_{l,d}^{(2)} = \sum_{m=1}^{D_{\text{size}}} \sum_{j=1}^D W_{d,j,m}^{(1)} x_{l-m+1,j}^{(1)},$$

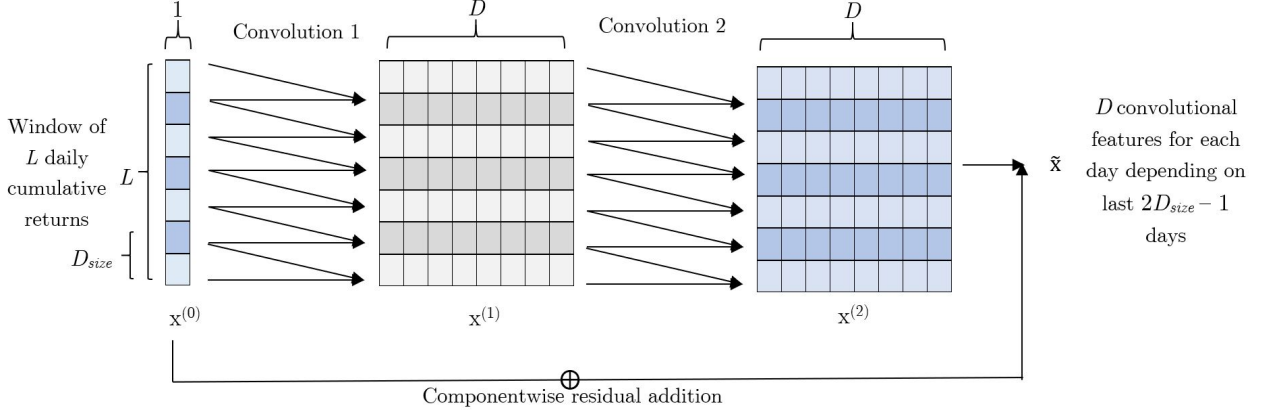
$$x_{l,d}^{(2)} = \text{ReLU} \left(y_{l,d}^{(2)} \right).$$

The final output of the CNN is $\tilde{x} \in \mathbb{R}^{L \times D}$. Our benchmark model is a 2-layered convolutional neural network. The number of layers is a hyperparameter selected on the validation data. Figure 3 illustrates the structure of the 2-layer CNN. While this description captures all the conceptual elements, the actual implementation includes additional details, such as bias terms, instance normalization and residual connection to improve the implementation as explained in Appendix B.C.

For a 1-layer CNN without the final nonlinear transformation, i.e. for a simple local linear filter, the patterns can be visualized by the vectors $W_m^{(0)}$. In our case of a 2-layer CNN the local filter can capture more complex patterns as it applies a 3-dimensional weighting scheme in the array $W^{(1)}$ and nonlinear transformations. In order to visualize the type of patterns, we project the local filter into a simple local linear filter. We want to find the basic patterns that activate only one of the D filters, but none of the others, i.e. we are looking for an orthogonal representation of the projection.⁷

⁷A local filter can be formalized as a mapping from the local D_{size} points of a sequence to the activation of the D filters: $\phi : \mathbb{R}^{D_{\text{size}}} \rightarrow \mathbb{R}^D$. Denote by $e_d \in \mathbb{R}^D$ a vector that is 0 everywhere except for the value 1 at position d , i.e. $e_d = (0 \ \cdots \ 1 \ 0 \ \cdots 0)$. Fundamentally, we want to invert the local filter to obtain $\phi^{-1}(e_d)$ to find the local sequences that only activates filter d . In general, the inverse is a set and not unique. Our example basic patterns in

Figure 3: Convolutional Network Architecture



This figure shows the structure of our convolutional network. The network takes as input a window of L consecutive daily cumulative returns a residual, and outputs D features for each block of D_{size} days. Each of the features is a nonlinear function of the observations in the block, and captures a common pattern.

The example plots for local filters in Figure 2 are projections of our higher dimensional nonlinear filter into two-dimensional linear filters. The examples show some of the most important local filters for our empirical benchmark model. While these projections are of course not complete representations of the nonlinear filters of the CNN, they provide an intuition for the type of patterns which are activated by specific filters. Our 2-layer CNN network has a local window size of $D_{\text{size}} = 2$, but because of the 2-layer structure it captures information from two neighboring points. Hence, the projection on a one-dimensional linear filter has a local window size of three as depicted in Figure 2.

The output of the CNN $\tilde{x} \in \mathbb{R}^{L \times D}$ is used as an input to the transformer. The CNN projection provides a more informative representation of the dynamics than the original time-series as it captures the relative local dependencies between data points. However, by construction the CNN is only a local representation, and we need the transformer network to detect the global patterns. A transformer network is a model of temporal dependencies between local filters. Given the local structure \tilde{x} the transformer estimates the temporal interactions between the L different blocks by computing a “global pattern projection”:

Assume there are H different global patterns. The transformer will calculate projections on these H patterns with the “attention weights”. We first introduce a simplified linear projection model before extending it to the actual transformer. For each of the $i = 1, \dots, H$ patterns we have projections defined by $\alpha_i \in \mathbb{R}^{L \times L}$:

$$h_i^{\text{simple}} = \sum_{j=1}^L \alpha_{i,j} \tilde{x}_j \quad \text{for } i = 1, \dots, H.$$

Figure 2 solve

$$\text{argmin}_{x_{\text{loc},d} \in \mathbb{R}^{D_{\text{size}}}} \|\phi(x_{\text{loc},d}) - e_d\|_2 \quad \text{for } d = 1, \dots, D.$$

The “attention function” $\alpha_i(\cdot, \cdot) \in [0, 1]$ captures dependencies between the last local patterns \tilde{x}_L and the prior local patterns \tilde{x}_j :

$$\alpha_{i,j} = \alpha_i(\tilde{x}_L, \tilde{x}_j) \quad \text{for } i = 1, \dots, H.$$

Each projection h_i^{simple} is called an “attention head”. These attention heads h_i^{simple} could be interpreted as “loadings” or “exposure” for a specific “pattern factor” α_i . For example, a global upward trend can be captured by an attention function that puts weight on subsequent local upward trends. Another example would be sinusoidal mean reversion patterns which would put weights on alternating “curved” local basis patterns. The projection on these weights captures how much a specific time-series \tilde{x} is exposed to this global pattern. Hence, h_i^{simple} measures the exposure to the global pattern i of the time-series \tilde{x} . Each attention head can focus on a specific global pattern, which we then combine to obtain our signal.

The fundamental challenge is to learn attention functions that can model complex dependencies. The crucial innovation in transformers is their modeling of the attention functions α_i and attention heads h_i . In order to deal with the high dimensionality of the problem, transformers consider lower dimensional projections of \tilde{x} into $\mathbb{R}^{D/H}$ and use the lower-dimensional scaled dot product attention mechanism for α_i as explained in Appendix B.C. More specifically, each attention head $h_i \in \mathbb{R}^{L \times D/H}$ is based on⁸ the projected input $\tilde{x}W_i^V$ with $W_i^V \in \mathbb{R}^{D \times D/H}$ and $\alpha_i \in \mathbb{R}^{L \times L}$:

$$h_i = \alpha_i \tilde{x}W_i^V \quad \text{for } i = 1, \dots, H.$$

The projection on all global basis patterns $h \in \mathbb{R}^{L \times D/H}$ is given by a weighted linear combination of the different attention heads

$$h^{\text{proj}} = \begin{pmatrix} h_1 & \dots & h_H \end{pmatrix} W^O$$

with $W^O \in \mathbb{R}^{D \times D}$. This final projection can, for example, model a combination of a global trend and mean reversion patterns. In conclusion, h^{proj} represents the time-series in terms of the H global patterns. This is analogous to a Fourier filter, but without pre-specifying the global patterns a priori. All parts of the CNN+Transformer network, i.e. the local patterns, the attention functions and the projections on global patterns, are estimated from the data.

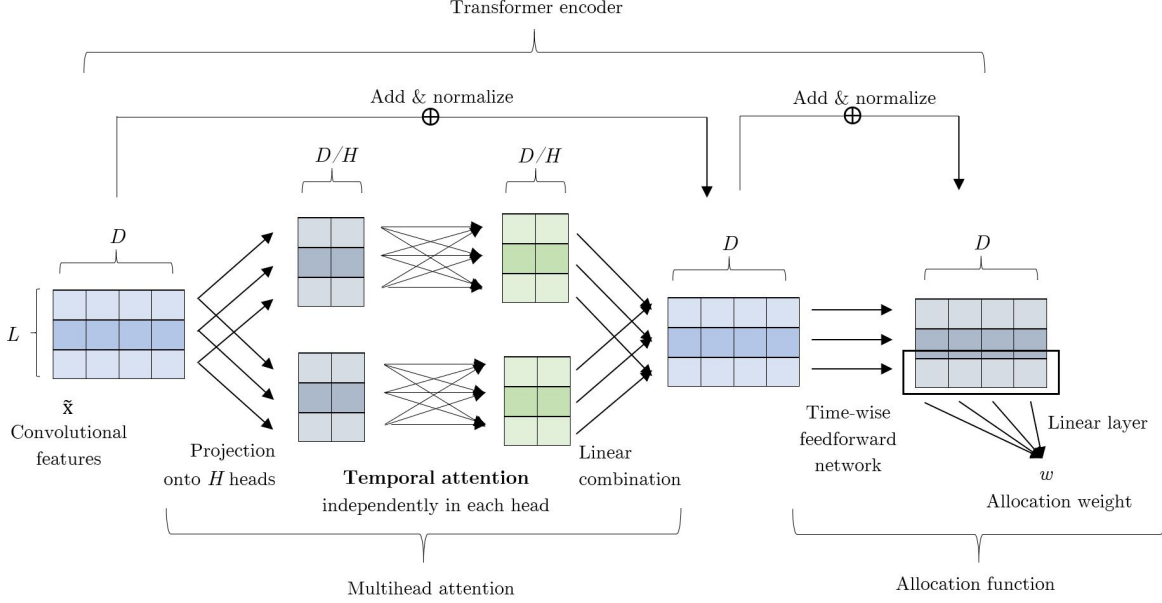
The trading signal $\theta^{\text{CNN+Trans}}$ equals the global pattern projection for the final cumulative return projection⁹ h_L^{proj} :

$$\theta^{\text{CNN+Trans}} = h_L^{\text{proj}} \in \mathbb{R}^H,$$

⁸The actual implementation also includes bias terms which we neglect here for simplicity. The Appendix provides the implementation details.

⁹In principle, we can use the complete matrix $h \in \mathbb{R}^{L \times D}$ as the signal. However, conceptually the global pattern at the end of the time period should be the most relevant for the next realization of the process. We have also implemented a transformer that uses the full matrix, with similar results and the variable importance rankings suggest that only h_L is selected in the allocation function.

Figure 4: Transformer Network Architecture



This figure shows the structure of our transformer network. The model takes as input the matrix $\tilde{x} \in \mathbb{R}^{L \times D}$ that we obtain as output of the convolutional network depicted in Figure 3, which contains D features for each of the L blocks of the original time series. These features are projected onto H attention heads, which capture the global temporal dependency patterns. The projections on these attention heads represent our arbitrage signals, which are the input to the feedforward network that estimates the allocation weight for the residual on the next day.

which is then used as input to a time-wise feedforward network allocation function

$$w^{\epsilon|\text{CNN+Trans}}(\theta^{\text{CNN+Trans}}) = g^{\text{FFN}}(\theta^{\text{CNN+Trans}}).$$

The separation between signal and allocation is not uniquely identified as we use a joint optimization problem. We have chosen a separation that maps naturally into the classical examples considered in the previous subsections. Figure 4 illustrates the transformer network architecture. We have presented a 1-layer transformer network, which is our benchmark model. The transformed data can be used as input in more iterations of the transformer to obtain a multi-layer transformer.

We illustrate the CNN+Transformer model in the first row of Figure A.2 in the Appendix for an empirical residual example. First, it is apparent that the cumulative returns of the strategy in subplot (c) outperforms the previous two models. This is because the allocation weights in subplot (a) capture not only the low frequency reversal patterns, but also the high-frequency cycles and trend components. This also implies that the allocation weights change more frequently to capture the higher frequency components. This more sophisticated allocation function requires a more complex signal as illustrated in subplot (b). Each change in the allocation can be traced back to changes in at least one of the signals. While the signals themselves are hard to interpret, we will leverage the transformer structure to extract interpretable “global dependency factors” in our main analysis. Figure A.3 in the Appendix provides another example to illustrate the differences between the three models. This example has a strong negative trend component with a superimposed mean-

reversion. Only the CNN+Transformer captures both type of patterns.

III. Empirical Analysis

A. Data

We collect daily equity return data for the securities on CRSP from January 1978 through December 2016. We use the first part of the sample to estimate the various factor models, which gives us the residuals for the time period from January 1998 to December 2016 for the arbitrage trading. The arbitrage strategies trade on a daily frequency at the close of each day. We use the daily adjusted returns to account for dividends and splits and the one-month Treasury bill rates from the Kenneth French Data Library as the risk-free rate. In addition, we complement the stock returns with the 46 firm-specific characteristics from Chen et al. (2022), which are listed in Table A.I. All these variables are constructed either from accounting variables from the CRSP/Compustat database or from past returns from CRSP. The full details on the construction of these variables are in the Internet Appendix of Chen et al. (2022).

Our analysis uses only the most liquid stocks in order to avoid trading and market friction issues. More specifically, we consider only the stocks whose market capitalization at the previous month was larger than 0.01% of the total market capitalization at that previous month, which is the same selection criterion as in Kozak et al. (2020). On average this leaves us with approximately the largest 550 stocks, which correspond roughly to the S&P 500 index. This is an unbalanced dataset, as the stocks that we consider each month need not be the same as in the next month, but it is essentially balanced on a daily frequency in rolling windows of up to one year in our trading period from 1998 through 2016. For each stock we have its cross-sectionally centered and rank-transformed characteristics of the previous month. This is a standard transformation to deal with the different scales which is robust to outliers and time-variation, and has also been used in Chen et al. (2022), Kozak et al. (2020), Kelly et al. (2019), and Freyberger et al. (2020).

Our daily residual time-series start in 1998 as we have a large number of missing values in daily individual stock returns prior to this date, but almost no missing daily values in our sample.¹⁰ We want to point out that the time period after 1998 also seems to be more challenging for arbitrage trading or factor trading, and hence our results can be viewed as conservative lower bounds.

B. Factor model estimation

As discussed in Section II.A, we construct the statistical arbitrage portfolios by using the residuals of a general factor model for the daily excess returns of a collection of stocks. In particular, we consider the three empirically most successful families of factor models in our implementation.

¹⁰Of all the stocks that have daily returns observed in a the local lookback window of $L = 30$ days, only 0.1% have a missing return the next day for the out-of-sample trading, in which case we do not trade this stock. Hence, our data set of stocks with market capitalization higher than 0.01% of the total market capitalization, has essentially no missing daily values on a local window for the time period after 1998.

For each family, we conduct a rolling window estimation to obtain daily residuals out of sample from 1998 through 2016. This means that the residual composition matrix Φ_{t-1} of equation (1) depends only on the information up to time $t - 1$, and hence there is no look-ahead bias in trading the residuals. The rolling window estimation is necessary because of the time-variation in risk exposure of individual stocks and the unbalanced nature of a panel of individuals stock returns.

The three classes of factor models consists of pre-specified factors, latent unconditional factors and latent conditional factors:

1. **Fama-French factors:** We consider 1, 3, 5 and 8 factors based on various versions and extensions of the Fama-French factor models and downloaded from the Kenneth French Data Library. We consider them as tradeable assets in our universe. Each model includes the previous one and adds additional characteristic-based risk factors:
 - (a) $K = 1$: CAPM model with the excess return of a market factor
 - (b) $K = 3$: Fama-French 3 factor model includes a market, size and value factor
 - (c) $K = 5$: Fama-French 3 factor model + investment and profitability factors
 - (d) $K = 8$: Fama-French 5 factor model + momentum, short-term reversal and long-term reversal factors.

We estimate the loadings of the individual stock returns daily with a linear regression on the factors with a rolling window on the previous 60 days and compute the residual for the current day out-of-sample. This is the same procedure as in Carhart (1997). At each day we only consider the stocks with no missing observations in the daily returns within the rolling window, which in any window removes at most 2% of the stocks given our market capitalization filter.

2. **PCA factors:** We consider 1, 3, 5, 8, 10, and 15 latent factors, which are estimated daily on a rolling window. At each time $t - 1$, we use the last 252 days, or roughly one trading year, to estimate the correlation matrix from which we extract the PCA factors.¹¹ Then, we use the last 60 days to estimate the loadings on the latent factors using linear regressions, and compute residuals for the current day out-of-sample. At each day we only consider the stocks with no missing observations in the daily returns during the rolling window, which in any window removes at most 2% of the stocks given our market capitalization filter.
3. **IPCA factors:** We consider 1, 3, 5, 8, 10, and 15 factors in the Instrumented PCA (IPCA) model of Kelly et al. (2019). This is a conditional latent factor model, in which the loadings β_{t-1} are a linear function of the asset characteristics at time $t - 1$. As the characteristics change at most each month, we reestimate the IPCA model on rolling window every year using the monthly returns and characteristics of the last 240 months. The IPCA provides the factor weights and loadings for each stock as a function of the stock characteristics. Hence, we do not need to estimate the loadings for individual stocks with an additional time-series regression, but use the loading function and the characteristics at time $t - 1$ to obtain the

¹¹This is the same procedure as in Avellaneda and Lee (2010).

out-of-sample residuals at time t . The other details of the estimation process are carried out in the way outlined in Kelly et al. (2019).

In addition to the factor models above, we also include the excess returns of the individual stocks without projecting out the factors. This “zero-factor model” simply consists of the original excess returns of stocks in our universe and is denoted as $K = 0$. For each factor model, in our empirical analysis we observe that the cumulative residuals exhibit consistent and relatively regular mean-reverting behavior. After taking out sufficiently many factors, the residuals of different stocks are only weakly correlated.

C. Implementation

Given the daily out-of-sample residuals from 1998 through 2016 we estimate the trading signal and policy on a rolling window to obtain the out-of-sample returns of the strategy. For each strategy we calculate the annualized sample mean μ , annualized volatility σ and annualized Sharpe ratio¹² $SR = \frac{\mu}{\sigma}$. The Sharpe ratio represents a risk-adjusted average return. Our main models estimate arbitrage strategies to maximize the Sharpe ratio without transaction costs. In Section III.E we also consider a mean-variance objective and in Section III.J we include transaction costs in the estimation and evaluation.

Our strategies trade the residuals of all stocks, which are mapped back into positions of the original stocks. We use the standard normalization that the absolute values of the individual stock portfolio weights sums up to one, i.e. we use the normalization $\|\omega_{t-1}^R\|_1 = 1$. This normalization implies a leverage constraint as short positions are bounded by one. The trading signal is based on a local lookback window of $L = 30$ days. We show in Section III.I, that the results are robust to this choice and are very comparable for a lookback window of $L = 60$ days. Our main results use a rolling window of 1,000 days to estimate the deep learning models. For computational reasons we re-estimate the network only every 125 days using the previous 1,000 days. Section III.I shows that our results are robust to this choice. Our main results show the out-of-sample trading performance from January 2002 to December 2016 as we use the first four years to estimate the signal and allocation function.

The hyperparameters for the deep learning models are based on the validation results summarized in Appendix C.A. Our benchmark model is a 2-layer CNN with $D = 8$ local convolutional filters and local window size of $D_{size} = 2$ days. The transformer has $H = 4$ attention heads, which can be interpreted as capturing four different global patterns. The results are extremely robust to the choice of hyperparameters. Appendix B.D includes all the technical details for implementing the deep learning models.

¹²We obtain the annualized metrics from the daily returns using the standard calculations $\mu = \frac{252}{T} \sum_{t=1}^T R_t$ and $\sigma = \sqrt{\frac{252}{T} \sum_{t=1}^T (R_t - \mu)^2}$.

Table I: OOS Annualized Performance Based on Sharpe Ratio Objective

Factors		Fama-French			PCA			IPCA		
Model	K	SR	μ	σ	SR	μ	σ	SR	μ	σ
CNN + Trans	0	1.64	13.7%	8.4%	1.64	13.7%	8.4%	1.64	13.7%	8.4%
	1	3.68	7.2%	2.0%	2.74	15.2%	5.5%	3.22	8.7%	2.7%
	3	3.13	5.5%	1.8%	3.56	16.0%	4.5%	3.93	8.6%	2.2%
	5	3.21	4.6%	1.4%	3.36	14.3%	4.2%	4.16	8.7%	2.1%
	8	2.49	3.4%	1.4%	3.02	12.2%	4.0%	3.95	8.2%	2.1%
	10	-	-	-	2.81	10.7%	3.8%	3.97	8.0%	2.0%
	15	-	-	-	2.30	7.6%	3.3%	4.17	8.4%	2.0%
Fourier + FFN	0	0.36	4.9%	13.6%	0.36	4.9%	13.6%	0.36	4.9%	13.6%
	1	0.89	3.2%	3.5%	0.80	8.4%	10.6%	1.24	6.3%	5.0%
	3	1.32	3.5%	2.7%	1.66	11.2%	6.7%	1.77	7.8%	4.4%
	5	1.66	3.1%	1.8%	1.98	12.4%	6.3%	1.90	7.7%	4.1%
	8	1.90	3.1%	1.6%	1.95	10.1%	5.2%	1.94	7.8%	4.0%
	10	-	-	-	1.71	8.2%	4.8%	1.93	7.6%	3.9%
	15	-	-	-	1.14	4.8%	4.2%	2.06	7.9%	3.8%
OU + Thresh	0	-0.18	-2.4%	13.3%	-0.18	-2.4%	13.3%	-0.18	-2.4%	13.3%
	1	0.16	0.6%	3.8%	0.21	2.1%	10.4%	0.60	3.0%	5.1%
	3	0.54	1.6%	3.0%	0.77	5.2%	6.8%	0.88	3.8%	4.3%
	5	0.38	0.9%	2.3%	0.73	4.4%	6.1%	0.97	3.8%	4.0%
	8	1.16	2.8%	2.4%	0.87	4.4%	5.1%	0.91	3.5%	3.8%
	10	-	-	-	0.63	2.9%	4.6%	0.86	3.1%	3.6%
	15	-	-	-	0.62	2.4%	3.8%	0.93	3.2%	3.5%

This table shows the out-of-sample annualized Sharpe ratio (SR), mean return (μ), and volatility (σ) of our three statistical arbitrage models for different numbers of risk factors K , that we use to obtain the residuals. We use the daily out-of-sample residuals from January 1998 to December 2016 and evaluate the out-of-sample arbitrage trading from January 2002 to December 2016. CNN+Trans denotes the convolutional network with transformer model, Fourier+FFN estimates the signal with a FFT and the policy with a feedforward neural network and lastly, OU+Thres is the parametric Ornstein-Uhlenbeck model with thresholding trading policy. The two deep learning models are calibrated on a rolling window of four years and use the Sharpe ratio objective function. The signals are extracted from a rolling window of $L = 30$ days. The $K = 0$ factor model corresponds to directly using stock returns instead of residuals for the signal and trading policy.

D. Main Results

Table I displays the main results for various arbitrage models. It reports the annualized Sharpe ratio, mean return and volatility for our principal deep trading strategy CNN+Transformer and the two benchmark models, Fourier+FFN and OU+Threshold, for every factor model described in Section III.B. The CNN+Transformer model and Fourier+FFN model are estimated with a Sharpe ratio objective. We obtain the daily out-of-sample residuals for different number of factors K for the time period January 1998 to December 2016. The daily returns of the out-of-sample arbitrage trading is then evaluated from January 2002 to December 2016, as we use a rolling window of four years to estimate the deep learning models.

First, we confirm that it is crucial to apply arbitrage trading to residuals and not individual stock returns. The stock returns, denoted as the $K = 0$ model, perform substantially worse than any type of residual within the same model and factor family. This is not surprising as residuals

for an appropriate factor model are expected to be better described by a model that captures mean reversion. Importantly, individual stock returns are highly correlated and a substantial part of the returns is driven by the low dimensional factor component.¹³ Hence, the complex nonparametric models are actually not estimated on many weakly dependent residual time-series, but most time-series have redundant information. In other words, the models are essentially calibrated on only a few factor time-series, which severely limits the structure that can be estimated. However, once we extract around $K = 5$ factors with any of the different factor models, the performance does not substantially increase by adding more factors. This suggests that most of commonality is explained by a small number of factors.

Second, the CNN+Transformer model strongly dominates the other benchmark models in terms of Sharpe ratio and average return. The Sharpe ratio is approximately twice as large as for a comparable Fourier+FFN model and four times higher for the corresponding parametric OU+Threshold model. Using IPCA residuals, the CNN+Transformer achieves the impressive out-of-sample Sharpe ratio of around 4, in spite of trading only the most liquid large cap stocks and the time period after 2002. The mean returns of the CNN+Transformer are similar to the Fourier+FFN model, but have substantially smaller volatilities, which results in the higher Sharpe ratios. The parametric mean-reversion model achieves positive mean returns with Sharpe ratios close to one for the IPCA residuals, but as expected is too restrictive relative to the flexible models. The Fourier+FFN has the same flexibility as the CNN+Transformer in its allocation function, but is restricted to a pre-specified signal structure. The difference in performance quantifies the importance of extracting the complex time-series signals.

Third, the average return of the arbitrage strategies is large in spite of the leverage constraints. Normalizing the individual stock weights w_{t-1}^R so sum up in absolute value to one limits the short-selling. The CNN+Transformer with a five-factor PCA residual achieves an attractive annual mean return of around 14%. This means that the strategies do not require an infeasible amount of leverage to yield an average return that might be required by investors. In other words, the high Sharpe ratios are not the results of vanishing volatility but a combination of high average returns with moderate volatility.

Fourth, the arbitrage strategies are qualitatively robust to the choice of factor models to obtain residuals. The Fama-French and PCA factor lead to very similar Sharpe ratio results, suggesting that they explain a similar amount of co-movement in the data. However, as the mean returns of PCA factors are usually higher than the mean returns of the Fama-French factors, the risk factors are different. This confirms the findings of Pelger (2020) and Lettau and Pelger (2020b), who show that PCA factors do not coincide with Fama-French type factors and explain different mean returns. The IPCA factors use the additional firm-specific characteristic information. The resulting residuals achieve the highest Sharpe ratios, which illustrates that conditional factor models can capture more information than unconditional models. Including the momentum and reversal

¹³Pelger (2020) shows that around one third of the individual stock returns is explained by a latent four-factor model.

Table II: Significance of Arbitrage Alphas based on Sharpe Ratio Objective

CNN+Trans model															
K	Fama-French					PCA					IPCA				
	α	t_α	R^2	μ	t_μ	α	t_α	R^2	μ	t_μ	α	t_α	R^2	μ	t_μ
0	11.6%	6.4***	30.3%	13.7%	6.3***	11.6%	6.4***	30.3%	13.7%	6.3***	11.6%	6.4***	30.3%	13.7%	6.3***
1	7.0%	14***	2.4%	7.2%	14***	14.9%	10***	0.6%	15.2%	11***	8.1%	12***	9.5%	8.7%	12***
3	5.5%	12***	1.2%	5.5%	12***	15.8%	14***	1.7%	16.0%	14***	8.2%	15***	6.0%	8.6%	15***
5	4.5%	12***	2.3%	4.6%	12***	14.1%	13***	1.3%	14.3%	13***	8.3%	16***	3.9%	8.7%	16***
8	3.3%	9.4***	2.1%	3.4%	9.6***	12.0%	12***	0.9%	12.2%	12***	7.8%	15***	5.0%	8.2%	15***
10	-	-	-	-	-	10.5%	11***	0.7%	10.7%	11***	7.7%	15***	4.0%	8.0%	15***
15	-	-	-	-	-	7.5%	8.8***	0.5%	7.6%	8.9***	8.1%	16***	4.2%	8.4%	16***

Fourier+FFN model															
K	Fama-French					PCA					IPCA				
	α	t_α	R^2	μ	t_μ	α	t_α	R^2	μ	t_μ	α	t_α	R^2	μ	t_μ
0	2.7%	0.8	8.6%	4.9%	1.4	2.7%	0.8	8.6%	4.9%	1.4	2.7%	0.8	8.6%	4.9%	1.4
1	3.0%	3.3**	3.3%	3.2%	3.5***	7.4%	2.7**	3.3%	8.4%	3.1**	4.8%	4.0***	16.4%	6.3%	4.8***
3	3.2%	4.7***	4.2%	3.5%	5.1***	10.9%	6.3***	2.2%	11.2%	6.4***	6.8%	6.4***	13.0%	7.8%	6.9***
5	2.9%	6.1***	3.5%	3.1%	6.4***	12.1%	7.5***	1.5%	12.4%	7.6***	6.7%	6.9***	13.3%	7.7%	7.4***
8	3.0%	7.2***	3.2%	3.1%	7.4***	10.0%	7.5***	0.9%	10.1%	7.6***	6.8%	7.0***	13.3%	7.8%	7.5***
10	-	-	-	-	-	8.0%	6.5***	1.0%	8.2%	6.6***	6.8%	7.1***	12.7%	7.6%	7.3***
15	-	-	-	-	-	4.7%	4.3***	0.4%	4.8%	4.4***	7.1%	7.6***	12.2%	7.9%	8.0***

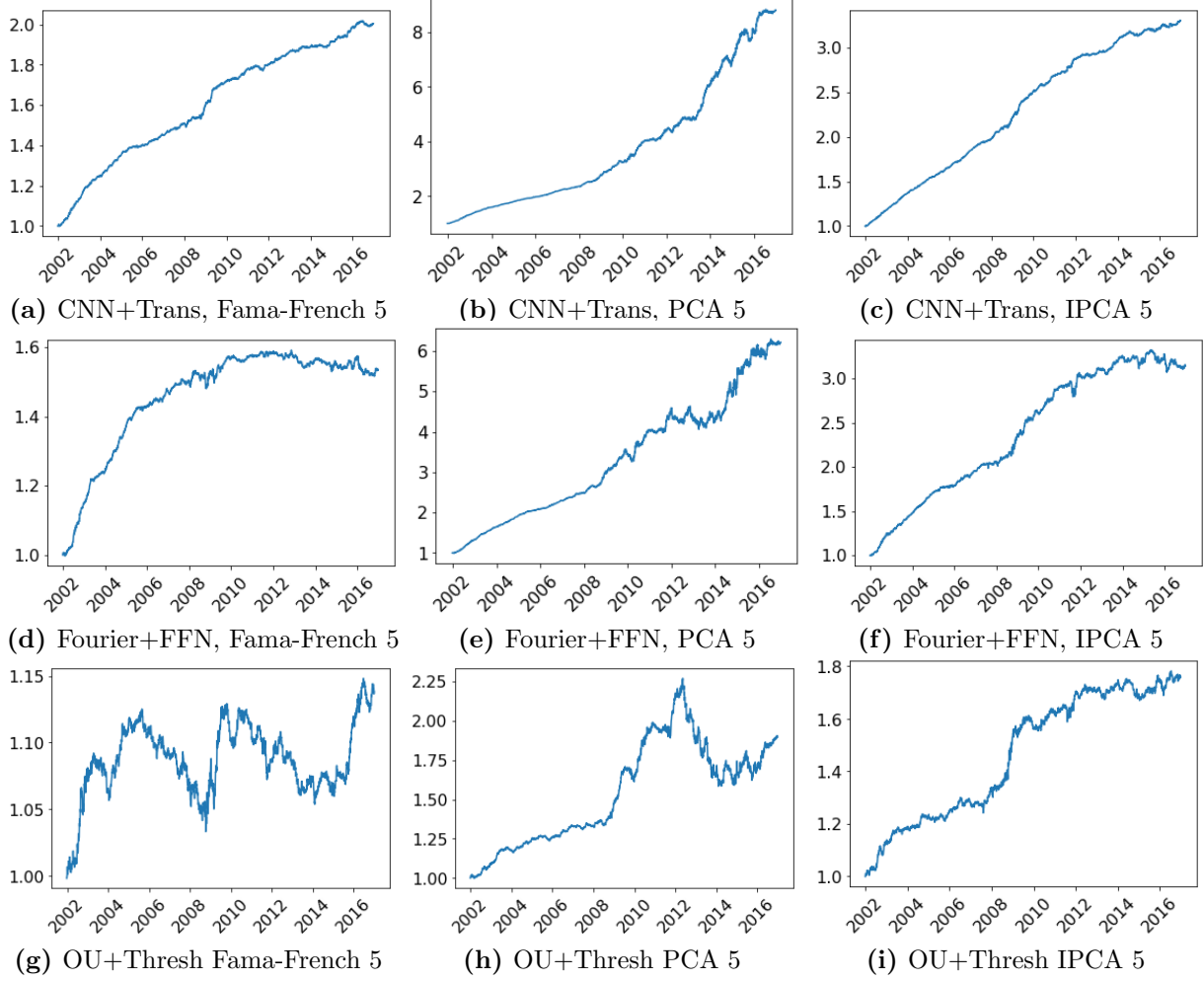
OU+Thresh model															
K	Fama-French					PCA					IPCA				
	α	t_α	R^2	μ	t_μ	α	t_α	R^2	μ	t_μ	α	t_α	R^2	μ	t_μ
0	-4.5%	-1.4	13.4%	-2.4%	-0.7	-4.5%	-1.4	13.4%	-2.4%	-0.7	-4.5%	-1.4	13.4%	-2.4%	-0.7
1	-0.2%	-0.2	13.5%	0.6%	0.6	0.7%	0.3	6.3%	2.1%	0.8	1.7%	1.4	18.9%	3.0%	2.3*
3	0.9%	1.2	10.4%	1.6%	2.1*	4.3%	2.5*	4.3%	5.2%	3.0**	2.6%	2.6**	18.8%	3.8%	3.4***
5	0.5%	0.9	6.8%	0.9%	1.5	3.7%	2.4*	3.2%	4.4%	2.8**	2.8%	3.0**	17.7%	3.8%	3.8***
8	0.6%	1.2	5.5%	1.0%	1.9	3.9%	3.0**	1.9%	4.4%	3.4***	2.3%	2.6**	17.6%	3.5%	3.6***
10	-	-	-	-	-	2.6%	2.2*	1.4%	2.9%	2.4*	2.1%	2.5*	17.6%	3.1%	3.3***
15	-	-	-	-	-	2.1%	2.1*	0.7%	2.4%	2.4*	2.3%	2.8**	18.1%	3.2%	3.6***

This table shows the out-of-sample pricing errors α of the arbitrage strategies relative of the Fama-French 8 factor model and their mean returns μ for the different arbitrage models and different number of factors K that we use to obtain the residuals. We run a time-series regression of the out-of-sample returns of the arbitrage strategies on the 8-factor model (Fama-French 5 factors + momentum + short-term reversal + long-term reversal) and report the annualized α , accompanying t-statistic value t_α , and the R^2 of the regression. In addition, we report the annualized mean return μ along with its accompanying t-statistic t_μ . The hypothesis test are two-sided and stars indicate p-values of 5% (*), 1% (**), and 0.1% (***). All results use the out-of-sample daily returns from January 2002 to December 2016 and the deep learning models are based on a Sharpe ratio objective.

factors in the Fama-French 8 factor models to obtain residuals still results in profitable arbitrage strategies. Hence, the arbitrage strategies are not simply capturing a conventional price trend risk premium.

The returns of the CNN+Transformer arbitrage strategies are statistically significant and not subsumed by conventional risk factors. Table II reports the out-of-sample pricing errors α of the arbitrage strategies relative of the Fama-French 8 factor model and their mean returns μ . We run a time-series regression of the out-of-sample returns of the arbitrage strategies on the 8-factor model (Fama-French 5 factors + momentum + short-term reversal + long-term reversal) and report the annualized α , accompanying t-statistic value t_α , and the R^2 of the regression. In addition, we report the annualized mean return μ along with its accompanying t-statistic t_μ . The arbitrage strategies

Figure 5. Cumulative OOS Returns of Different Arbitrage Strategies



These figures show the cumulative daily returns of the arbitrage strategies for our representative models on the out-of-sample trading period between January 2002 and December 2016. We estimate the optimal arbitrage trading strategies for our three benchmark models based on the out-of-sample residuals of the Fama-French, PCA and IPCA 5-factor models. The deep learning models use the Sharpe ratio objective.

for the CNN+Transformer model for $K \geq 1$ are all statistically significant and not explained by the Fama-French 5 factors or price trend factors. Importantly, the pricing errors are essentially as large as the mean returns, which implies that the returns of the CNN+Transformer arbitrage strategies do not carry any risk premium of these eight factors. This is supported by the R^2 values, which are close to zero for the Fama-French or PCA residuals, and hence confirm that these arbitrage portfolios are essentially orthogonal to the Fama-French 8 factors. In contrast, one third of the individual return variation for $K = 0$ is explained by those risk factors. However, even in that case the pricing errors are significant. The residuals of IPCA factors have a higher correlation with the Fama-French 8 factors, suggesting that the conditional IPCA factor model extracts factors that are inherently different from the conventional risk factors. Note that the residuals of a Fama-French 8 factor model are not mechanically orthogonal in the time-series regression on the Fama-French 8

factors, as we construct out-of-sample residuals based on rolling window estimates. The parametric arbitrage strategies are largely explained by conventional risk factors. The third subtable in Table II shows that the residuals of the OU+Threshold model for Fama-French or PCA residuals do not have statistically significant pricing errors on a 1% level.

The CNN+Transformer has a consistent out-of-sample performance and is not affected by various negative events. Figure 5 shows the cumulative out-of-sample returns of the arbitrage strategies for our representative models. We select the residuals of the various five-factor models as including additional factors has only minor effects on the performance. Note that the CNN+Transformer model has consistently almost always positive returns, while maintaining a low volatility and avoiding any large losses. Importantly, the performance of the CNN+Transformer is nearly completely immune to both the “quant quake” which affected quantitative trading groups and funds engaging in statistical arbitrage in August 2007 (Barr (2007)), and the period of poor performance in quant funds during 2011–2012 (Ebrahimi (2013)). The Fourier+FFN model also performs similarly well until the financial crisis, but its risk increases afterwards as displayed by the larger volatility and larger drawdowns. The performance of the parametric model is visibly inferior. This illustrates that although all strategies trade the same residuals, which should be orthogonal to common market risk, profitable arbitrage trading requires an appropriate signal and allocation policy.

E. Mean-Variance Objective

The deep learning statistical arbitrage strategies can achieve high average returns in spite of leverage constraints. Our main deep learning models are estimated with a Sharpe ratio objective. As the sum of absolute stock weights is normalized to one, the arbitrage strategies impose an implicit leverage constraint. We show that the average return can be increased while maintaining this leverage constraint. For this purpose we change the objective for the deep learning model to a mean-variance objective. In order to illustrate the effect of the different objective function, we set the risk aversion parameter to $\gamma = 1$.

Tables III and IV collect the results for the Sharpe ratio, mean, volatility and significance tests. As expected the Sharpe ratios are slightly lower compared to the corresponding model with Sharpe ratio objective, but the mean returns are substantially increased. The CNN+Transformer model achieves average annual returns around 20% with PCA and IPCA residuals while the volatility is only around half as large as the one of a market portfolio. The mean returns are statistically highly significant and not spanned by conventional risk factors or a price trend risk premium. The Fourier+FFN model can also obtain high average returns, but those come at the cost of a higher volatility. Overall, we confirm that the more flexible signal extraction function of the CNN+Transformer is crucial for the superior performance.

F. Unconditional Residual Means

The unconditional average of residuals is not a profitable strategy and does not provide information about the potential arbitrage profitability contained in the residuals. A natural question to

Table III: OOS Annualized Performance Based on Mean-Variance Objective

CNN+Trans strategy, mean-variance objective function										
K	Fama-French			PCA			IPCA			
	SR	μ	σ	SR	μ	σ	SR	μ	σ	
0	0.83	9.5%	11.4%	0.83	9.5%	11.4%	0.83	9.5%	11.4%	
1	3.15	10.5%	3.3%	2.21	27.3%	12.3%	2.83	15.9%	5.6%	
3	2.95	7.8%	2.6%	2.38	22.6%	9.5%	3.13	17.9%	5.7%	
5	3.03	5.9%	2.0%	2.75	19.6%	7.1%	3.21	18.2%	5.7%	
8	2.96	4.2%	1.4%	2.68	16.6%	6.2%	3.18	17.0%	5.4%	
10	-	-	-	2.67	15.3%	5.7%	3.21	16.6%	5.2%	
15	-	-	-	2.20	8.7%	4.0%	3.34	16.3%	4.9%	

Fourier+FFN strategy, mean-variance objective function										
K	Fama-French			PCA			IPCA			
	SR	μ	σ	SR	μ	σ	SR	μ	σ	
0	0.28	5.5%	19.3%	0.28	5.5%	19.3%	0.28	5.5%	19.3%	
1	0.38	2.5%	6.7%	0.48	16.6%	34.8%	0.56	9.7%	17.2%	
3	1.16	4.3%	3.7%	0.34	32.1%	93.1%	1.06	17.6%	16.7%	
5	1.30	3.1%	2.4%	0.37	22.5%	61.2%	1.17	17.0%	14.5%	
8	1.73	3.6%	2.0%	0.67	17.4%	25.9%	1.21	14.4%	11.9%	
10	-	-	-	0.45	7.4%	16.4%	1.06	12.6%	11.9%	
15	-	-	-	0.56	5.7%	10.2%	1.17	12.1%	10.4%	

This table shows the out-of-sample annualized Sharpe ratio (SR), mean return (μ), and volatility (σ) of our CNN+Transformer and Fourier+FFN models for different numbers of risk factors K , that we use to obtain the residuals. We use a mean-variance objective function with risk aversion $\gamma = 1$. We use the daily out-of-sample residuals from January 1998 to December 2016 and evaluate the out-of-sample arbitrage trading from January 2002 to December 2016. The two deep learning models are calibrated on a rolling window of four years. The signals are extracted from a rolling window of $L = 30$ days. The $K = 0$ factor model corresponds to directly using stock returns instead of residuals for the signal and trading policy.

ask is if the residuals themselves have a risk premium component and if trading an equally weighted portfolio of residuals could be profitable. Table A.VI in the Appendix shows the performance of this simple strategy. If we do not project out any factors ($K = 0$), this strategy essentially trades an equally weighted market portfolio. Table A.VII in the Appendix reports the test statistics relative to the Fama-French 8 factor model, which completely subsumes the market risk premium. Once we regress out at least 3 factors, the equally weighted residuals have a mean return of around 1% or lower. The low volatility confirms that the residuals are only weakly cross-sectionally dependent and are largely diversified away. The moderately large Sharpe ratios for PCA residuals is a consequence of the near zero volatility. Scaling up the mean returns to a meaningful magnitude would potentially require an unreasonable amount of leverage. Overall, we confirm that residuals need to be combined with a signal and trading policy that takes advantage of the time series patterns in order to achieve a profitable strategy.

IPCA factors are close to uncorrelated with conventional risk factors. The R^2 values in Table A.VII are as expected for the Fama-French factors and, not surprisingly, after regressing out all of those factors, the cross-sectional average of the residuals is essentially orthogonal to those factors. The PCA residuals show a very similar behavior. However, the conditional IPCA model leaves a

Table IV: Significance of Arbitrage Alphas based on Mean-Variance Objective

CNN+Trans model															
K	Fama-French					PCA					IPCA				
	α	t_α	R^2	μ	t_μ	α	t_α	R^2	μ	t_μ	α	t_α	R^2	μ	t_μ
0	5.8%	2.2*	19.6%	9.5%	3.2**	5.8%	2.2*	19.6%	9.5%	3.2**	5.8%	2.2*	19.6%	9.5%	3.2**
1	9.9%	12***	7.1%	10.5%	12***	26.3%	8.3***	1.6%	27.3%	8.6***	14.0%	11***	23.5%	15.9%	11***
3	7.5%	11***	5.3%	7.8%	11***	22.1%	9.1***	2.2%	22.6%	9.2***	16.6%	12***	17.6%	17.9%	12***
5	5.7%	11***	5.3%	5.9%	12***	19.0%	10***	3.2%	19.6%	11***	16.7%	12***	16.0%	18.2%	12***
8	4.4%	9.8***	3.6%	4.6%	10***	16.3%	10***	1.6%	16.6%	10***	15.5%	12***	18.3%	17.0%	12***
10	-	-	-	-	-	14.8%	10***	1.7%	15.3%	10***	15.2%	13***	20.6%	16.6%	12***
15	-	-	-	-	-	8.5%	8.4***	0.9%	8.7%	8.5***	14.8%	13***	21.6%	16.3%	13***

Fourier+FFN model															
K	Fama-French					PCA					IPCA				
	α	t_α	R^2	μ	t_μ	α	t_α	R^2	μ	t_μ	α	t_α	R^2	μ	t_μ
0	3.2%	0.7	8.4%	5.5%	1.1	3.2%	0.7	8.4%	5.5%	1.1	3.2%	0.7	8.4%	5.5%	1.1
1	2.8%	1.6	1.8%	2.5%	1.5	15.4%	1.7	1.3%	16.6%	1.9	7.9%	1.8	2.6%	9.7%	2.2*
3	4.1%	4.4***	3.4%	4.3%	4.5***	30.3%	1.3	0.1%	32.1%	1.3	17.4%	4.1***	1.9%	17.6%	4.1***
5	2.9%	4.8***	3.1%	3.1%	5.0***	21.0%	1.3	0.1%	22.5%	1.4	15.9%	4.3***	2.6%	17.0%	4.5***
8	3.5%	6.8***	2.3%	3.6%	7.0***	17.4%	2.6**	0.3%	17.2%	2.6**	12.9%	4.3***	4.4%	14.4%	4.7***
10	-	-	-	-	-	7.1%	1.7	0.3%	7.4%	1.8	11.7%	3.9***	3.5%	12.6%	4.1***
15	-	-	-	-	-	5.5%	2.1*	0.1%	5.7%	2.2*	11.3%	4.3***	4.0%	12.1%	4.5***

This table shows the out-of-sample pricing errors α of the arbitrage strategies relative of the Fama-French 8 factor model and their mean returns μ for the different arbitrage models and different number of factors K that we use to obtain the residuals. We use a mean-variance objective function with risk aversion $\gamma = 1$. We run a time-series regression of the out-of-sample returns of the arbitrage strategies on the 8-factor model (Fama-French 5 factors + momentum + short-term reversal + long-term reversal) and report the annualized α , accompanying t-statistic value t_α , and the R^2 of the regression. In addition, we report the annualized mean return μ along with its accompanying t-statistic t_μ . The hypothesis test are two-sided and stars indicate p-values of 5% (*), 1% (**), and 0.1% (***). All results use the out-of-sample daily returns from January 2002 to December 2016.

component in the residuals that it is highly correlated with conventional risk factors. In this sense, the IPCA factors extract a factor model that is quite different from the Fama-French factors.

Importantly, unconditional means and alphas of asset pricing residuals are a poor measure of arbitrage opportunities. The mean and alphas of residuals that are optimally traded based on their time series patterns have mean returns that can be larger by a factor of 50. This implies more generally, that the unconditional perspective of evaluating asset pricing models could potentially overstate the efficiency of markets and the pricing ability of asset pricing models.

G. Importance of Time-Series Signal

How important is the flexibility in the signal extraction function relative to the allocation function? So far, we have considered a rigid parametric model for the signal and allocation function and a flexible allocation function but either a pre-specified time-series filter or a data-driven flexible filter. In A.IX in Appendix we also report the results for two additional model variations, which serve as ablation tests emphasizing the central importance of applying a time-series model to extract a signal extraction function from the data.

The first model, OU+FFN, uses the same 4-dimensional OU signal as the OU+Threshold policy, but replaces the threshold allocation function with an FFN allocation function. This FFN

allocation function has the same architecture as that of the Fourier+FFN policy, except the input is 4-dimensional instead of 30-dimensional. The results show that even despite using a very flexible allocation function, the results are similar or even worse than the simple parametric thresholding rule. This points to the weakness of the OU signal representation: although the allocation function is a powerful universal approximator, it cannot accomplish much with an information-poor input. If the optimal allocation function given the simple OU signal is well approximated by the parametric thresholding rule, then the nonparametric FFN offers too much flexibility without comparable efficiency, which leads to a noisier estimate of a simple function and hence worse out-of-sample performance.

The second model does not extract a time-series signal from the residuals, but uses the residuals themselves as signal to a flexible FFN allocation function. As the allocation function uses the same type of network as for the CNN+Transformer, Fourier+FFN or OU+FFN, this setup directly assesses the relevance of using a time-series model for the signal. The FFN model also performs worse than the deep learning models that apply a time-series filter to the residuals. This is a good example to emphasize the importance of a time-series model. While FFNs are flexible in learning low dimensional functional relationships, they are limited in learning a complex dependency model if the training data is limited. For example, the FFN is not sufficiently efficient to learn an FFT-like transformation and hence has a substantially worse performance on the original time-series compared to frequency-transformed time-series.

In summary, the flexible data-driven signal extraction function of the CNN+Transformer model seems to be the critical element for statistical arbitrage. A flexible allocation function is not sufficient to compensate for an uninformative signal.

H. Dependency between Arbitrage Strategies

The trading strategies for different factor models are only weakly correlated. In Table A.VIII, we report the correlations of the returns of our CNN+Transformer strategies across factor models with 3, 5, and 10 factors, based on the Sharpe ratio objective function strategy.¹⁴ Notably, the correlations between strategies from different factor model families range from roughly 0.2 to 0.45, indicating that strategies for different factor model families can be used as part of a diversification strategy. While the performance of the arbitrage trading for the residuals obtained with different families of factor models is comparable, the factors themselves are different. Hence, even if the arbitrage signal and allocation functions are similar, the resulting strategies can be weakly correlated. The within-family correlations range from 0.4 to 0.85, indicating that the residuals from the same class of factor model capture similar patterns.

¹⁴The correlations for the mean-variance objective function are similar.

Table V: OOS Annualized Performance of CNN+Trans for 60 Days Lookback Window

	Fama-French			PCA			IPCA		
K	SR	μ	σ	SR	μ	σ	SR	μ	σ
0	1.50	13.5%	9.0%	1.50	13.5%	9.0%	1.50	13.5%	9.0%
1	2.95	9.6%	3.2%	2.68	15.8%	5.9%	3.14	8.8%	2.8%
3	3.21	8.7%	2.7%	3.49	16.8%	4.8%	3.84	9.6%	2.5%
5	3.23	6.8%	2.1%	3.54	16.0%	4.5%	3.90	9.2%	2.4%
8	2.96	4.2%	1.4%	3.02	12.5%	4.2%	3.93	8.7%	2.2%
10	-	-	-	2.67	9.9%	3.7%	3.98	9.2%	2.3%
15	-	-	-	2.36	8.1%	3.4%	4.24	9.6%	2.3%

This table shows the out-of-sample annualized Sharpe ratio (SR), mean return (μ), and volatility (σ) of the CNN+Transformer model for different numbers of risk factors K , that we use to obtain the residuals. The signals are extracted from a rolling window of $L = 60$ days. We use the daily out-of-sample residuals from January 1998 to December 2016 and evaluate the out-of-sample arbitrage trading from January 2002 to December 2016. The model is calibrated on a rolling window of four years and uses the Sharpe ratio objective function. The $K = 0$ factor model corresponds to directly using stock returns instead of residuals for the signal and trading policy.

I. Stability over Time

Our results are robust to length of the local window to extract the trading signal. We re-estimate the CNN+Transformer model on an extended rolling lookback window of $L = 60$ days, while keeping the rest of the model structure the same. Tables V and VI show that the results are robust to the choice of lookback window. Extending the local window to 60 trading days, which is close to three months, leads to essentially the same performance as using only the most recent $L = 30$ trading days to infer the signal. This is further evidence that the arbitrage signal is different from conventional momentum or reversal strategies that incorporate information from longer time periods. As the signal can be inferred from the most recent past, it implies that either the arbitrage signal depends only on the most recent days or that those days are sufficient to infer the relevant time-series structure. In the next section, we provide evidence that the arbitrage trading signals put strong emphasis on most recent two weeks prior to the trading.

A constant-in-time signal and allocation function captures a large fraction of the arbitrage information. We re-estimate the CNN+Transformer model with a constant model instead of the rolling window calibration. Our main models are estimated on a rolling window of four years, which allows the models to adopt to changing economic conditions. Here we use either the first $T_{\text{train}} = 4$ years (1,000 trading days) or $T_{\text{train}} = 8$ years (2,000 trading days) to estimate the signal and allocation function, and then keep those functions constant for the remaining out-of-sample trading period. The results are reported in Tables VII and VIII. As expected the performance decreases relative to a time-varying model with re-estimation, which suggests that there is some degree of time-variation in the signal and allocation function. The longer training window of 8 years results in slightly higher Sharpe ratios than the 4 year window, as the model has more data and more variety in the market environment to learn the arbitrage information. Importantly, the constant CNN+Transformer still substantially outperforms the other benchmark models, Fourier+FFN and OU+Threshold, even if those are estimated on a rolling window. We conclude that the constant signal and allocation

Table VI: Significance of Arbitrage Alphas for 60 Days Lookback Window

CNN+Trans Model , Sharpe objective function, $L = 60$ days lookback window															
K	Fama-French					PCA					IPCA				
	α	t_α	R^2	μ	t_μ	α	t_α	R^2	μ	t_μ	α	t_α	R^2	μ	t_μ
0	11.8%	5.6***	19.5%	13.5%	5.8***	11.8%	5.6***	19.5%	13.5%	5.8***	11.8%	5.6***	19.5%	13.5%	5.8***
1	9.1%	11***	7.2%	9.6%	11***	15.5%	10***	1.2%	15.8%	10***	8.2%	12***	10.1%	8.8%	12***
3	8.3%	12***	7.1%	8.7%	12***	16.5%	13***	2.5%	16.8%	14***	9.2%	15***	9.3%	9.6%	15***
5	6.5%	12***	6.0%	6.8%	13***	15.6%	13***	2.2%	16.0%	14***	8.8%	15***	10.3%	9.2%	15***
8	4.1%	11***	3.2%	4.2%	11***	12.2%	11***	1.6%	12.5%	12***	8.3%	15***	8.9%	8.7%	15***
10	-	-	-	-	-	9.7%	10***	1.0%	9.9%	10***	8.8%	15***	8.3%	9.2%	15***
15	-	-	-	-	-	8.1%	9.1***	0.7%	8.1%	9.1***	9.2%	16***	9.3%	9.6%	16***

This table shows the out-of-sample pricing errors α of the arbitrage strategies relative of the Fama-French 8 factor model and their mean returns μ for the CNN+Transformer model and different number of factors K that we use to obtain the residuals. The signals are extracted from a rolling window of $L = 60$ days. We run a time-series regression of the out-of-sample returns of the arbitrage strategies on the 8-factor model (Fama-French 5 factors + momentum + short-term reversal + long-term reversal) and report the annualized α , accompanying t-statistic value t_α , and the R^2 of the regression. In addition, we report the annualized mean return μ along with its accompanying t-statistic t_μ . The hypothesis test are two-sided and stars indicate p-values of 5% (*), 1% (**), and 0.1% (***). All results use the out-of-sample daily returns from January 2002 to December 2016 and are based on a Sharpe ratio objective.

Table VII: OOS Annualized Performance of CNN+Trans for Constant Model

$T_{\text{train}} = 4 \text{ years}$										
K	Fama-French			PCA			IPCA			
	SR	μ	σ	SR	μ	σ	SR	μ	σ	
0	1.10	8.5%	7.8%	1.10	8.5%	7.8%	1.10	8.5%	7.8%	
1	1.90	4.5%	2.3%	0.66	5.2%	7.9%	0.94	3.1%	3.3%	
3	1.60	3.6%	2.2%	1.65	8.7%	5.3%	1.82	5.3%	2.9%	
5	1.81	3.0%	1.7%	1.93	9.8%	5.1%	2.09	5.4%	2.6%	
8	1.70	2.5%	1.5%	2.04	9.6%	4.7%	1.89	5.0%	2.6%	
10	-	-	-	2.06	9.1%	4.4%	1.77	4.7%	2.7%	
15	-	-	-	1.82	7.0%	3.9%	2.09	5.5%	2.7%	

$T_{\text{train}} = 8 \text{ years}$										
K	Fama-French			PCA			IPCA			
	SR	μ	σ	SR	μ	σ	SR	μ	σ	
0	1.33	12.0%	9.0%	1.33	12.0%	9.0%	1.33	12.0%	9.0%	
1	2.06	5.0%	2.4%	1.81	15.2%	8.4%	2.02	8.5%	4.2%	
3	2.46	5.3%	2.2%	2.04	13.1%	6.4%	2.47	7.5%	3.0%	
5	1.82	3.2%	1.8%	1.91	11.9%	6.2%	2.64	7.6%	2.9%	
8	1.48	2.5%	1.7%	1.89	10.8%	5.7%	2.71	8.3%	3.1%	
10	-	-	-	1.82	10.0%	5.5%	2.68	8.2%	3.1%	
15	-	-	-	1.38	6.2%	4.5%	2.70	7.8%	2.9%	

This table shows the out-of-sample annualized Sharpe ratio (SR), mean return (μ), and volatility (σ) of the CNN+Transformer model for different numbers of risk factors K . We estimate the model on only once on the first T_{train} days and keep it constant on the remaining test set. We use the daily out-of-sample residuals from January 1998 to December 2016 and evaluate the out-of-sample arbitrage trading from January 1998 + T_{train} to December 2016. The signals are extracted from a rolling window of $L = 30$ days and we use the Sharpe ratio objective function.

function for the CNN+Transformer model already capture a substantial amount of arbitrage information. Therefore, the constant functions serve as a meaningful model to analyze in more detail

Table VIII: Significance of Arbitrage Alphas for Constant Model

CNN+Trans model, Sharpe objective function, $T_{\text{train}} = 4$ years															
K	Fama-French					PCA					IPCA				
	α	t_α	R^2	μ	t_μ	α	t_α	R^2	μ	t_μ	α	t_α	R^2	μ	t_μ
0	8.4%	4.2***	3.0%	8.5%	4.3***	8.4%	4.2***	3.0%	8.5%	4.3***	8.4%	4.2***	3.0%	8.5%	4.3***
1	4.0%	6.8***	5.9%	4.5%	7.3***	4.1%	2.0*	4.5%	5.2%	2.5*	3.1%	3.7***	1.6%	3.1%	3.6***
3	3.2%	5.7***	4.9%	3.6%	6.2***	8.2%	6.1***	2.7%	8.7%	6.4***	5.3%	7.4***	11.7%	5.3%	7.0***
5	2.8%	6.6***	4.3%	3.0%	7.0***	9.3%	7.1***	1.8%	9.8%	7.5***	5.5%	8.6***	8.3%	5.4%	8.1***
8	2.3%	6.1***	5.1%	2.5%	6.6***	9.0%	7.5***	2.2%	9.6%	7.9***	5.0%	7.7***	8.2%	5.0%	7.3***
10	-	-	-	-	-	8.6%	7.5***	1.9%	9.1%	8.0***	5.1%	8.0***	16.6%	4.7%	6.9***
15	-	-	-	-	-	6.8%	6.8***	1.0%	7.0%	7.1***	5.8%	9.3***	17.6%	5.5%	8.1***

CNN+Trans model, Sharpe objective function, $T_{\text{train}} = 8$ years															
K	Fama-French					PCA					IPCA				
	α	t_α	R^2	μ	t_μ	α	t_α	R^2	μ	t_μ	α	t_α	R^2	μ	t_μ
0	10.1%	4.1***	18.1%	12.0%	4.4***	10.1%	4.1***	18.1%	12.0%	4.4***	10.1%	4.1***	18.1%	12.0%	4.4***
1	4.4%	6.5***	14.3%	5.0%	6.8***	14.5%	5.8***	2.5%	15.2%	6.0***	7.0%	6.6***	30.6%	8.5%	6.7***
3	4.9%	7.9***	11.6%	5.3%	8.2***	12.8%	6.7***	2.7%	13.1%	6.8***	7.0%	7.9***	8.2%	7.5%	8.2***
5	2.9%	5.8***	12.3%	3.2%	6.0***	11.6%	6.2***	1.6%	11.9%	6.3***	7.1%	8.7***	12.1%	7.6%	8.7***
8	2.3%	4.7***	5.4%	2.5%	4.9***	10.2%	6.0***	3.1%	10.8%	6.3***	7.7%	9.0***	14.6%	8.3%	9.0***
10	-	-	-	-	-	9.4%	5.7***	2.6%	10.0%	6.0***	7.7%	8.9***	11.3%	8.2%	8.9***
15	-	-	-	-	-	6.0%	4.4***	0.9%	6.2%	4.6***	7.4%	8.9***	11.2%	7.8%	8.9***

This table shows the out-of-sample pricing errors α of the arbitrage strategies relative of the Fama-French 8 factor model and their mean returns μ for the CNN+Transformer model and different number of factors K . We estimate the model on only once on the first T_{train} days and keep it constant on the remaining test set. We use the daily out-of-sample residuals from January 1998 to December 2016 and evaluate the out-of-sample arbitrage trading from January 1998 + T_{train} to December 2016. The signals are extracted from a rolling window of $L = 30$ days and we use the Sharpe ratio objective function. We run a time-series regression of the out-of-sample returns of the arbitrage strategies on the 8-factor model (Fama-French 5 factors + momentum + short-term reversal + long-term reversal) and report the annualized α , accompanying t-statistic value t_α , and the R^2 of the regression. In addition, we report the annualized mean return μ along with its accompanying t-statistic t_μ . The hypothesis test are two-sided and stars indicate p-values of 5% (*), 1% (**), and 0.1% (***).

in Section III.N.

J. Market Frictions and Transaction Costs

Our deep learning arbitrage strategies remain profitable in the presence of realistic trading frictions. In practice, trading costs associated with high turnover or large short-selling positions can diminish the profitability of arbitrage trading. In order to ensure that our model produces economically meaningful results, we extend it to the setting in which both transaction costs and holding costs are accounted for. We do not model market frictions associated with market impact, as in our empirical analysis we restrict the asset universe to stocks with large market capitalization, which are especially liquid.

In our market-friction extension, the daily returns R_t of the strategy now have constant linear penalties associated with the daily turnover and the proportion of short trades. These penalties quantify proportional transaction costs, which are used to model trading fees, size of the bid-ask spread, etc., and holding costs, which are used to model short borrow rate fees charged by a brokerage. In particular, we incorporate a subset of the market friction models proposed by Boyd

Table IX: OOS Performance of CNN+Trans with Trading Frictions

IPCA factor model							
K	Sharpe ratio			Mean-variance			
	SR	μ	σ	SR	μ	σ	
0	0.52	8.5%	16.3%	0.22	2.6%	11.9%	
1	0.85	5.9%	6.9%	0.86	5.5%	6.4%	
3	1.24	6.6%	5.4%	1.16	6.9%	5.9%	
5	1.11	5.5%	5.0%	1.02	5.3%	5.3%	
10	0.98	5.1%	5.2%	1.04	5.4%	5.2%	
15	0.94	4.8%	5.1%	1.02	5.1%	5.0%	

This table shows the out-of-sample annualized Sharpe ratio (SR), mean return (μ), and volatility (σ) for the CNN+Transformer model with trading frictions on IPCA residuals. We use the daily out-of-sample residuals from January 1998 to December 2016 and evaluate the out-of-sample arbitrage trading from January 2002 to December 2016. The models are calibrated on a rolling window of four years and use either the Sharpe ratio or mean-variance objective function with trading costs ($\text{cost}(w_{t-1}^R, w_{t-2}^R) = 0.0005\|w_{t-1}^R - w_{t-2}^R\|_{L^1} + 0.0001\|\min(w_{t-1}^R, 0)\|_{L^1}$). The signals are extracted from a rolling window of $L = 30$ days.

et al. (2017), which are commonly used in the statistical arbitrage literature.¹⁵ Mathematically, we subtract the market-friction costs

$$\text{cost}(w_{t-1}^R, w_{t-2}^R) = 0.0005\|w_{t-1}^R - w_{t-2}^R\|_{L^1} + 0.0001\|\min(w_{t-1}^R, 0)\|_{L^1}$$

from the portfolio returns and use these net portfolio returns in the optimization problem of section II.C, where $w_{t-1}^R \in \mathbb{R}^{N_{t-1}}$ is the strategy’s allocation weight vector at time $t - 1$. The first penalty term represents a slippage/transaction cost of 5 basis points per transaction, whereas the second one is a holding cost of 1 basis point per short position. Both costs are universal for all times and all stocks. This corresponds to a modification of the objective function in the training and evaluation parts of our algorithm. We use this model for the sake of illustration and simplicity given that in our empirical study we trade a universe of highly liquid US stocks, but more complicated models¹⁶ may be included in the computations without any significant structural changes.

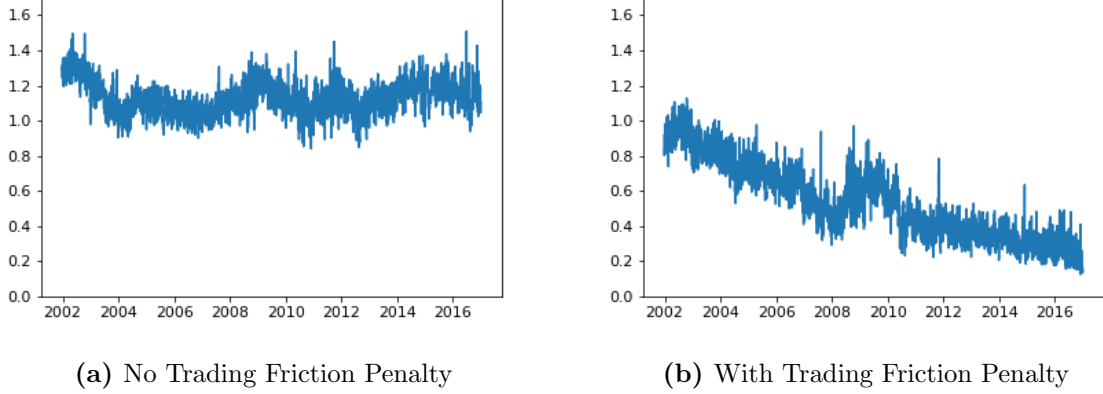
Table IX displays the Sharpe ratios, average returns, and volatility of our CNN+Transformer model under market frictions for IPCA residuals. The results for PCA residuals are collected in the Appendix in Table A.X with very similar findings. We exclude the Fama-French factor model from the analysis with market frictions, as we take the traded factors from Kenneth French Data Library as given, which are based on a larger stock universe with different trading costs and, hence, would not be directly comparable to the IPCA and PCA results.¹⁷ As expected the Sharpe ratios are lower and range from 0.94 to 1.24 for a reasonable number of IPCA factors. The Sharpe ratio and mean-

¹⁵See for example Avellaneda and Lee (2010), Yeo and Papanicolaou (2017) and Krauss et al. (2017).

¹⁶For example, those considering time and stock-dependent transaction costs or market impact of the trades on the stock prices.

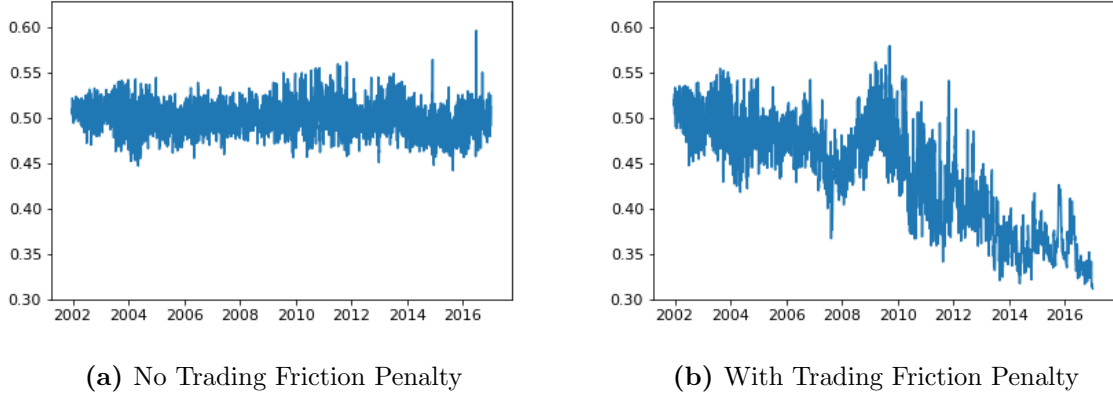
¹⁷Regardless, each factor corresponds to a portfolio of traded assets, and thus the residuals of this model could be traded in a number of ways under suitable extensions. For example, we could include ETFs which try to track a value or size premium, project these latent factors onto our asset universe, or approximate each factor with a number of sparse subset of assets in our asset universe as in Pelger and Xiong (2021). However, these changes constitute differences that would make the results incomparable to the PCA and IPCA results.

Figure 6: Turnover of CNN+Transformer Model with and without Trading Friction Objective



These figures show the daily turnover of CNN+Transformer model with and without trading friction objective on the representative IPCA 5-factor residuals for the out-of-sample trading period between January 2002 and December 2016. The models are calibrated on a rolling window of four years and use the Sharpe ratio objective function with or without trading costs ($\text{cost}(w_{t-1}^R, w_{t-2}^R) = 0.0005\|w_{t-1}^R - w_{t-2}^R\|_{L^1} + 0.0001\|\min(w_{t-1}^R, 0)\|_{L^1}$). We define turnover as the ℓ_1 norm of the difference between allocation weight vectors at consecutive times, i.e. $\|w_{t-1}^R - w_{t-2}^R\|_{L^1}$.

Figure 7: Proportion of Short Allocation Weights of CNN+Transformer Model with and without Trading Friction Objective



These figures show the daily fraction of short trades of the CNN+Transformer strategies with and without trading friction objective on the representative IPCA 5-factor residuals for the out-of-sample trading period between January 2002 and December 2016. Each plot shows the absolute value of the sum of negative weights $\|\min(w_{t-1}^R, 0)\|_{L^1}$ relative to the sum of absolute values of all weights, which is normalized to $\|w_{t-1}^R\|_1 = 1$. The models are calibrated on a rolling window of four years and use the Sharpe ratio objective function with or without trading costs ($\text{cost}(w_{t-1}^R, w_{t-2}^R) = 0.0005\|w_{t-1}^R - w_{t-2}^R\|_{L^1} + 0.0001\|\min(w_{t-1}^R, 0)\|_{L^1}$).

variance objective have the desired effects, but lead to overall very similar results. Importantly, the arbitrage strategies retain their economic significance even in the presence of trading costs.

These results present a lower bound on the profitability under trading frictions, as we have made four simplifying assumptions. First, in the current implementation the factor composition cannot be changed due to trading costs. A possible extension could construct the latent risk factors by including the trading friction objective. For example, the sparse representation of latent factors as in Pelger and Xiong (2020) would reduce trading costs. Second, because the policy with frictions is recursive, we are conducting an approximate training process to maintain parallelization

given our computational resources and the large volume of data, but this may lead to suboptimal optimization results. However, it would be possible to conduct an exact sequential training process at the cost of more computation. Third, our modified architecture with the market-friction objective is given by the simplest modification to our architecture without frictions, but it is possible that the optimal transaction and holding cost-minimizing strategy has a more complicated functional form or is not Markovian and requires additional previous allocations. Last but not least, we keep the hyperparameters of our main analysis, but we could potentially improve the performance by employing hyperparameter tuning.

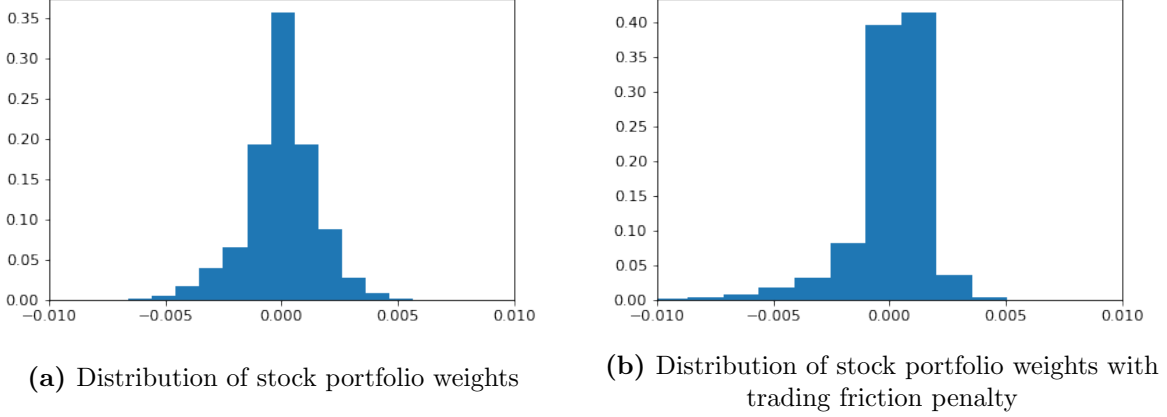
The effect of trading frictions is time-varying and our model can exploit particularly profitable arbitrage time periods by increasing trading and short positions. In Figure 6 we analyze the daily turnover of a representative CNN+Transformer strategy based on IPCA 5-factor residuals and a Sharpe ratio objective. Broadly, we see that our model with trading friction penalty is able to adapt by decreasing daily turnover. However, our model seems to reduce turnover based on trading opportunities. During the times of high market volatility such as 2007–2009, arbitrage trading could be potentially be more profitable, which our model takes advantage of. On the other hand, during the later years of the calm bull market from 2011–2015, strategies with less turnover could maintain profitability. This pattern is confirmed in Figure 7 which shows the daily proportion of allocation weights, which are short stocks in our universe. As expected the holding cost friction model reduces the overall proportion of short trades. Interestingly, our model is able to intelligently choose time periods during which it can maximize performance by taking positions with higher short proportion, such as the market turmoil at the end of 2015 and the financial crisis of 2008. Effectively, this indicates that the CNN+Transformer trading policy has learned to avoid holding and transaction costs by generally modifying the original strategy’s allocations to be less short-biased on average, and to more appropriately enter short-dominant positions during relevant subperiods.

K. Portfolio Weight Concentration

In this section we study the portfolio weight concentration of successful statistical arbitrage trading. We show that our arbitrage portfolios are well-diversified, but we can still achieve a large fraction of the profitability when restricted to a sparse set of assets. In this and the following sections, the benchmark model is the CNN+Transformer based on IPCA 5-factor residuals and a Sharpe ratio objective. The results hold qualitatively for alternative factor specifications. We study the out-of-sample portfolio weights w_t^R for individual stocks.

Figure 8 shows that the optimal portfolio weights are well-diversified and do not rely on excessively large weights on individual stocks. The left subplot shows the histogram of the distribution of stock weights w_t^R aggregated over time. The weights are approximately normally distributed and centered at zero. Hence, most weights concentrate around values in $[-0.5\%, +0.5\%]$, which implies a relatively well-diversified portfolio. Second, the portfolios correspond to long-short positions with approximately similar weights on each of the two legs. The right subplot estimates the

Figure 8: Distribution of Portfolio Weights



These figures show histograms of the distribution of stock weights w_t^R aggregated over time. Subplot (a) shows the out-of-sample weights for our empirical benchmark model, which is the CNN+Transformer model based on IPCA 5-factor residuals. Subplot (b) estimates the baseline model with trading friction penalty. The out-of-sample trading period is between January 2002 and December 2016.

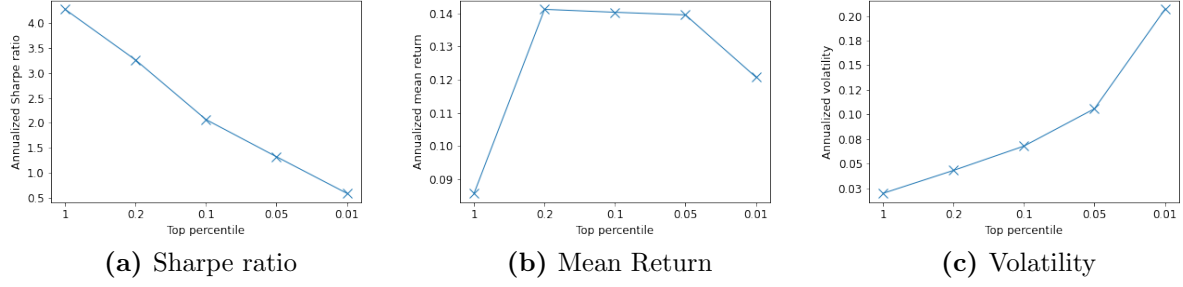
baseline model with the trading friction penalty from Section III.J. While a trading friction penalty increases the kurtosis, which implies sparser weights, we still do not observe excessive weights on individual stocks. The trading friction penalty also reduces short sales, which is consistent with Figure 7.

Our statistical arbitrage trading policy does not target specific industries. Figure A.5 in the Appendix shows the rolling industry concentration of portfolio weights standardized by the population industry concentration. The fraction invested in a specific industry follows very closely the sample proportion of stocks in the corresponding industry. While there is some minor variation in the industry concentration over time, it deviates less than 20% from the population concentration. This suggests that stocks in all industries offer statistical arbitrage opportunities.

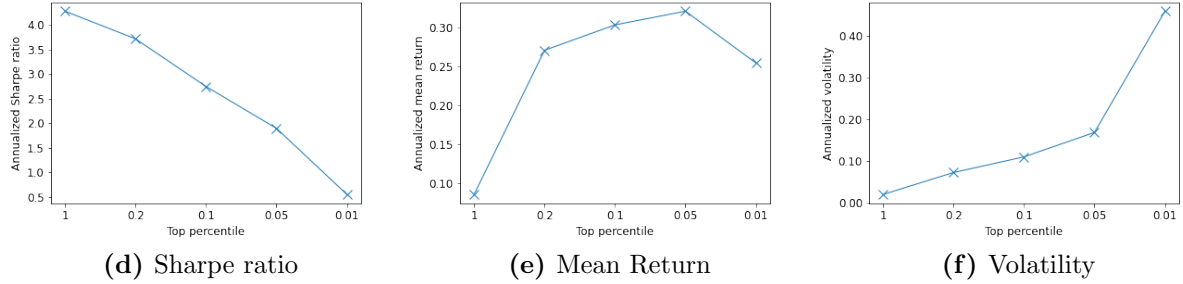
While our statistical arbitrage portfolios are well-diversified, a subset of a few stocks can already achieve most of their performance. This finding is important for optimization under trading frictions. We construct sparse trading policies by selecting only the proportion p of the stock weights w_t^R with the largest absolute value for trading. We compare the full model with sparse models, which invest only in $p = 1\%$, 5% , 10% or 20% of the stocks. Note that this represents only a lower bound for the performance of sparse portfolios, as we are not including the sparsity constraint in the optimization.

Figure 9 in panel A shows the annualized out-of-sample Sharpe ratio, mean return and volatility of arbitrage strategies based only the most extreme portfolio weights. Portfolios with less stocks are less diversified and as expected have a higher volatility. However, focussing on the extreme weights can increase the mean return of the portfolios. The Sharpe ratio of sparse portfolios is generally decreasing in the degree of sparsity, as the loss in diversification dominates the effect of higher expected returns. However, a sparse portfolio can capture a substantial amount of the profitability. We achieve out-of-sample Sharpe ratios above two with only 10% of the stocks. These

Figure 9: Performance of Sparse Portfolios
PANEL A: Largest Stock Portfolio Weights

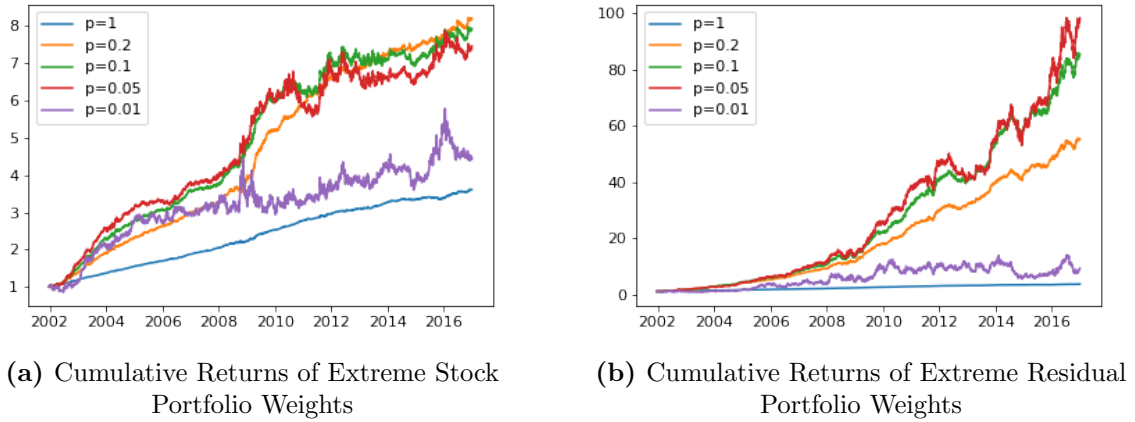


PANEL B: Largest Residual Portfolio Weights



These figures show the annualized out-of-sample Sharpe ratio, mean return and volatility of arbitrage strategies based on selecting only the largest portfolio weights in absolute value. Panel A selects the proportion p of the most extreme stock weights w_t^R for trading, while panel B selects the proportion p of the most extreme residual weights w_t^ϵ for the trading policy. The baseline model is the CNN+Transformer model based on IPCA 5-factor residuals for the out-of-sample trading period between January 2002 and December 2016. We consider the full model $p = 1$ and the fraction $p = 0.01, 0.05, 0.1$ and 0.2 .

Figure 10: Cumulative Returns of Sparse Portfolios



These figures show the cumulative returns of sparse portfolio weights in the stock and residual weight vectors. Subplot (a) selects the proportion p of the stock weights w_t^R with the largest absolute value for trading, while subplot (b) selects the proportion p of the residual weights w_t^ϵ with the largest absolute value for the trading policy. The baseline model is the CNN+Transformer model based on IPCA 5-factor residuals for the out-of-sample trading period between January 2002 and December 2016. We consider the full model $p = 1$ and the fraction $p = 0.01, 0.05, 0.1$ and 0.2 .

are lower bounds as we use the model that is optimized for non-sparse weights, and select only the extreme weights. It is noteworthy, that using only 5% of the stocks, which corresponds to roughly

25 stocks in our sample, achieves mean returns of 14%. However, the performance deteriorates when our portfolio consists of only 1%, corresponding to around 5 stocks. The cumulative return time series in Figure 10 further illustrate the different effect of sparsity on the mean and variance of the strategies.

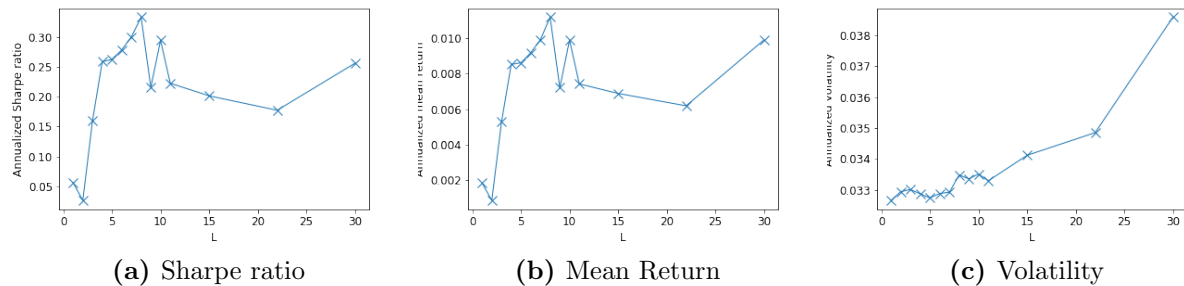
In our second analysis, we construct sparse residual portfolio weights w_t^ϵ . Similar to the sparse stock weights, we select the proportion p of the most extreme residual weights w_t^ϵ for the trading policy. A sparse stock portfolio weight w_t^R combines a sparse factor representation and a sparse trading policy in residuals. By studying the largest portfolio weights in residuals, we can separate the effect of sparse factors from a sparse trading policy in residuals. This is relevant as some factors could be approximated by a sparse set of traded assets, for example ETFs. Panel B in Figure 9 shows the out-of-sample Sharpe ratio, mean return and volatility for sparse residual portfolio weights w_t^ϵ . The Sharpe ratio effects are very similar, as targeting the most extreme residual portfolios results in larger mean returns, while it increases the variance. However, a sparse residual portfolio can achieve around twice the expected return of a sparse stock portfolio.

L. Complexity of Arbitrage Trading

Our CNN+Transformer solution can discover complex trading signals and policies. As a robustness check, we study how much simple reversal strategies can earn. Given the residuals from our baseline IPCA-5-factor model, we construct long-short trading strategies for different time lags. Such high-minus-low strategies have been motivated in He et al. (2022). In more detail, the portfolio weights of the simple trading strategy are long-short portfolios, that buy the 20% lowest residuals and sell the 20% highest residuals from L periods in the past.

Figure 11 shows the out-of-sample Sharpe ratio, mean return and volatility of simple reversal strategies. First, these simple reversal strategies yield positive returns and Sharpe ratios. The variance is increasing for longer lags. The reversal returns increase substantially with a lag of at least one week (five trading days). The Sharpe ratios are primarily driven by the low variance and achieve Sharpe ratios of up to 0.3 for lags between one and two weeks.

Figure 11: Simple Reversal Trading



These figures show the annualized out-of-sample Sharpe ratio, mean return and volatility of simple reversal strategies based on IPCA 5-factor residuals. The portfolio weights of the simple trading strategy are long-short portfolios, that buy the 20% lowest residuals and sell the 20% highest residuals for L periods in the past. The out-of-sample trading period is between January 2002 and December 2016.

Simple reversal strategies result in substantially lower mean returns and Sharpe ratios than our complex arbitrage strategies. This confirms that simple ad-hoc approaches are not sufficient to leverage mispricing and successful arbitrage trading is more complex than simple reversal patterns. The findings also suggest that there is profitability in longer holding periods for signals that are further in the past. We will study this aspect in depth in the next section.

M. Persistence of Arbitrage

We study arbitrage trading for different holding periods and show that statistical arbitrage signals are persistent. Given the out-of-sample portfolio weights w_t^R , we document the portfolio performance for longer holding periods. As in the previous sections, our benchmark model is the CNN+Transformer based on IPCA 5-factor residuals and a Sharpe ratio objective.

First, we consider longer holding periods, that can overlap. An investment with weights w_t^R is held for B trading days, ranging from 1 to 30 trading days. The trading with longer holding periods is overlapping and the fraction $1/B$ is invested based on new weights every trading day. Assuming log returns, this is equivalent to the portfolio weights

$$w_t^{R,B\text{-days}} = \frac{1}{B} \sum_{l=0}^{B-1} w_{t-l}^R.$$

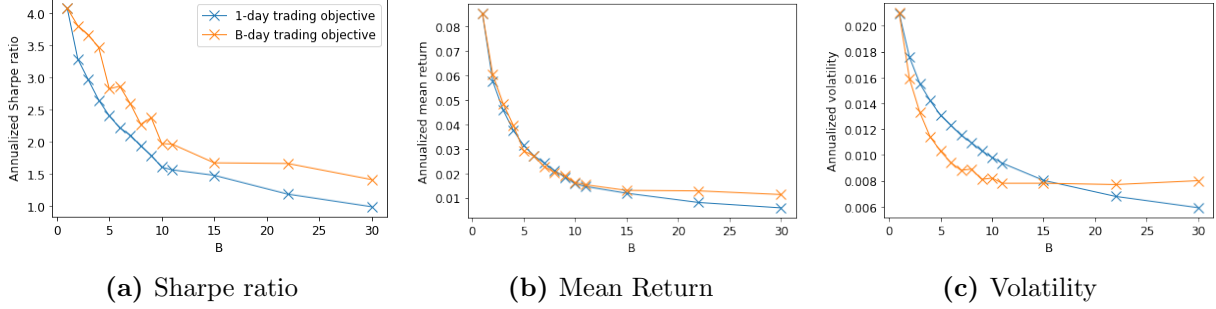
Panel A in Figure 12 shows the annualized out-of-sample Sharpe ratio, mean return and volatility for different overlapping holding periods. Daily trading indeed generates the highest payoff in terms of mean returns and Sharpe ratios. The half-life in terms of Sharpe ratios is around seven trading days. In fact, the Sharpe ratio is still above one with a one month (22 business days) holding period, when using signals estimated with a 1-day trading objective. As expected, the lower trading frequency can reduce the volatility. This shows that statistical arbitrage is long-lived and persists for several days and even weeks. We also include the results, when we change the estimation to optimize the Sharpe ratio of the overlapping multi-horizon holding periods. It is possible to achieve out-of-sample Sharpe ratios around 1.5 with a one month holding period, when directly optimizing for longer holding periods. The mean returns for a strategy based on the B -day trading objective decline less than for a 1-day trading objective. For longer horizons this comes at the cost of a slightly higher variance. For shorter horizons, the B -day trading objective reduces the variance by taking advantage of additional diversification.

Overlapping trading generates diversification effects between strategies. It is a valid measure of how fast signals are dying out, but it is still implicitly based on daily trading. Optimizing for a longer holding period can take advantage of this diversification effects and increase the mean return without strongly increasing the variance. This is one reason why we can maintain Sharpe ratios of 1.5 for one month holding periods.

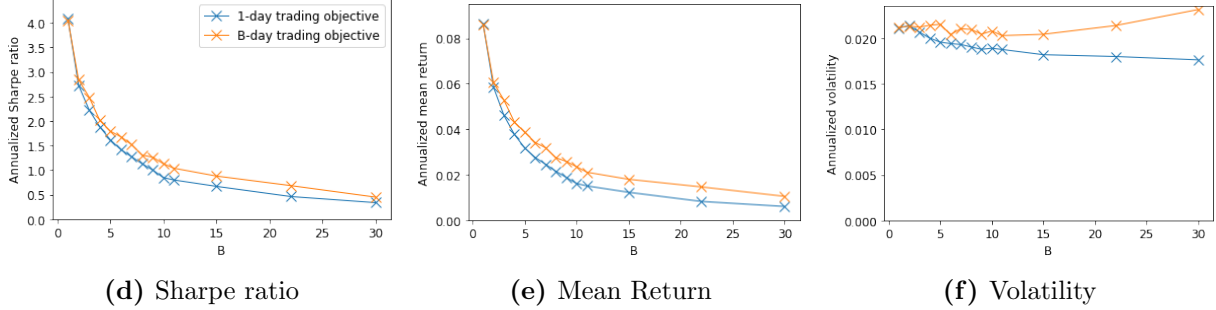
An alternative analysis actually trades only every B days without overlap. As there are B different starting days, this yields B possible implementations of a B -day holding strategy. We

Figure 12: Performance for Longer Holding Periods

PANEL A: Overlapping Trading



PANEL B: Non-overlapping Trading



These figures show the annualized out-of-sample Sharpe ratio, mean return and volatility for different holding periods for our empirical benchmark model, which is the CNN+Transformer model based on IPCA 5-factor residuals. An investment with weights w_t^R is held for B trading days, ranging from 1 to 30 trading days. The blue line indicates a model that is estimated with a daily trading objective (that is, our baseline model), while the orange line displays a model that is estimated with a B -holding day objective. In panel A the trading with longer holding periods is overlapping and the fraction $1/B$ is invested based on new weights every trading day. In panel B, we estimate for a holding period of B days, the performance of the B different trading strategies starting at different days and report the average results. Hence, panel B reports results for non-overlapping portfolios. The out-of-sample trading period is between January 2002 and December 2016.

report the average performance for each of the possible B starting days, that is, we average the performance metrics, but do not create a portfolio of overlapping returns. Panel B in Figure 12 shows the corresponding results. By construction, the mean returns for weights based on the 1-day trading objective are identical to overlapping trading. The difference between the two analyses comes from the variance. The overlapping trading generates large diversification benefits, which are not achieved with the separate non-overlapping trading. As a result the Sharpe ratios for non-overlapping trading are lower. However, even with a one month (22 business days) holding period, we still achieve an out-of-sample Sharpe ratio of around 0.5. There is little improvement when optimizing the trading for a longer holding period with non-overlapping trading.

Overall, we have two main findings. First, arbitrageurs do indeed correct prices quickly. Depending on the analysis around half of the Sharpe ratio vanishes after one or two weeks. Arbitrageurs do engage in arbitrage trading as signals do eventually die out. Second, a large fraction of the statistical arbitrage signal is persistent. Even with holding periods of over one month, the signals

can be highly profitable. This has important economic implications. The persistence in arbitrage signals could be explained by the limited capacity of arbitrageurs, that is, arbitrageurs might have insufficient capital to fully exploit temporal mispricing quickly. An alternative explanation could relate to strategic trading. Arbitrageurs might try to take advantage of temporal mispricing, while at the same time limit their market impact to avoid revealing their detected signal. A third explanation could relate to behavioral trading. In the presence of noise traders or uninformed traders, the adjustment of prices also depends on how quickly the non-arbitrageurs adjust their expectations. The persistence of arbitrage has also practical implications. It explains our findings from Section III.J, why statistical arbitrage can also be exploited in the presence of transaction costs by avoiding frequent trading.

N. *Estimated Structure*

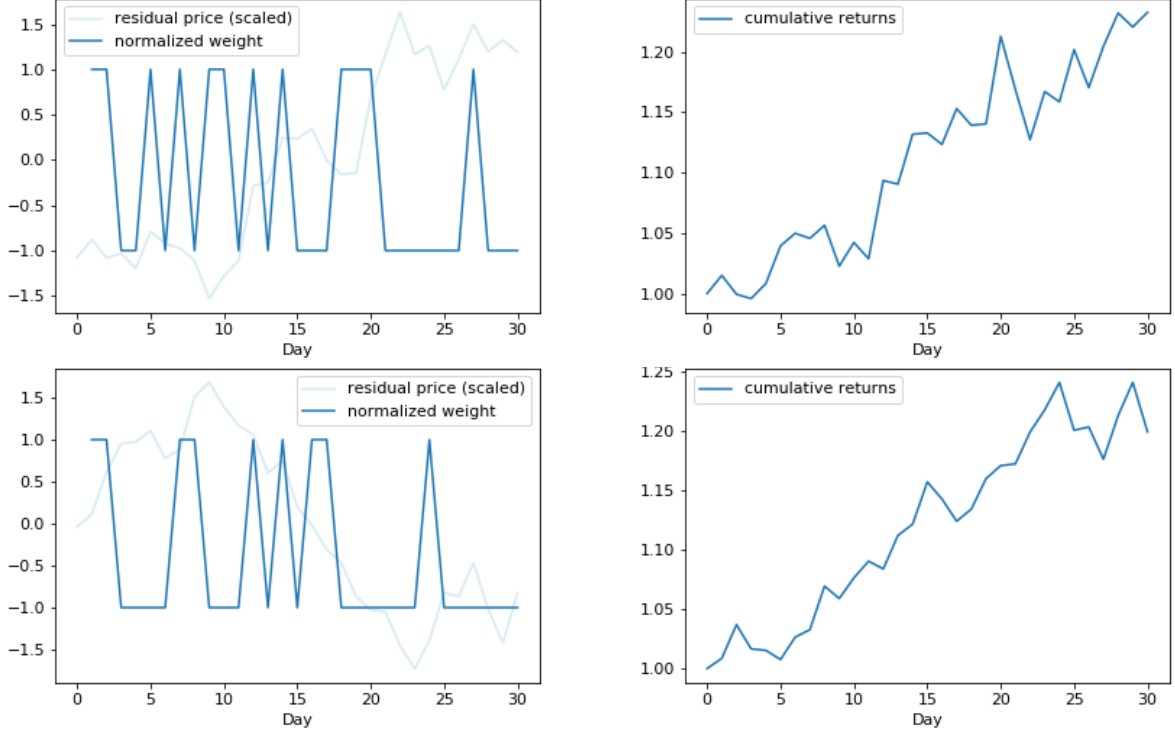
What are the patterns that our CNN+Transformer model can learn and exploit? In order to answer this question, we analyze the different building blocks of our benchmark model and show their structure on representative and informative residuals inputs. Our goal is to ascertain, characterize, and explain the role that the convolutional features and attention heads play in the determination of the final allocation weight and recognition of salient time series patterns. The benchmark model for this section is the CNN+Transformer based on IPCA 5-factor residuals and a Sharpe ratio objective. The model is calibrated on the first 8 years of data and kept constant, which allows us to study the signal and allocation function.

As an illustrative example, Figure 13 shows the allocation and return on representative residuals. The left subplot displays an out-of-sample time-series of cumulative returns of a randomly selected residual and its value in the allocation function. We normalize the allocation weight to have an absolute value of one, that is, for this illustrative example we only trade this particular residual. The right subplots depicts the payoff of trading the specific residual with the displayed allocation function. The first residual shows mean-reversion patterns, which are successfully detected and exploited by the function $\mathbf{w}^{\epsilon|\text{CNN+Trans}}$. The second residual has a downward trend, which is also correctly detected and taken advantage of by the model.¹⁸ These examples suggest that the CNN+Transformer model can learn mean-reversion and trend patterns. Figures A.2 and A.3 are further examples with the same takeaways.

Next, we “dissect” the CNN+Transformer model to understand what type of functions it can estimate. Our analysis begins with the eight basic convolutional patterns learned by the convolutional layers of our network, which are displayed in Figure 14. The CNN represents a given time-series as a matrix of exposures to local basic patterns. As explained in Section II.D.3, these local filters are more complicated than simple local linear filters, but we can project our CNN filters into two-dimensional orthogonal linear filters, which are more interpretable. These local patterns are the building blocks to construct global patterns. We see that these basic patterns display a

¹⁸Note that our in our empirical study the model trades in all residuals and is not limited to trade only in one residual. Hence, the empirical performance is substantially better as shown in Figure 5.

Figure 13: Examples of Allocation and Returns of CNN+Transformer Strategy



These plots display representative examples of the CNN+Transformer out-of-sample arbitrage trading on a sample of residuals from the IPCA 5-factor model. The left subplots show the normalized cumulative returns of the residuals and the normalized allocation weight, which the specific residual has in the trading strategy. The right subplots illustrates the payoff of trading the specific residual with the displayed allocation function. The model is calibrated on the first 8 years of data and kept constant.

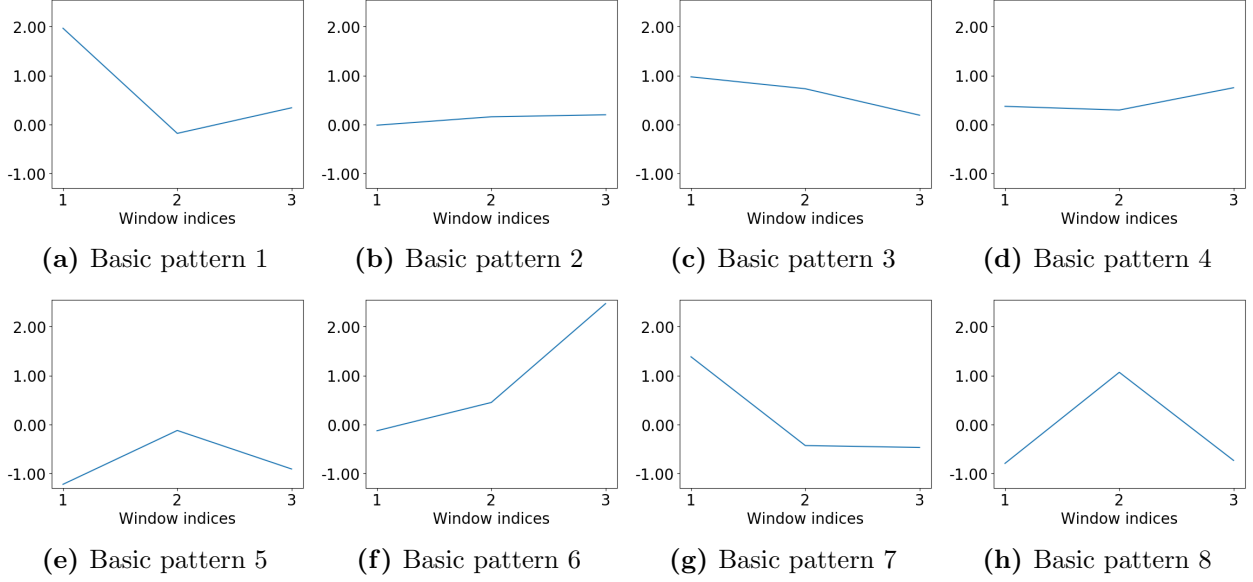
variety of salient price behavior which are considered to be important. Basic patterns 4 and 6 capture local upward trends, basic patterns 3 and 7 track local downward trends and basic patterns 1, 5 and 8 learn reversion patterns. However, the basis patterns do not include very spiked, sharp changes. Overall, the building blocks seem to be sufficient to construct any smooth trend and mean-reversion pattern.

We can understand the global patterns learned by the transformer by studying the attention function. The attention functions $\alpha_i(.,.)$ of each attention head $i = 1, \dots, H = 4$ capture the dependencies between the local patterns. Our arbitrage signal can be interpreted as “loadings” to these “attention factors”. We use the same H attention functions for all residuals, but in order to visualize them, we evaluate them for a given residual time-series, which yield the attention weights per head:

$$\alpha_{i,j} = \alpha_i(\tilde{x}_L, \tilde{x}_j) \quad \text{for } i = 1, \dots, H.$$

As our signal only depends on the final cumulative return projection h_L^{proj} , the attention weights $\alpha_{i,j}$ for $i = 1, \dots, H$ and $j = 1, \dots, L$ contain all the “global factor” information. Hence, we will plot the $H \times L$ dimensional attention weights of the attention heads to understand which global

Figure 14: Local Basic Patterns of Benchmark Model



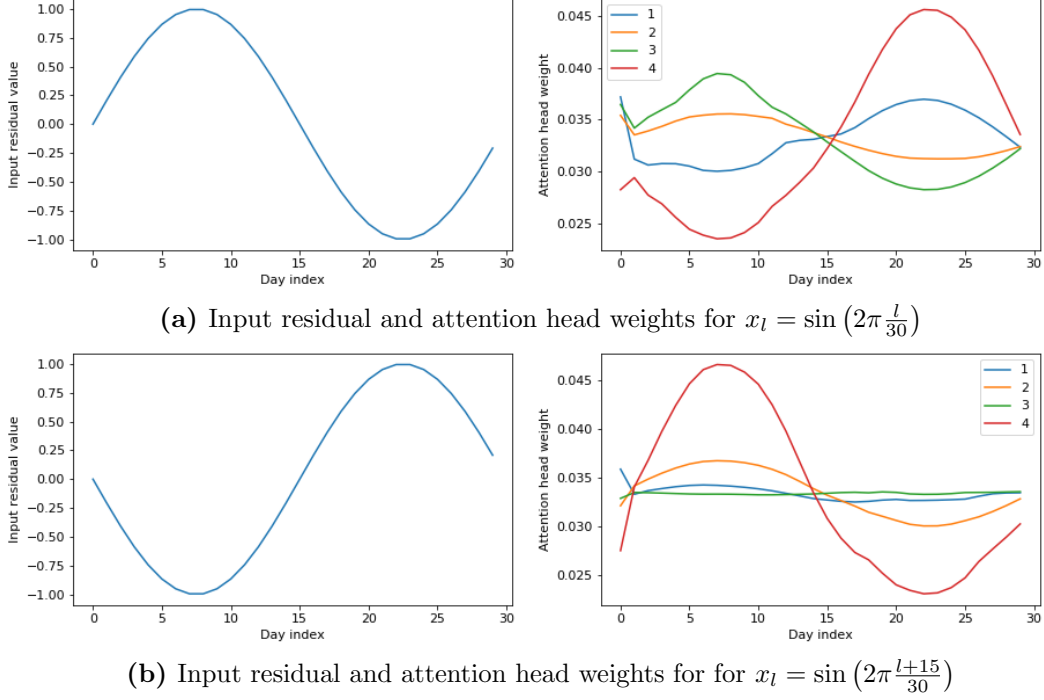
These figures show the $D = 8$ local filters of the CNN estimated for the benchmark model in our empirical analysis. These are projections of our higher dimensional nonlinear filter from a 2-layer CNN into two-dimensional linear filters. These building blocks are labeled “basic patterns”. The benchmark model is the CNN+Transformer model based on IPCA 5-factor residuals. We estimate the model on only once on the first $T_{\text{train}}=8$ years based on the Sharpe ratio objective.

patterns are activated by specific time-series.

Figure 15 plots the attention head weights for simulated sinusoidal residual input time-series. Note that the attention head weights discover the sinusoidal pattern although the model was estimated on the empirical data and not specifically trained for this simulated input. The different attention heads capture different patterns. The fourth attention head displayed in red has the strongest activation and capture high-frequency mean reversion patterns. These attention head weights are positive for negative realizations. We will label these fourth attention head weights a “negative reversal” pattern. The third attention head weights depicted by the green curve co-move with the mean-reversion patterns of the original time-series, that is they are positive for high values, but seem to be only activated if this positive “hilltop” appears at the beginning of the time-series. If the mean-reversion cycle achieves its positive values at the end, the third attention head is not activated. We will label these third attention head weights the “early reversal” pattern. The first attention head in blue seems to be a “dampened” version of the fourth red attention head. Figure A.4 in the Appendix shows additional simulated input time-series that confirm this interpretation. In summary, the different attention head weights can be assigned to specific global patterns.

In Figure 16, we plot the different components of the CNN+Transformer model evaluated on a randomly selected, representative 30-day empirical residual. The cumulative residual in subfigure (a) is the input to the CNN. This $L = 30$ dimensional vector is represented by the CNN in terms of its “exposure” to local basic pattern. The subfigures (d)–(k) show this $D \times L$ dimensional representation, which is the output of the CNN. As we have $D = 8$ local filters, we obtain eight time-series that display the activation to each filter. For example, basic pattern 1 is associated with

Figure 15: Example Attention Weights for Sinusoidal Residual Inputs

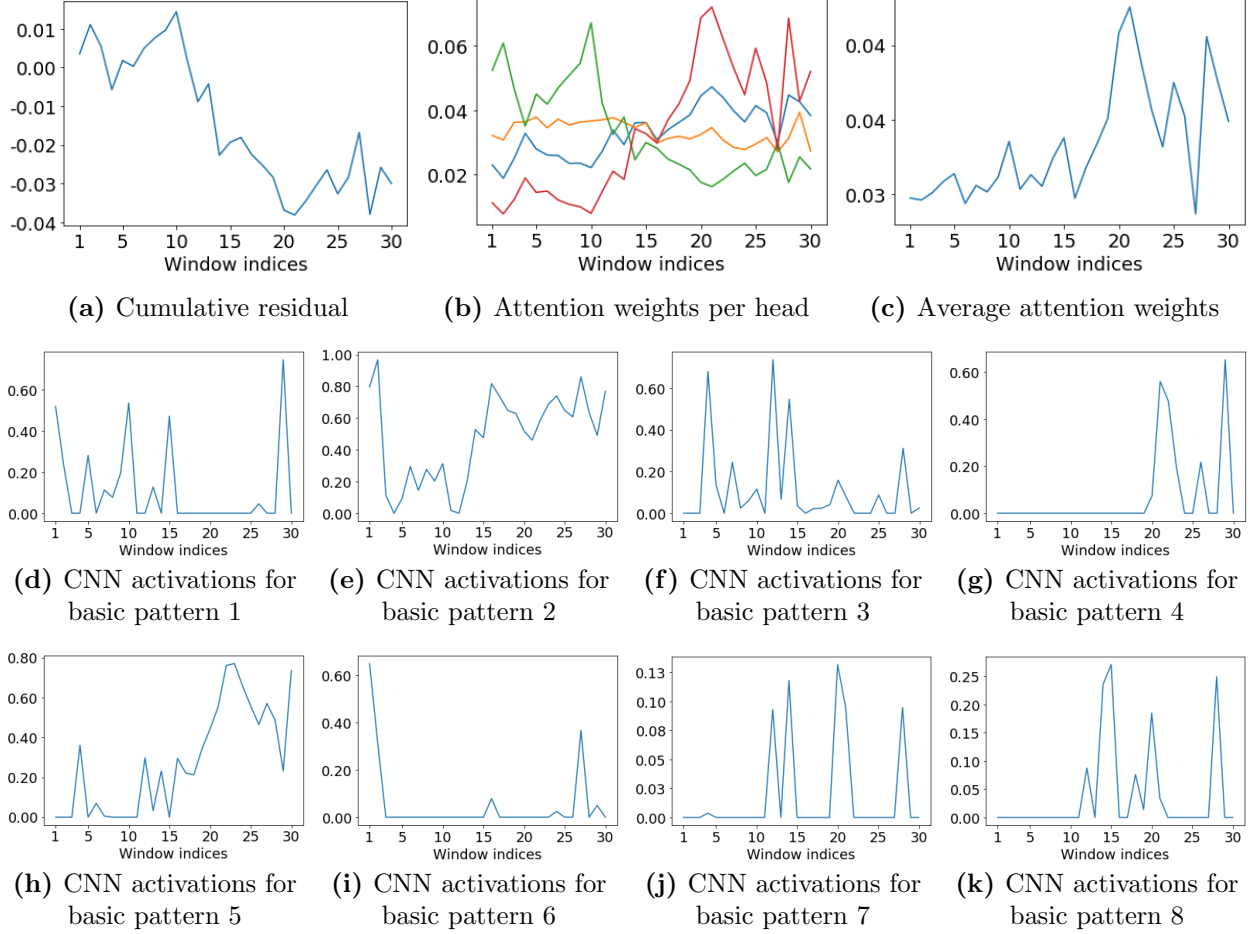


These plots show the attention head weights of the CNN+Transformer benchmark model for simulated sinusoidal residual input time series. Both sine functions have a cycle of 30 days and the second is shifted by 15 days. The right subplot shows the attention weights for the $H = 4$ attention heads for the specific residuals. The empirical benchmark model is the CNN+Transformer model based on IPCA 5-factor residuals. We estimate the model only once on the first $T_{\text{train}}=8$ years based on the Sharpe ratio objective.

a “reversal kink” in subfigure 14(a) and hence has the strongest activation to this basic pattern on day 28, when the residual has a downward spike. This $D \times L$ matrix of exposures to local patterns is the input to the transformer. The attention head weights in subfigure (b) connect the local patterns to a global pattern. The fourth attention head weight in red has its highest values during the “bottom” of the residual movements, confirming our previous intuition that this attention head activates during bad times. The third attention head weight in green spikes during the “top” at the beginning of the residual time-series, which is in line with our interpretation as an early reversal pattern. The first attention head in blue is a dampened version of the red attention head. The average over the four attention head weights depicted in subfigure (c) suggests that the heads attend on average more closely to the latter half of the time series.

In Figure 17 we generalize the analysis of Figure 16 to study the model structure of the benchmark model over time. While Figure 16 represents a “snapshot” for one point in time, we now display the allocation weights and attention head weights of a single representative residual for different times. Subfigure 17(a) shows the cumulative residual time-series. For a specific point in time we use the lagged $L = 30$ days as an input to obtain the allocation weights and attention head weights for that time. The out-of-sample allocation weights correctly change the directions to exploit the patterns in the residual time-series. The attention head weights over time offer additional insights into the structure of the global patterns. Each vertical slice from window index 1

Figure 16: CNN+Transformer Model Structure for Representative Residual

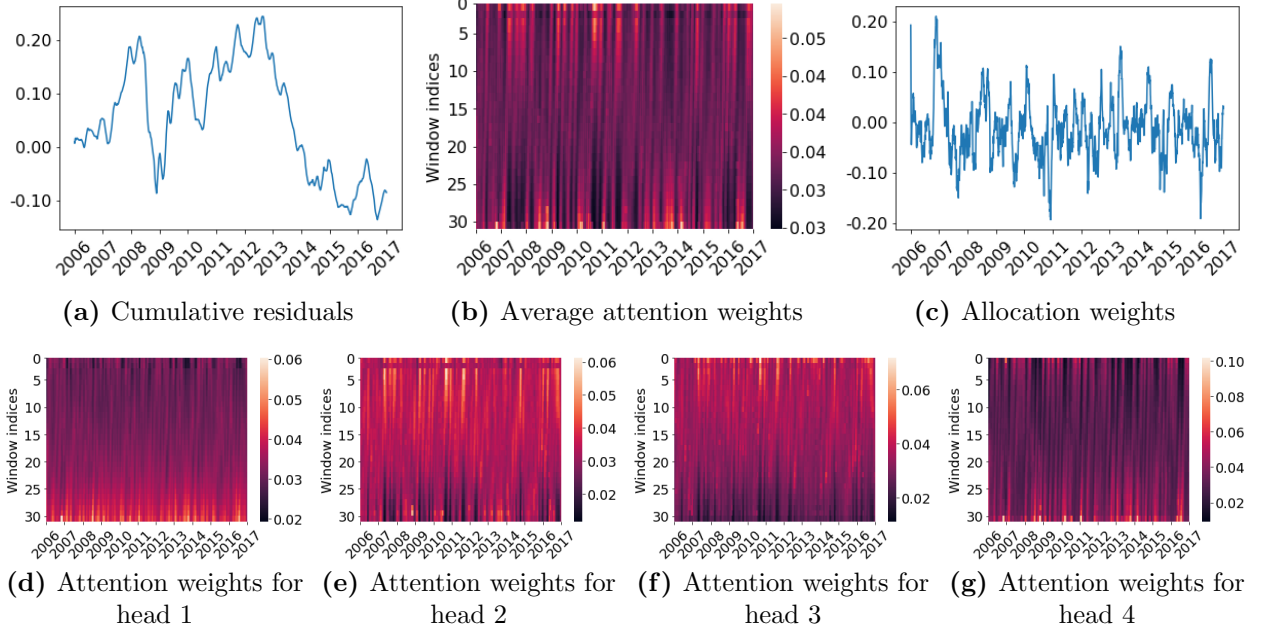


These figures illustrate the different components of the CNN+Transformer benchmark model evaluated for a randomly selected, representative empirical residual. The cumulative residual returns, which are the input to the model, are plotted in (a). The convolutional activations (d)–(k) quantify the exposure of the residual time-series to local basis filters. Subplot (b) displays the attention weights for the $H = 4$ attention heads, which represent global dependency patterns. Subplot (c) shows the average of these four attention head weights. The empirical benchmark model is the CNN+Transformer model based on IPCA 5-factor residuals. We estimate the model on only once on the first $T_{\text{train}}=8$ years based on the Sharpe ratio objective.

to window index 30 displays the normalized attention weights for the time point under the slice. The third attention head, which was displayed in green in Figures 15 and 16 has the largest values during “up-patterns” of the residual, for example for 2007, 2010 and 2012. Importantly, the attention weights focus on the early days within the 30-day window. This confirms our previous interpretation as an “early reversal” pattern. Attention head four, which was previously represented as a red line, has the highest values during down-times, such as 2009, 2014 and the middle of 2016. In contrast to attention head 3, this head focuses on the immediate past within the local window. Attention head 1, which is a dampened down-version, focuses more uniformly on all the values within the local window.

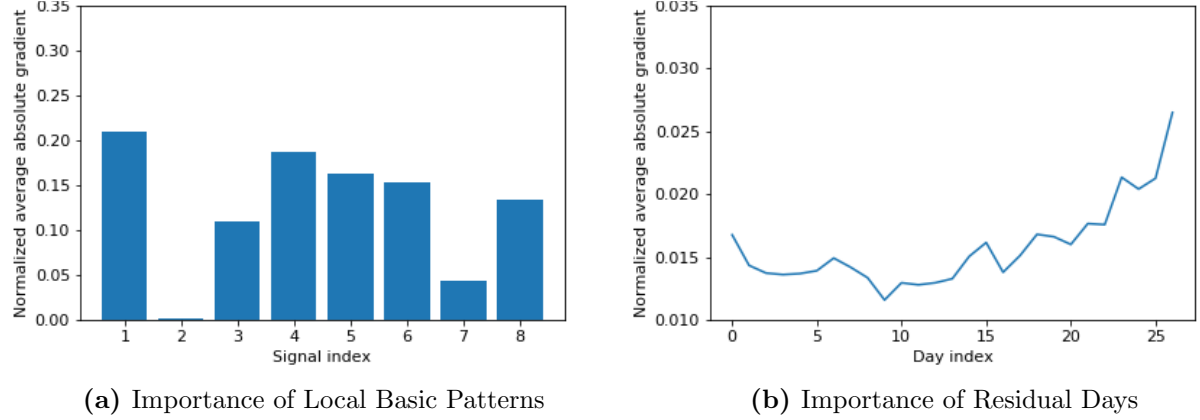
The average attention weights in (b) illustrate the asymmetric response of the transformer network. During uptrends, it focuses on the residual prices which are further in the past part of the

Figure 17: CNN+Transformer Model Structure for Representative Residual Over Time



These figures illustrate the out-of-sample behavior from 2006 to 2016 of the CNN+Transformer benchmark model for a single residual time-series. The cumulative residual returns are plotted in (a), and the suggested allocation weights before cross-sectional normalization are plotted in (c). The attention head weights (d)–(g) quantify the activation for each attention head over time. Subplot (b) shows the average of these weights over the four heads for different times. All time-series have been smoothed using a simple moving average with a 30-day window for better presentation. The empirical benchmark model is the CNN+Transformer model based on IPCA 5-factor residuals. We estimate the model on only once on the first $T_{\text{train}}=8$ years based on the Sharpe ratio objective.

Figure 18: Variable Importance for Allocation Weight



These figures show the normalized average absolute gradient (NAAG) of the allocation weight with respect to various inputs to intermediate layers in the CNN+Transformer benchmark network. A higher NAAG indicates a higher importance. Subplot (a) quantifies the importance of the $D=8$ different convolutional filters, that is, we display the gradient with respect to the output of the convolutional network, which is the input to the self-attention layer. In (b), we report the importance of the first 27 days of the input residual time series. Each average absolute gradient is normalized by dividing each element by the sum of all elements. The empirical benchmark model is the CNN+Transformer model based on IPCA 5-factor residuals. We estimate the model on only once on the first $T_{\text{train}}=8$ years based on the Sharpe ratio objective.

window to decide which to position to take; however, during downtrends, it focuses on the most re-

cent cumulative residual prices in the lookback window, which indicates that it is taking into account the latest data in order to decide what position to take. This indicates that our CNN+Transformer policy network has learned to act swiftly during downtrends, and more slowly during uptrends. This shows that our model learns in particular the commonly repeated wisdom that “markets take escalators up and elevators down”. This asymmetric policy is a key benefit of the attention-based model, which cannot easily be replicated by the parametric Ornstein-Uhlenbeck or fixed basis pattern benchmark models we compare against. The convolutional subnetwork’s patterns provide translation invariant information about what kind of trend is present within each 3-day subwindow of the 30-day cumulative residual price lookback window, which allows the transformer subnetwork to form a stable attention function that results in this unique policy.

Figure 18 sheds further light on which days and patterns are important. The figure shows the normalized average absolute gradient (NAAG) of the allocation weight with respect to various inputs to intermediate layers in the CNN+Transformer benchmark network. A higher NAAG indicates a higher importance. Subplot (a) quantifies the importance of the $D = 8$ different basic patterns. We observe that the flat basic pattern 2 has a negligible weight, while basis patterns that are needed for trend or reversal patterns have high importance. In (b), we report the importance of the first 27 days of the input residual time series.¹⁹ Crucially, all previous days matter, which emphasizes that the trading allocation depends on the past dynamics. The most recent 14 days seem to get on average more attention for the trading decisions. However, as indicated in Figure 17, the importance of the days seems to be asymmetric for different global patterns.

IV. Conclusion

In this paper, we introduce a unifying conceptual framework to compare different statistical arbitrage approaches based on the decomposition into (1) arbitrage portfolio generation, (2) signal extraction and (3) allocation decision. We develop a novel deep learning statistical arbitrage approach. It uses conditional latent factors to generate arbitrage portfolios. The signal is estimated with a CNN+Transformer, which combines global dependency patterns with local filters. The allocation is estimated with a nonparametric FFN based on a global trading objective.

We conduct a comprehensive empirical out-of-sample study on U.S. equities and demonstrate the potential of machine learning methods in arbitrage trading. Our CNN+Transformer substantially outperforms all benchmark approaches. The implied trading strategies are not spanned by conventional risk factors, including price trend factors, and survive realistic transaction and holding costs. Our model provides insights into optimal trading policies which are based on asymmetric trend and reversion patterns. In particular, our study shows that the trading signal extraction is the most challenging and separating element among different statistical arbitrage approaches.

Our findings contribute to the debate on efficiency of markets. We quantify the scope of profits that arbitrageurs can achieve in equity markets. Importantly, the substantial profitability of our

¹⁹As the attention head weights are determined relative to the last local 3-day window, that subwindow has mechanically a larger weight and is not comparable to the other 27 days.

arbitrage strategies is not inconsistent with equilibrium asset pricing, following similar arguments as in Gatev et al. (2006). It could rather be viewed as empirical evidence about how efficiency is maintained in practice. We document non-declining profitability of arbitrage trading over time, which suggests that the profits are compensation for arbitrageurs to enforce the law of one price.

REFERENCES

- AVELLANEDA, M. AND J.-H. LEE (2010): “Statistical arbitrage in the US equities market,” *Quantitative Finance*, 10, 761–782.
- BALI, T. G., A. GOYAL, D. HUANG, F. JIANG, AND Q. WEN (2022): “Predicting Corporate Bond Returns: Merton Meets Machine Learning,” *Working paper*.
- BARR, A. (2007): “Quant quake shakes hedge-fund giants,” *Marketwatch*.
- BIANCHI, D., M. BÜCHNER, AND A. TAMONI (2019): “Bond risk premia with machine learning,” *Working paper*.
- BOYD, S., E. BUSSETI, S. DIAMOND, R. N. KAHN, K. KOH, P. NYSTRUP, J. SPETH, ET AL. (2017): “Multi-period trading via convex optimization,” *Foundations and Trends in Optimization*, 3, 1–76.
- BRYZGALOVA, S., M. PELGER, AND J. ZHU (2019): “Forest through the Trees: Building Cross-Sections of Stock Returns,” *Working paper*.
- CARHART, M. M. (1997): “On persistence in mutual fund performance,” *Journal of Finance*, 52, 57–82.
- CARTEA, A. AND S. JAIMUNGAL (2016): “Algorithmic trading of co-integrated assets,” *International Journal of Theoretical and Applied Finance*, 19, 165038.
- CHEN, L., M. PELGER, AND J. ZHU (2022): “Deep learning in asset pricing,” *Management Science*, *forthcoming*.
- CHEN, Y., W. CHEN, AND S. HUANG (2018): “Developing Arbitrage Strategy in High-frequency Pairs Trading with Filterbank CNN Algorithm,” in *2018 IEEE International Conference on Agents (ICA)*, 113–116.
- CONG, L., K. TANG, J. WANG, AND Y. ZHANG (2020): “Single-Step Portfolio Construction through Reinforcement Learning and Economically Interpretable AI,” *Working paper*.
- D’ASPREMONT, A. (2011): “Identifying small mean-reverting portfolios,” *Quantitative Finance*, 11, 351–364.
- DEMIGUEL, V., J. GIL-BAZO, F. NOGALES, AND A. SANTOS (2022): “Machine Learning and Fund Characteristics Help to Select Mutual Funds with Positive Alpha,” *Working paper*.
- DUNIS, C., J. LAWS, AND B. EVANS (2006): “Modelling and trading the soybean-oil crush spread with recurrent and higher order networks: a comparative analysis,” *Neural Network World*, 16, 193–213.
- EBRAHIMI, H. (2013): “Hedge fund quants lose money in 2012,” *The Telegraph*.
- ELLIOTT, R., J. VAN DER HOEK, AND W. MALCOLM (2005): “Pairs trading,” *Quantitative Finance*, 5, 513–545.
- FAMA, E. F. AND K. R. FRENCH (1993): “Common risk factors in the returns on stocks and bonds,” *Journal of*.
- (2015): “A five-factor asset pricing model,” *Journal of financial economics*, 116, 1–22.

- FISCHER, T. G., C. KRAUSS, AND A. DEINERT (2019): “Statistical arbitrage in cryptocurrency markets,” *Journal of Risk and Financial Management*, 12, 31.
- FREYBERGER, J., A. NEUHIERL, AND M. WEBER (2020): “Dissecting characteristics nonparametrically,” *Review of Financial Studies*, 33, 2326–2377.
- GATEV, E., W. N. GOETZMANN, AND K. ROUWENHORST (2006): “Pairs trading: performance of a relative-value arbitrage rule,” *Review of Financial Studies*, 19, 797–827.
- GIGLIO, S. AND D. XIU (2021): “Asset Pricing with Omitted Factors,” *Journal of Political Economy*, 129, 1947–1990.
- GU, S., B. KELLY, AND D. XIU (2021): “Autoencoder Asset Pricing Models,” *Journal of Econometrics*, 222, 429–450.
- GU, S., B. T. KELLY, AND D. XIU (2020): “Empirical Asset Pricing Via Machine Learning,” *Review of Financial Studies*, 33, 2223–2273.
- HE, A., S. HE, D. HUANG, AND G. ZHOU (2022): “Testing Asset Pricing Models Using Pricing Error Information,” *Working paper*.
- HUCK, N. (2009): “Pairs selection and outranking: An application to the S&P 100 index,” *European Journal of Operational Research*, 196, 819–825.
- JIANG, J., B. KELLY, AND D. XIU (2022): “(Re-)Imag(in)ing Price Trends,” *Journal of Finance*, *forthcoming*.
- JUREK, J. W. AND H. YANG (2007): “Dynamic portfolio selection in arbitrage,” in *EFA 2006 Meetings Paper*.
- KANIEL, R., Z. LIN, M. PELGER, AND S. VAN NIEUWERBURGH (2022): “Machine-Learning the Skill of Mutual Fund Managers,” *Working paper*.
- KELLY, B., S. PRUITT, AND Y. SU (2019): “Characteristics Are Covariances: A Unified Model of Risk and Return,” *Journal of Financial Economics*, 134, 501–524.
- KIM, T. AND H. Y. KIM (2019): “Optimizing the Pairs-Trading Strategy Using Deep Reinforcement Learning with Trading and Stop-Loss Boundaries,” *Complexity*, 2019.
- KOZAK, S., S. NAGEL, AND S. SANTOSH (2020): “Shrinking the Cross Section,” *Journal of Financial Economics*, 135, 271–292.
- KRAUSS, C., X. A. DOA, AND N. HUCK (2017): “Deep neural networks, gradient-boosted trees, random forests: Statistical arbitrage on the S&P 500,” *European Journal of Operational Research*, 259, 689–702.
- LETTAU, M. AND M. PELGER (2020a): “Estimating Latent Asset Pricing Factors,” *Journal of Econometrics*, 218, 1–31.
- (2020b): “Factors that Fit the Time-Series and Cross-Section of Stock Returns,” *Review of Financial Studies*, 33, 2274–2325.
- LEUNG, T. AND X. LI (2015): “Optimal mean reversion trading with transaction costs and stop-loss exit,” *International Journal of Theoretical and Applied Finance*, 18, 1550020.
- LI, S. AND Y. TANG (2022): “Automated Risk Forecasting,” *Working paper*.
- LIM, B. AND S. ZOHREN (2020): “Time Series Forecasting With Deep Learning: A Survey,” *Working paper*.
- LINTILHAC, P. S. AND A. TOURIN (2016): “Model-based pairs trading in the bitcoin markets,” *Quantitative Finance*, 17, 703–716.

- MUDCHANATONGSUK, S., J. A. PRIMBS, AND W. WONG (2008): “Optimal pairs trading: A stochastic control approach,” in *2008 American Control Conference*, IEEE, 1035–1039.
- MULVEY, J. M., Y. SUN, M. WANG, AND J. YE (2020): “Optimizing a portfolio of mean-reverting assets with transaction costs via a feedforward neural network,” *Quantitative Finance*, forthcoming.
- MURRAY, S., H. XIAO, AND Y. XIA (2021): “Charting By Machines,” *Working paper*.
- PELGER, M. (2020): “Understanding Systematic Risk: A High-Frequency Approach,” *Journal of Finance*, 74, 2179–2220.
- PELGER, M. AND R. XIONG (2020): “Interpretable Sparse Proximate Factors for Large Dimensions,” *Journal of Business & Economic Statistics*, *Conditionally accepted*.
- (2021): “Interpretable sparse proximate factors for large dimensions,” *Journal of Business & Economic Statistics*, *conditionally accepted*.
- RAD, H., R. K. Y. LOW, AND R. FAFF (2016): “The profitability of pairs trading strategies: distance, cointegration and copula methods,” *Quantitative Finance*, 16, 1541–1558.
- VASWANI, A., N. SHAZEER, N. PARMAR, J. USZKOREIT, L. JONES, A. GOMEZ, L. KAISER, AND I. POLOSUKHIN (2017): “Attention Is All You Need,” *NIPS Conference on Neural Information Processing Systems*.
- VIDYAMURTHY, G. (2004): *Pairs Trading: Quantitative Methods and Analysis*, Wiley.
- XIAOHONG CHEN AND H. WHITE (1999): “Improved rates and asymptotic normality for nonparametric neural network estimators,” *IEEE Transactions on Information Theory*, 45, 682–691.
- YEO, J. AND G. PAPANICOLAOU (2017): “Risk control of mean-reversion time in statistical arbitrage,” *Risk and Decision Analysis*, 6, 263–290.

Appendix A. Data

Appendix A. List of the Firm-Specific Characteristics

Table A.I: Firm Characteristics by Category

<u>Past Returns</u>			<u>Value</u>		
(1)	r2_1	Short-term momentum	(26)	A2ME	Assets to market cap
(2)	r12_2	Momentum	(27)	BEME	Book to Market Ratio
(3)	r12_7	Intermediate momentum	(28)	C	Ratio of cash and short-term investments to total assets
(4)	r36_13	Long-term momentum	(29)	CF	Free Cash Flow to Book Value
(5)	ST_Rev	Short-term reversal	(30)	CF2P	Cashflow to price
(6)	LT_Rev	Long-term reversal	(31)	D2P	Dividend Yield
			(32)	E2P	Earnings to price
<u>Investment</u>			(33)	Q	Tobin's Q
(7)	Investment	Investment	(34)	S2P	Sales to price
(8)	NOA	Net operating assets	(35)	Lev	Leverage
(9)	DPI2A	Change in property, plants, and equipment			
(10)	NI	Net Share Issues	<u>Trading Frictions</u>		
			(36)	AT	Total Assets
<u>Profitability</u>			(37)	Beta	CAPM Beta
(11)	PROF	Profitability	(38)	IdioVol	Idiosyncratic volatility
(12)	ATO	Net sales over lagged net operating assets	(39)	LME	Size
(13)	CTO	Capital turnover	(40)	LTurnover	Turnover
(14)	FC2Y	Fixed costs to sales	(41)	MktBeta	Market Beta
(15)	OP	Operating profitability	(42)	Rel2High	Closeness to past year high
(16)	PM	Profit margin	(43)	Resid_Var	Residual Variance
(17)	RNA	Return on net operating assets	(44)	Spread	Bid-ask spread
(18)	ROA	Return on assets	(45)	SUV	Standard unexplained volume
(19)	ROE	Return on equity	(46)	Variance	Variance
(20)	SGA2S	Selling, general and administrative expenses to sales			
(21)	D2A	Capital intensity			
<u>Intangibles</u>					
(22)	AC	Accrual			
(23)	OA	Operating accruals			
(24)	OL	Operating leverage			
(25)	PCM	Price to cost margin			

This table shows the 46 firm-specific characteristics sorted into six categories. More details on the construction are in the Internet Appendix of Chen et al. (2022).

Appendix B. Implementation of Different Models

Appendix A. Feedforward Neural Network (FFN)

In the Fourier+FFN and FFN models, we utilize a feedforward network with L^{FFN} layers as illustrated in Figure A.1. Each hidden layer takes the output from the previous layer and transforms

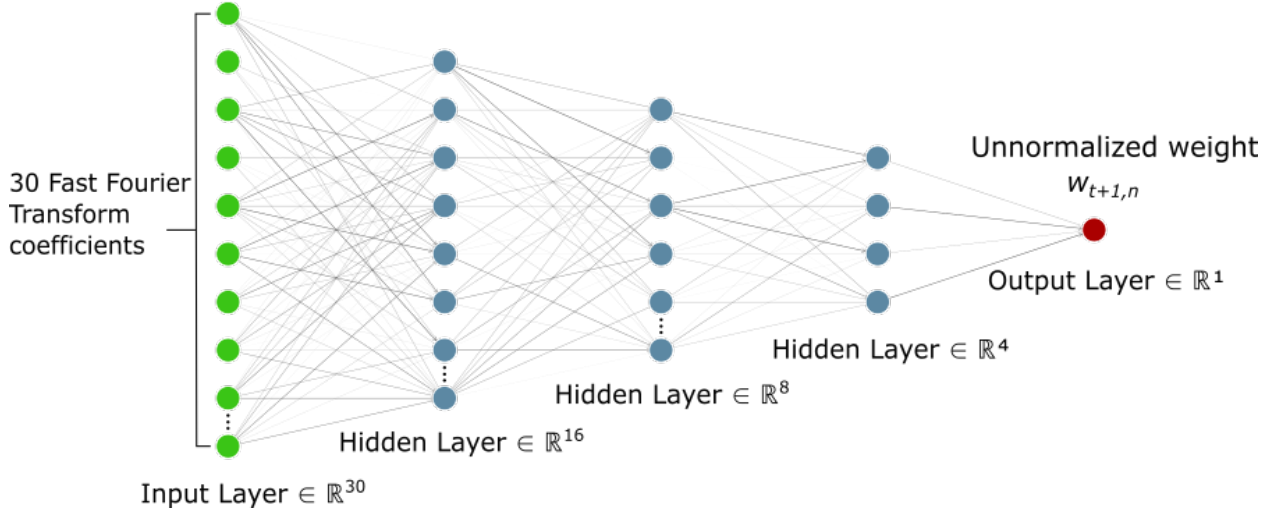
it into an output as

$$x^{(l)} = \text{ReLU} \left(W^{\text{FFN},(l-1)\top} x^{(l-1)} + w_0^{\text{FFN},(l-1)} \right) = \text{ReLU} \left(w_0^{\text{FFN},(l-1)} + \sum_{k=1}^{K^{(l-1)}} w_k^{\text{FFN},(l-1)} x_k^{(l-1)} \right)$$

$$y = W^{\text{FFN},(L^{\text{FFN}})\top} x^{(L)} + w_0^{\text{FFN},(L^{\text{FFN}})}$$

with hidden layer outputs $x^{(l)} = (x_1^{(l)}, \dots, x_{K^{(l)}}^{(l)}) \in \mathbb{R}^{K^{(l)}}$, parameters $W^{(\text{FFN},l)} = (w_1^{\text{FFN},(l)}, \dots, w_{K^{(l)}}^{\text{FFN},(l)}) \in \mathbb{R}^{K^{(l)} \times K^{(l-1)}}$ for $l = 0, \dots, L^{\text{FFN}} - 1$ and $W^{\text{FFN},(L^{\text{FFN}})} \in \mathbb{R}^{K^{(L)}}$, and where $\text{ReLU}(x_k) = \max(x_k, 0)$.

Figure A.1. Feedforward Network Architecture



Appendix B. Ornstein-Uhlenbeck Model

Following Avellaneda and Lee (2010) and Yeo and Papanicolaou (2017) we model X_t as an Ornstein-Uhlenbeck (OU) process

$$dX_t = \kappa (\mu - X_t) dt + \sigma dB_t$$

for a Brownian motion B_t . As the analytical solution of the above stochastic differential equation is

$$X_{t+\Delta t} = (1 - e^{-\kappa\Delta t})\mu + e^{-\kappa\Delta t}X_t + \sigma \int_t^{t+\Delta t} e^{-\kappa(t+\Delta t-s)} dB_s$$

for any Δt , we can without loss of generality set $\Delta t = 1$, and estimate the parameters κ, μ and σ from the AR(1) model

$$X_{t+1} = a + bX_t + e_t,$$

where each e_t is a normal, independent and identically distributed random variable with mean 0. The parameters are estimated with a standard linear regression, which yields

$$\hat{\kappa} = -\frac{\log(\hat{b})}{\Delta t}, \quad \hat{\mu} = \frac{\hat{a}}{1 - \hat{b}}, \quad \frac{\hat{\sigma}}{\sqrt{2\hat{\kappa}}} = \sqrt{\frac{\hat{\sigma}_e^2}{1 - \hat{b}^2}}.$$

The strategy depends on the ratio $\frac{X_L - \hat{\mu}}{\hat{\sigma}\sqrt{2\hat{\kappa}}}$. Note that this is only defined for $b < 1$ which is equivalent to parameter restrictions that the OU process is mean-reverting. The trading policy depends on the thresholds c_{thresh} and c_{crit} , which are hyperparameters. These hyperparameters are selected on the validation data from the candidate values $c_{\text{thresh}} \in \{1, 1.25, 1.5\}$ and $c_{\text{crit}} \in \{0.25, 0.5, 0.75\}$. Our benchmark model has the values $c_{\text{thresh}} = 1.25$ and $c_{\text{crit}} = 0.25$, which coincides with the optimal values in Avellaneda and Lee (2010) and Yeo and Papanicolaou (2017).

Appendix C. Convolutional Neural Network with Transformer

Appendix C.1. Convolutional Neural Network

In our empirical application, we consider a 2-layered convolutional network with some standard technical additions. The network takes as input a window $x^{(0)} = x \in \mathbb{R}^L$ of L consecutive daily cumulative returns or log prices of a residual, and outputs the feature matrix $\tilde{x} \in \mathbb{R}^{L \times F}$ given by computing the following quantities for $l = 1, \dots, L, d = 1, \dots, D$

$$y_{l,d}^{(0)} = b_d^{(0)} + \sum_{m=1}^{D_{\text{size}}} W_{d,m}^{(0)} x_{l-m+1}^{(0)}, \quad x_{l,d}^{(1)} = \text{ReLU} \left(\frac{y_{l,d}^{(0)} - \mu_d^{(0)}}{\sigma_d^{(0)}} \right). \quad (\text{A.1})$$

$$y_{l,d}^{(1)} = b_d^{(1)} + \sum_{m=1}^{D_{\text{size}}} \sum_{j=1}^D W_{d,j,m}^{(1)} x_{l-m+1,j}^{(1)}, \quad x_{l,d}^{(2)} = \text{ReLU} \left(\frac{y_{l,d}^{(1)} - \mu_d^{(1)}}{\sigma_d^{(1)}} \right), \quad (\text{A.2})$$

$$\tilde{x}_{l,d} = x_{l,d}^{(2)} + x_l^{(0)}, \quad (\text{A.3})$$

where

$$\mu_k^{(i)} = \frac{1}{L} \sum_{l=1}^L y_{l,k}^{(i)}, \quad \sigma_k^{(i)} = \sqrt{\frac{1}{L} \sum_{l=1}^L \left(y_{l,k}^{(i)} - \mu_k^{(i)} \right)^2}.$$

and $b^{(0)}, b^{(1)} \in \mathbb{R}^D$, $W^{(0)} \in \mathbb{R}^{D \times D_{\text{size}}}$ and $W^{(1)} \in \mathbb{R}^{D \times D \times D_{\text{size}}}$ are parameters to be estimated. Compared with the simple convolutional network introduced in the main text, the previous equations incorporate three standard technical improvements commonly used in deep learning practice. First, they include “bias terms” $b^{(i)}$ in the first part of equations A.1 and A.2 to allow for more flexible modeling. Second, they include so-called “instance normalization” before each activation function to speed up the optimization and avoid vanishing gradients caused by the saturation of the ReLU activations. Third, they include a “residual connection” in equation A.3 to facilitate gradient propagation during training.

Appendix C.2. Transformer Network

The benchmark model in our empirical application is a one-layer transformer, following the implementation of the seminal paper of Vaswani et al. (2017). First, the sequence of features $\tilde{x} \in \mathbb{R}^{L \times D}$ is projected onto D/H -dimensional subspaces (called the “attention heads”) for an integer H dividing D , obtaining, for $1 \leq i \leq H$,

$$V_i = \tilde{x}W_i^V + b_i^V \in \mathbb{R}^{L \times D/H}, \quad K_i = \tilde{x}W_i^K + b_i^K \in \mathbb{R}^{L \times D/H}, \quad Q_i = \tilde{x}W_i^Q + b_i^Q \in \mathbb{R}^{L \times D/H},$$

where $W_i^V, W_i^K, W_i^Q \in \mathbb{R}^{D \times F/H}$, $b_i^V, b_i^K, b_i^Q \in \mathbb{R}^{D/H}$ are parameters to be estimated. Next, each projection V_i is processed temporally obtaining the hidden states $h_i \in \mathbb{R}^{L \times D/H}$, with

$$h_{i,l} = \sum_{j=1}^L w_{l,j,i} V_{i,j} \in \mathbb{R}^{D/H}, \quad w_{l,j,i} = \frac{\exp(K_{i,l} \cdot Q_{i,j})}{\sum_{m=1}^L \exp(K_{i,l} \cdot Q_{i,m})} \in [0, 1] \quad l = 1, \dots, L \text{ and } i = 1, \dots, D/H.$$

These states are then concatenated and linearly combined, obtaining the last hidden state

$$h = \text{Concat}(h_1, \dots, h_h)W^O + b^O \in \mathbb{R}^{L \times D},$$

where $W^O \in \mathbb{R}^{F \times F}$, $b^O \in \mathbb{R}^F$ are parameters to be estimated.

Finally, h is normalized and processed time-wise though a 2-layered feedforward network as described in detail in the original paper (Vaswani et al. (2017)). The number of hidden units in the intermediate layer is a technical hyperparameter that we call HDN in section C.A. This network also has dropout regularization with hyperparameter called DRP in section C.A.

Appendix D. Network Estimation Details

As explained in Section II.C, we estimate the parameters of the models with neural networks by solving the optimization problems introduced in equation (4) or in equation (6) of section II.C, depending on the model and the objective function. In all cases, this is done by replacing the mean and variance by their annualized sample counterpart over a training set, and by finding the optimal network parameters with stochastic gradient descent using PyTorch’s Adam optimizer and the optimization hyperparameters learning rate and number of optimization epochs described in detail in section C.A.

As mentioned in Section III.C, our main results use rolling windows of 1,000 days as training sets. The networks are reestimated every 125 days to strike a balance between computational efficiency and adaptation to changing economic conditions, and the strategies’ returns are always obtained out-of-sample. Additionally, to be able to train our model over these long windows without running into memory issues, we split each training window into temporal “batches”, as is commonly done in deep learning applications. Each batch contains the returns and residuals for all the stocks in a subwindow of 125 days of the original training window, with the subwindows being consecutive and non-overlapping (i.e., for a training window of 1000 days, we split it into the subwindow containing

the first 125 days, the subwindow containing the days between the 126th day and the 250th day, etc.). The optimization process is applied successively to each batch, completing the full sequence of batches before starting a new optimization iteration or epoch.

In the implementation of our optimization procedure under market frictions, we found it useful to include the last allocation as an additional input to the allocation function \mathbf{w}^ϵ , as the inclusion of the cost term makes the objective function depend on it. However, the inclusion of the previous allocations in either the objective function or the architecture of the model complicates the parallelization of the training and evaluation computations, because after this change the model requires the output of previous lookback window in order to compute the output of the current window. To allow training to remain parallelized, which is desirable for reasonable computational speed given the volume of data of our empirical application, in our implementation of the training function in each epoch, we take the previous allocations from the output of the previous epoch and use them as a pre-computed approximation of the allocations for the current epoch. This approximation converges in our empirical experiments and allows us to maintain parallelization, but may produce suboptimal results. For evaluation purposes, however, everything is computed exactly and with no approximations using a sequential approach.

Throughout section III, all presented results have been computed with PyTorch 1.5 and have been parallelized across 8 NVIDIA GeForce GTX Titan V GPUs, on a server with two Intel Xeon E5-2698v3 32-core CPUs and 1 TB of RAM. The full rationale for the hyperparameter choices are described in detail in section C.A, but for a CNN+Transformer model with a lookback window of 30 days, 8 convolutional filters with a filter size of 2, 4 attention heads, 125-day reestimation using a rolling lookback window of 1000, it takes our deep model approximately 7 hours to be periodically estimated and run in our 19 years of daily out-of-sample data with our universe of on average ~ 550 stocks per month.

Appendix C. Additional Empirical Results

Appendix A. Robustness to Hyperparameter Selection

In this subsection, we describe our hyperparameter selection procedure and explore additional hyperparameter choices to show that the performance of our strategies is extremely robust to our choices. These results complement the time stability checks we exhibited in Section III.I. To decide which hyperparameters we would select for use in our network, we fixed a validation dataset as follows: we took the first 1000 trading days of our data set of residuals (all trading days from January 1, 1998 through December 31, 2001) of the 5-factor IPCA-based model, which is estimated with a 20-year rolling window. Because it is solely used for training in our rolling train/test procedures used to compute strategy returns, this data is completely in-sample, and thus completely avoids look-ahead bias which would influence any of our out-of-sample trading results in the main text. We started with a reasonable set for our hyperparameters, and tested also additional points adjacent

Table A.II: Hyperparameter options for the network in the empirical analysis

Notation	Hyperparameters	Candidates	Chosen
D	Number of filters in the convolutional network	8, 16	8
ATT	Number of attention heads	2, 4	4
HDN	Number of hidden units in the transformer’s linear layer	2D, 3D	2D
DRP	Dropout rate in the transformer	0.25, 0.5	0.25
D_{size}	Filter size in the convolutional network	2	2
LKB	Number of days in the residual lookback window	30	30
WDW	Number of days in the rolling training window	1000	1000
RTFQ	Number of days of the retraining frequency	125	125
BTCH	Batch size, in days	125	125
LR	Learning rate	0.001	0.001
EPCH	Number of optimization epochs	100	100
OPT	Optimization method	Adam	Adam

This table shows the parameters for our network architecture with respect to the Sharpe ratio on our validation data and the candidates we tried. In DRP, we follow the convention that the dropout rate p is the proportion of units which are removed.

to these sets.²⁰ For each model represented by a point on the grid, we trained the model using the Sharpe ratio objective on the first 750 days of the 1000 trading days, and evaluated it by its out-of-sample Sharpe ratio on the last 250 days of the 1000 trading days. We tested 16 combinations of hyperparameters, which are illustrated in Table A.II. The results of our test on the last 250 days of our validation data are displayed in Table A.III.

The results in Table A.III show that all Sharpe ratios fall within a tight range of values, which is roughly $[3.5, 4.2]$. Means and volatilities concentrate similarly, falling within $[13\%, 17.8\%]$ and $[3.6\%, 4.3\%]$. Computation of 95% bootstrapped confidence intervals for mean return shows that all models’ confidence intervals contain the interval $[10\%, 20\%]$, with volatilities similarly contained. Hence, these models are statistically not distinguishable. Given the statistical insignificance of the differences in performance of these models, we chose the model displayed in Table A.II, which is the most parsimonious one, that is it has the smallest number of parameters, and hence benefits low GPU memory usage and ease of interpretability.

To ensure that our results are stable across several choices of hyperparameters, we study the results of four additional models with perturbed hyperparameters. This complements our robustness results of Section III.I regarding the size of the lookback window and the retraining frequency. The four additional networks and their hyperparameter configurations are listed in Table A.IV, with Network 1 being the network studied throughout this empirical section. Network 2 corresponds to more filters and commensurately more hidden units to consume them, and higher dropout rates to more strongly regularize the additional parameters. Network 3 halves the number of attention heads from our original specification. Networks 4 and 5 modify the size of the rolling training window from 1000 trading days to 1250 and 750 trading days, respectively, which corresponds closely to three and five calendar years. These additional hyperparameter configurations constitute local perturbations in hyperparameter space, to which our strategies’ performance are relatively robust.

²⁰Note the computation over a large set of hyperparameters is computationally infeasible, which requires us to restrict the set to reasonable values.

Table A.III: Performance of candidate models on the last year of the validation data set

D	ATT	HDN	DRP	SR	μ	σ
8	2	2	0.25	3.81	16.3%	4.3%
8	2	2	0.50	3.92	16.0%	4.1%
8	2	3	0.25	3.79	16.2%	4.3%
8	2	3	0.50	4.00	16.4%	4.1%
8	4	2	0.25	3.81	15.6%	4.1%
8	4	2	0.50	4.13	17.8%	4.3%
8	4	3	0.25	3.82	15.6%	4.1%
8	4	3	0.50	4.16	17.4%	4.2%
16	2	2	0.25	4.00	14.8%	3.7%
16	2	2	0.50	4.06	16.2%	4.0%
16	2	3	0.25	4.11	14.9%	3.6%
16	2	3	0.50	4.06	16.6%	4.1%
16	4	2	0.25	3.93	15.6%	4.0%
16	4	2	0.50	3.66	13.9%	3.8%
16	4	3	0.25	4.18	16.8%	4.0%
16	4	3	0.50	3.51	13.0%	3.7%

This table shows the model performance with respect to the Sharpe ratio, mean, and volatility on our validation data set for the candidate models implied by Table A.II. The models are trained on the first three years of the validation data set (1998–2000) and tested on the last year (2001). In DRP, we follow the convention that the dropout rate p is the proportion of units which are removed.

Table A.IV: Alternative best performing models on the data from 2002–2016

Model	FLNB	FLSZ	ATT	HDN	DRP	LKB	WDW
Network 1	[1,8]	2	4	16	0.25	30	1000
Network 2	[1,16]	2	4	32	0.5	30	1000
Network 3	[1,8]	2	2	16	0.25	30	1000
Network 4	[1,8]	2	4	16	0.25	30	1250
Network 5	[1,8]	2	4	16	0.25	30	750

This table reports four of the best performing models for our network architecture with respect to the Sharpe ratio on our data from 2002–2016 and the candidates described in Table A.II. Our original network, which is studied throughout this section, is labeled as Network 1.

Table A.V: Performance of the alternative models on our benchmark residual datasets, 2002–2016

Model	Fama-French 5			PCA 5			IPCA 5		
	SR	μ	σ	SR	μ	σ	SR	μ	σ
Network 1	3.21	4.6%	1.4%	3.36	14.3%	4.2%	4.16	8.7%	2.1%
Network 2	3.16	4.6%	1.4%	3.26	13.9%	4.3%	4.35	8.4%	1.9%
Network 3	3.30	4.8%	1.4%	3.17	13.4%	4.2%	4.00	8.4%	2.1%
Network 4	2.93	4.1%	1.4%	2.74	11.7%	4.3%	3.96	7.9%	2.0%
Network 5	3.13	4.9%	1.6%	3.52	15.0%	4.3%	3.77	8.6%	2.3%

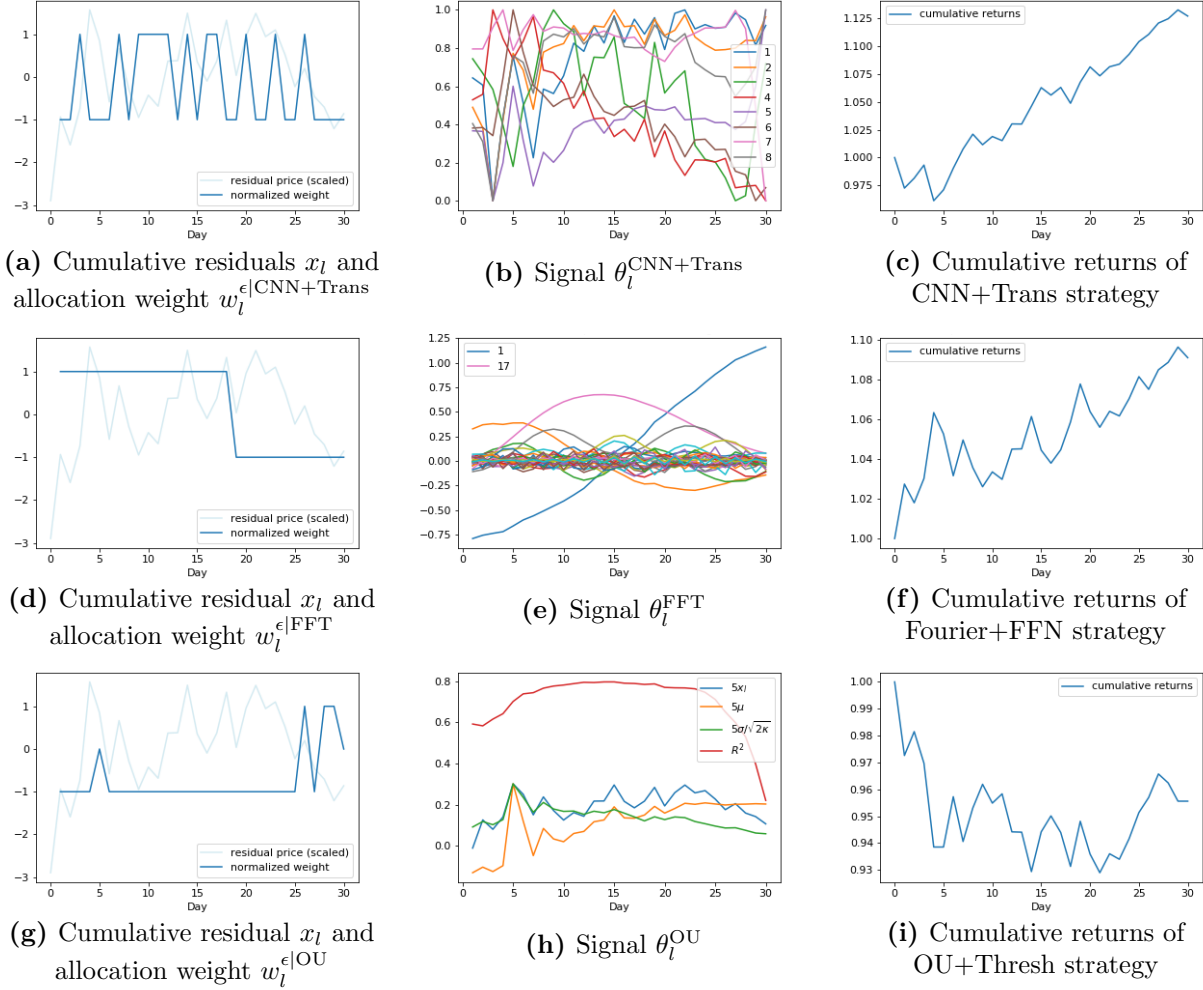
This table shows the average annualized returns, volatilities and Sharpe ratios of our alternative models from Table A.IV on our three benchmark residual datasets, trained with the Sharpe ratio objective function.

In Table A.V, we report the results of these models on a representative subset of 5-factor models, which are now evaluated on the full out-of-sample data. We see that the Sharpe ratios are broadly similar across all three different perturbations of network architecture hyperparameters (i.e., number of filters, number of attention heads, and dropout rate). The small range of values induced by these choices shows that our network performs similarly over a variety of sensible network parameters, and highlights the efficacy of our reasonable choice of convolutional, attentional, and feedforward subnetworks which specialize in finding small temporal patterns, arranging these patterns throughout time, and deciding on allocations based on these arranged patterns.

For the allocation function feedforward network (FFN) utilized for the Fourier+FFN model, we choose a reasonable architecture based on deep learning conventions and have verified that the results are robust to this choice. Because the input of the network are the $L = 30$ coefficients of the Fourier decomposition of each residual window $(X_l^{(n,t)})_{1 \leq l \leq L}$ and the output is the corresponding allocation weight $w_{n,t} \in \mathbb{R}$, we follow standard deep learning practices and consider 3 hidden layers with dimensions 16,8,4 regularized with a dropout rate of 0.25. We use the ReLU activation function, and train using the same procedure outlined in B.D, with the same batch size, learning rate, number of optimization epochs, and optimization method as in Table A.II.

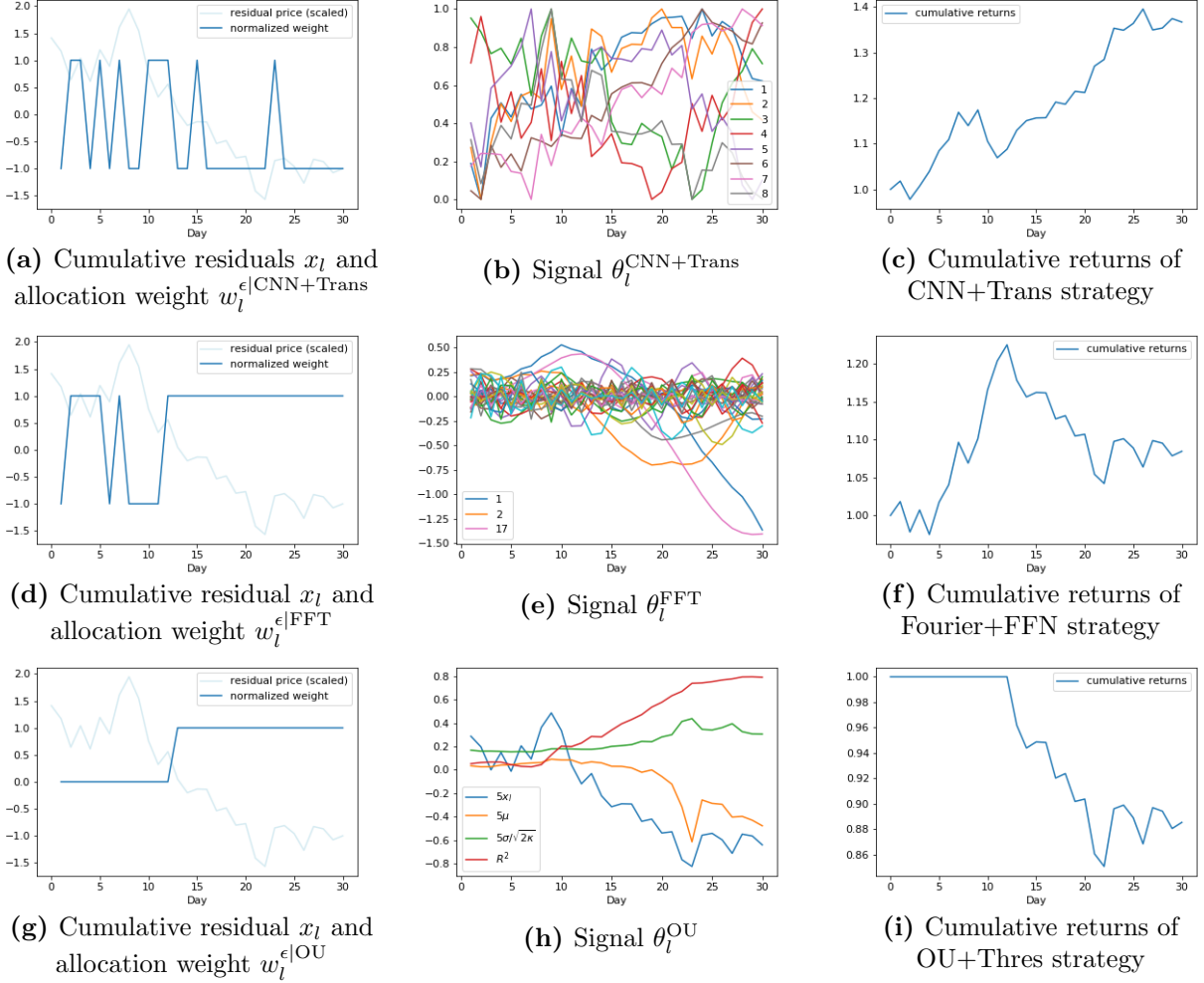
Appendix B. Interpretation

Figure A.2: Illustrative Example of Allocation Weights and Signals for Different Methods



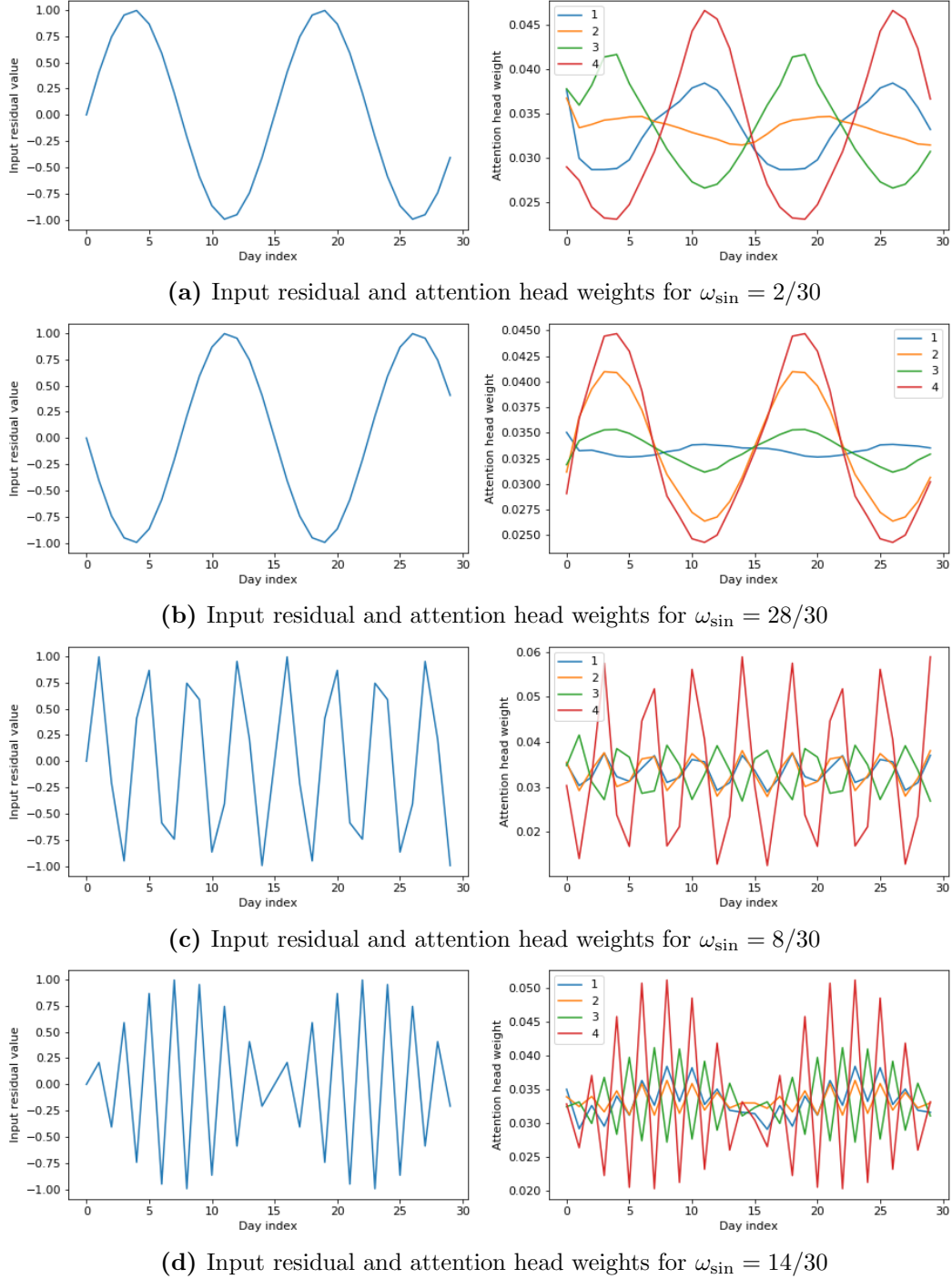
These plots are an illustrative example of the allocation weights and signals of the Ornstein-Uhlenbeck with Threshold (OU+Thres), Fast Fourier Transform (FFT) with Feedforward Neural Network (FFN), and Convolutional Neural Network (CNN) with Transformer models for a specific cumulative residual. The models are estimated on the empirical data, and the residual is a representative empirical example. In more detail, we consider the residuals from five IPCA factors and estimate the benchmark models as explained in Section III.N. The left subplots display the cumulative residual process along with the out-of-sample allocation weights $w_l^{\epsilon|}$ that each model assigns to this specific residual. In this example, we consider trading only this specific residual and hence normalize the weights to $\{-1, 0, 1\}$. The middle column plots show the time-series of estimated out-of-sample signals for each model, by applying the θ_l^{ϵ} arbitrage signal function to the previous L cumulative returns of the residual. The right column plots display the out-of-sample cumulative returns of trading this particular residual based on the corresponding allocation weights. We use a rolling lookback window of $L = 30$ days to estimate the signal and allocation, which we evaluate for the out-of-sample trading on the next 30 days. The plots only show the out-of-sample period. The evaluation of this illustrative example is a simplification of the general model that we use in our empirical main analysis, where we trade all residuals and map them back into the original stock returns.

Figure A.3: Additional Examples of Allocation Weights and Signals



These plots are an illustrative example of the allocation weights and signals of the Ornstein-Uhlenbeck with Threshold (OU+Thres), Fast Fourier Transform (FFT) with Feedforward Neural Network (FFN), and Convolutional Neural Network (CNN) with Transformer models for a specific cumulative residual. The models are estimated on the empirical data, and the residual is a representative empirical example. In more detail, we consider the residuals from five IPCA factors and estimate the benchmark models as explained in Section III.N. The left subplots display the cumulative residual process along with the out-of-sample allocation weights $w_l^{\epsilon|}$ that each model assigns to this specific residual. In this example, we consider trading only this specific residual and hence normalize the weights to $\{-1, 0, 1\}$. The middle column plots show the time-series of estimated out-of-sample signals for each model, by applying the θ_l^i arbitrage signal function to the previous L cumulative returns of the residual. The right column plots display the out-of-sample cumulative returns of trading this particular residual based on the corresponding allocation weights. We use a rolling lookback window of $L = 30$ days to estimate the signal and allocation, which we evaluate for the out-of-sample on the next 30 days. The plots only show the out-of-sample period. The evaluation of this illustrative example is a simplification of the general model that we use in our empirical main analysis, where we trade all residuals and map them back into the original stock returns.

Figure A.4: Example Attention Weights for Sinusoidal Residual Inputs



These plots show the attention head weights of the CNN+Transformer benchmark model for simulated sinusoidal residual input time series. The inputs are $x_l = \sin(2\pi\omega_{\sin}l)$, for various ω_{\sin} and $l \in \{0, \dots, 29\}$. The right subplot shows the attention weights for the $H = 4$ attention heads for the specific residuals. The empirical benchmark model is the CNN+Transformer model based on IPCA 5-factor residuals. We estimate the model on only once on the first $T_{\text{train}}=8$ years based on the Sharpe ratio objective.

Appendix C. Unconditional Residual Means

Table A.VI: OOS Annualized Performance of Unconditional Average Residuals

Equally Weighted Residuals										
K	Fama-French			PCA			IPCA			
	SR	μ	σ	SR	μ	σ	SR	μ	σ	
0	0.52	11.2%	21.4%	0.52	11.2%	21.4%	0.52	11.2%	21.4%	
1	0.39	1.9%	4.8%	-0.23	-0.4%	1.5%	0.76	3.2%	4.2%	
3	0.18	0.7%	3.7%	0.34	0.3%	0.9%	0.76	2.0%	2.7%	
5	0.22	0.8%	3.5%	0.93	0.7%	0.7%	0.63	1.4%	2.3%	
8	-0.17	-0.5%	2.9%	1.04	0.6%	0.5%	0.66	1.4%	2.2%	
10	-	-	-	0.90	0.4%	0.5%	0.65	1.3%	2.1%	
15	-	-	-	1.08	0.4%	0.4%	0.62	1.3%	2.0%	

This table shows the out-of-sample annualized Sharpe ratio (SR), mean return (μ), and volatility (σ) of equally weighted residuals. We evaluate the out-of-sample arbitrage trading from January 2002 to December 2016. The $K = 0$ factor model corresponds to directly using stock returns instead of residuals for the signal and trading policy.

Table A.VII: Significance of Arbitrage Alphas Based on Unconditional Average Residuals

Equally Weighted Residuals															
K	Fama-French					PCA					IPCA				
	α	t_α	R^2	μ	t_μ	α	t_α	R^2	μ	t_μ	α	t_α	R^2	μ	t_μ
0	1.4%	1.4	97.0%	11.2%	2.0*	1.4%	1.4	97.0%	11.2%	2.0*	1.4%	1.4	97.0%	11.2%	2.0*
1	0.4%	0.4	36.6%	1.9%	1.5	0.0%	0.0	25.8%	-0.4%	-0.9	0.4%	1.1	85.0%	3.2%	2.9**
3	0.4%	0.4	9.6%	0.7%	0.7	0.4%	1.9	13.1%	0.3%	1.3	0.9%	3.3**	84.1%	2.0%	2.9**
5	0.2%	0.2	7.0%	0.8%	0.9	0.7%	4.2***	5.9%	0.7%	3.6***	0.4%	2.0*	89.4%	1.4%	2.4*
8	-0.6%	-0.8	0.7%	-0.5%	-0.7	0.6%	4.5***	4.1%	0.6%	4.0***	0.4%	2.1*	89.3%	1.4%	2.5*
10	-	-	-	-	-	0.5%	3.8***	3.0%	0.4%	3.5***	0.3%	1.9	89.4%	1.3%	2.5*
15	-	-	-	-	-	0.4%	4.3***	2.0%	0.4%	4.2***	0.3%	1.6	89.0%	1.3%	2.4*

This table shows the out-of-sample pricing errors α of cross-sectionally equally weighted residuals relative of the Fama-French 8 factor model and their mean returns μ for the different arbitrage models and different number of factors K that we use to obtain the residuals. We run a time-series regression of the out-of-sample returns of the arbitrage strategies on the 8-factor model (Fama-French 5 factors + momentum + short-term reversal + long-term reversal) and report the annualized α , accompanying t-statistic value t_α , and the R^2 of the regression. In addition, we report the annualized mean return μ along with its accompanying t-statistic t_μ . The hypothesis test are two-sided and stars indicate p-values of 5% (*), 1% (**), and 0.1% (***). All results use the out-of-sample daily returns from January 2002 to December 2016.

Appendix D. Dependency between Arbitrage Strategies

Table A.VIII: Correlations between the Returns of the CNN+Transformer Arbitrage Strategies

	Fama-French 3	PCA 3	IPCA 3	Fama-French 5	PCA 5	IPCA 5	PCA 10	IPCA 10
Fama-French 3	1.00	0.32	0.44	0.62	0.25	0.43	0.21	0.44
PCA 3	0.32	1.00	0.32	0.34	0.62	0.35	0.41	0.36
IPCA 3	0.44	0.32	1.00	0.37	0.28	0.81	0.21	0.75
Fama-French 5	0.62	0.34	0.37	1.00	0.28	0.39	0.23	0.40
PCA 5	0.25	0.62	0.28	0.28	1.00	0.29	0.47	0.31
IPCA 5	0.43	0.35	0.81	0.39	0.29	1.00	0.23	0.84
PCA 10	0.21	0.41	0.21	0.23	0.47	0.23	1.00	0.25
IPCA 10	0.44	0.36	0.75	0.40	0.31	0.84	0.25	1.00

This table reports the correlations of our CNN+Transformer strategies for some representative choices of the factor models. The correlations are calculated with returns of the out-of-sample arbitrage trading from January 2002 to December 2016. The models are calibrated on a rolling window of four years and use the Sharpe ratio objective function. The signals are extracted from a rolling window of $L = 30$ days.

Appendix E. Time-Series Signal

In this appendix, we report the OOS returns of strategies using alternative models for the ablation tests in Section III. For the FFN feedforward network, we use the same architecture, hyperparameters, optimization settings, etc. as in the Fourier+FFN model utilized throughout the empirical results section and described in Appendix C.A. For the OU+FFN model, because the input is the low-dimensional OU signal in \mathbb{R}^4 , we consider a 3 hidden layer with dimensions 4,4,4 regularized with a dropout rate of 0.25. We use the sigmoid activation function, and estimate it using the same procedure outlined in section B.D, with the same batch size, learning rate, number of optimization epochs, and optimization method as in Table A.II.

Table A.IX: OOS Annualized Performance Based on Sharpe Ratio Objective

Factors		Fama-French			PCA			IPCA		
Model	K	SR	μ	σ	SR	μ	σ	SR	μ	σ
OU + FFN	0	0.50	10.6%	21.3%	0.50	10.6%	21.3%	0.50	10.6%	21.3%
	1	0.34	0.8%	2.3%	0.05	0.7%	11.9%	0.60	4.8%	8.0%
	3	0.16	0.2%	1.4%	0.44	3.4%	7.8%	0.70	4.6%	6.6%
	5	0.17	0.2%	1.2%	0.68	4.7%	7.0%	0.66	4.2%	6.3%
	8	-0.34	-0.3%	1.0%	0.51	3.1%	6.0%	0.60	3.9%	6.2%
	10	-	-	-	0.26	1.3%	5.0%	0.56	3.5%	6.2%
	15	-	-	-	0.31	1.4%	4.3%	0.54	3.3%	6.1%
FFN	0	0.57	8.8%	15.3%	0.57	8.8%	15.3%	0.57	8.8%	15.3%
	1	0.60	2.0%	3.3%	0.53	6.2%	11.7%	1.07	6.5%	6.1%
	3	1.02	2.6%	2.6%	1.15	8.2%	7.2%	1.50	7.6%	5.0%
	5	1.32	2.3%	1.7%	1.42	9.8%	6.9%	1.55	7.3%	4.7%
	8	1.31	2.1%	1.6%	1.05	6.4%	6.2%	1.52	7.2%	4.7%
	10	-	-	-	0.70	3.5%	5.0%	1.48	7.0%	4.7%
	15	-	-	-	0.51	2.4%	4.8%	1.68	7.5%	4.5%

This table shows the out-of-sample annualized Sharpe ratio (SR), mean return (μ), and volatility (σ) of our three statistical arbitrage models for different numbers of risk factors K , that we use to obtain the residuals. We use the daily out-of-sample residuals from January 1998 to December 2016 and evaluate the out-of-sample arbitrage trading from January 2002 to December 2016. OU+FFN denotes a parametric Ornstein-Uhlenbeck model to extract the signal, but a flexible feedforward neural network to estimate the allocation function. FFN takes the residuals directly as signals and estimates an allocation function with a feedforward neural network. The deep learning models are calibrated on a rolling window of four years and use the Sharpe ratio objective function. The signals are extracted from a rolling window of $L = 30$ days. The $K = 0$ factor model corresponds to directly using stock returns instead of residuals for the signal and trading policy.

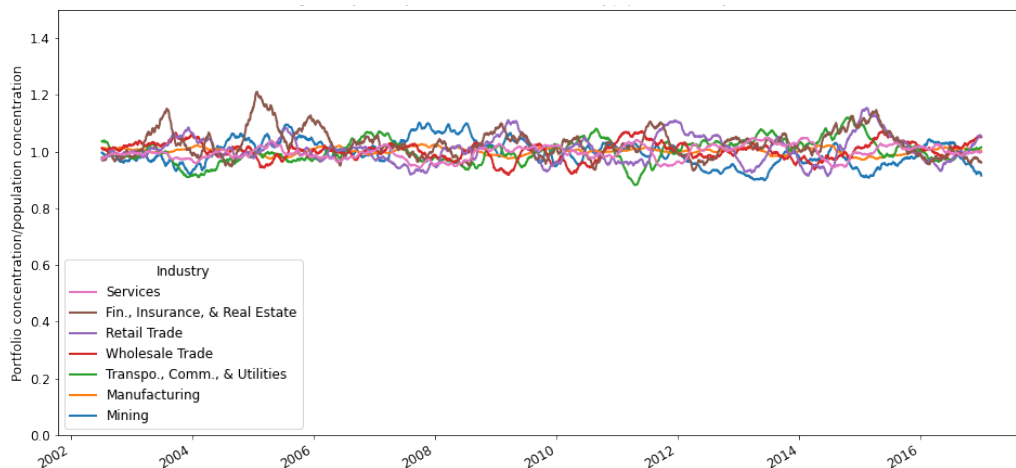
Appendix F. Trading Friction Results for PCA Residuals

Table A.X: OOS Performance of CNN+Trans with Trading Frictions

PCA factor model						
K	Sharpe ratio			Mean-variance		
	SR	μ	σ	SR	μ	σ
0	0.52	8.5%	16.3%	0.22	2.6%	11.9%
1	0.88	7.3%	8.4%	0.79	9.0%	11.4%
3	0.90	5.7%	6.3%	0.62	4.7%	7.6%
5	0.81	4.5%	5.6%	0.68	4.4%	6.4%
10	-0.08	-0.4%	4.8%	-0.08	-0.4%	4.6%
15	-0.87	-3.7%	4.3%	-0.96	-3.5%	3.7%

This table shows the out-of-sample annualized Sharpe ratio (SR), mean return (μ), and volatility (σ) for the CNN+Transformer model with trading frictions on PCA residuals. We use the daily out-of-sample residuals from January 1998 to December 2016 and evaluate the out-of-sample arbitrage trading from January 2002 to December 2016. The models are calibrated on a rolling window of four years and use either the Sharpe ratio or mean-variance objective function with trading costs $\text{cost}(w_{t-1}^R, w_{t-2}^R) = 0.0005\|w_{t-1}^R - w_{t-2}^R\|_{L^1} + 0.0001\|\min(w_{t-1}^R, 0)\|_{L^1}$. The signals are extracted from a rolling window of $L = 30$ days.

Figure A.5: Industry Concentration of Portfolio Weights



This figure shows the rolling 132-day industry concentration of portfolio weights standardized by the population industry concentration. The stock portfolio weights w_t^R are for the empirical benchmark CNN+Transformer model based on IPCA 5-factor residuals and for the out-of-sample trading period between January 2002 and December 2016. We use standard SIC industry classifications.